GEOTECHNICAL

ENGINEERING

GEOTECHNICAL ENGINEERING

VOLUME 20   NUMBER 2   DECEMBER 1989

Papers: **Page**

GEOTECHNICAL ISSUES

T. William Lambe

INTRODUCTION

In this volume and subsequent volumes to the Journal I shall identify important and controversial issues in the practice of geotechnical engineering. I invite you to state your position and its basis on the issues I raise. Send your response to the Editor of the Journal who will consider it for publication. In an appropriate volume of the Journal, I will summarize, compare and comment on the discussions sent to the Editor.

At the Society's tenth conference (April 1990 in Taipei) I will chair a panel which will address the case described in Figure 1. The case raises four important issues.

I suggest you study the problem in Figure 1 prior to your coming to the Taipei conference. Such study will enable you to enjoy and profit more from the panel discussion at the Taipei conference.

Please submit to the Editor of the Journal a statement on your position relative to "strength" in the case, Figure 1.

THE PROBLEM

The contractor plans to construct a clay Embankment in nine months. Flexibility considerations require that you place the compacted clay no dryer than 1% below the optimum water content as determined by the Standard Proctor Test. Address the following issues considering only the End-of-Construction State. Do not consider slope protection, piping, earthquake loading etc. – consider only stability against a shear slide immediately after completion of the embankment.

A. Allowable Factor of Safety: State the minimum factor of safety and the basis for your choice.

T. William Lambe, Consulting Geotechnical Engineer, Florida, USA

B. Strength: State the procedure you would use to select the strength for the stability analysis. If you call for laboratory tests, state type(s) of lab tests and specify the stress and drainage conditions.

C. Stability Analysis: State (with references) the method of stability analysis you would use. Identify the parameters needed and the method of getting each parameter.

D. Construction Control: State the procedure you would use to ensure that the completed embankment has the minimum permissible factor of safety and the parameters used in your stability analysis.
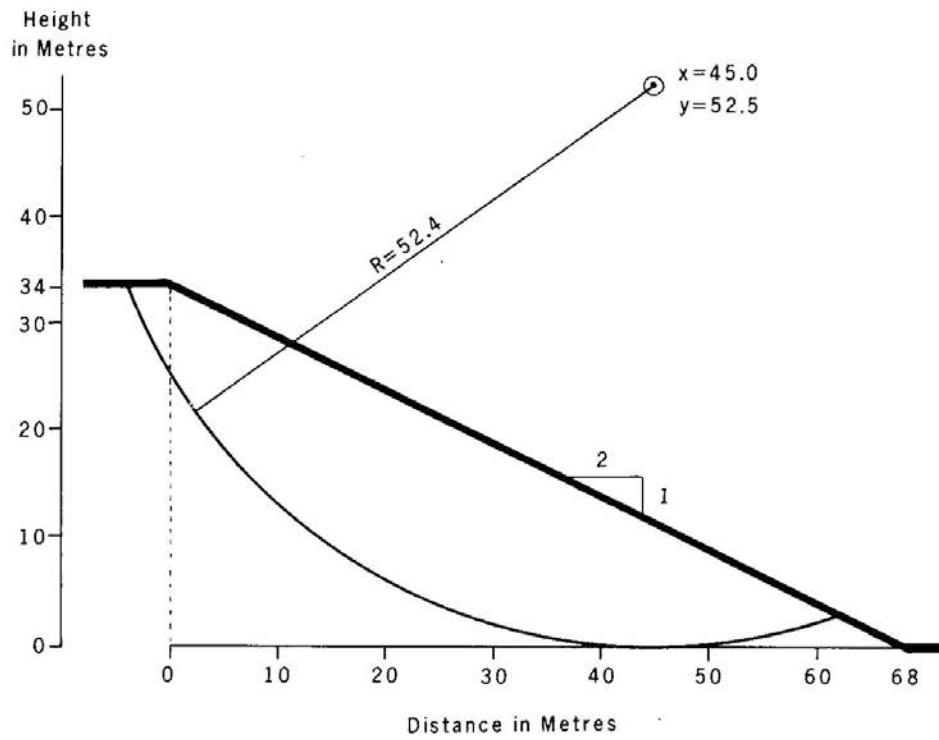
YOUR RESPONSE

Send or FAX your response to:
Peter Whiteside
The Editor, "Geotechnical Engineering"
c/o Geotechnical Control Office
6/F Empire Centre
68 Mody Road
Kowloon
HONG KONG

FAX (852) 369 0007

If your response is in time, it will be considered at the Taipei conference as well as for publication in Geotechnical Engineering.

Slope composed of Compacted Clay

Liquid & Plastic Limits : $\omega_\ell = 65\%$, $\omega_P = 22\%$

Compaction - Std. Proctor

$\omega_o = 20.0\%$, $\gamma_{d_{max}} = 1.66$ t/m^3

Unconfined Strength

$\triangle\omega_o$	-2	0	2	4	6	%
$P/2A_f$	20.0	13.7	9.2	6.2	4.2	t/m^2

Fig. 1. Problem Slope

TEST DRIVING OF 75M LONG H BEARING-PILES IN CHINA

L. Weber*

SYNOPSIS

In the Shanghai area, the soil conditions are such that bearing-piles have become an essential foundation part of the new high-rise buildings. In order to reduce the settlements under the high working loads, the pile tip has to penetrate into the compact sand layer, situated at approx. 60-70m depth. No H-piles have yet been tested under these conditions in Shanghai. This paper describes the driving of H bearing-piles with different shapes and with lengths varying from 45m to 75m. Dynamic measurements were performed during driving and after a wait time of approx. 40 hours in order to assess the change in bearing capacity as a function of time and in order to get an idea about the resistance distribution along the piles by using a stress wave analysis program (CAPWAP). One month after driving, two piles of 75m length were statically test loaded both in the vertical and in horizontal directions.

From these tests, it can be concluded that these H-pile sections can be installed smoothly in the typical Shanghai subsoil to the dense second sand layer without any sign of pile buckling. The full penetration welds of the splices have no observable influence on the pile driving behavior. The amount of set-up is very important; as a consequence, the axial driving stresses are low. One test pile was statically loaded in compression to 2.6 times the working load without any sign of pile or soil failure. The permanent displacements from the vertical and horizontal loading tests are small.

INTRODUCTION TO THE DRIVING TESTS

Although some long H-piles have already been driven, mainly in the USA, no comparison allows for the prediction of the H-pile behavior during driving and load testing under the specific soil conditions in the Shanghai area. The main concerns of the Chinese Building Authorities are:

– the prevention of pile buckling during driving and load testing
– the amount of dynamic stresses introduced in the pile during driving through compact layers
– the amount of horizontal displacement under twice the working load, especially about the Y-axis of the H-pile
– the influence of the pile splices on the pile performance

---

*Technical Advisory Dept., ARBED, Luxemburg

TEST PROGRAM

The test program is as follows:

- drive 6 reaction piles and 2 test piles. Due to the given number of piles at the site, different pile lengths have to be fixed. In order to get an idea about the influence of the pile shape on bearing capacity, two different types of reinforcements are used.
- monitor force and acceleration during driving and restrike in order to determine the bearing capacity and the resistance distribution along the piles by stress wave analysis (CAPWAP program).
- execute two vertical static tests, one to twice the working load ($2\times40=80$kN), one against the X-axis and one against the Y-axis of the section. The max. allowable displacement of the pile head is 40mm. Since, in the final structure, the pile top is embedded in the concrete slab, it was decided to fix the head in a manner which does not allow for any inclination against the vertical.

SUBSOIL CONDITIONS AT THE TEST SITE

The Lotus Mansion site is located in the Hong Qiao district between downtown Shanghai and the airport. The soil profile at the site is shown in figure 1 and consists, starting at the surface, of approx. 1.5m of fill, underlain by $\simeq$14m of mucky loam and clay. Beneath, until a depth of 46m, a saturated plastic clay and loam occurs. Within the depths of 46m and 52m, the soil consists of a medium dense sandy loam, underlain by slight to medium plastic loam extending to a depth of 65m. Beneath, an intermediary layer of sandy loam reaches the depth of 68m; an underlying medium to very dense silty sand is found to about 93m depth.

PILE DRIVING TESTS

Piles

All piles were sections HP $360\times410\times176$ (HP $14\times16\times118$) in steel quality BS4360 grade 50B (yield point = 345MPa). The piles were driven in segments of 15m length, except the piles A1, 2, 4, 5, for which the 1st segment presents a length of 10m. The pile segments are welded together by full penetration welds and a 45° beveling of the upper element surface as shown on figure 2.

86

.

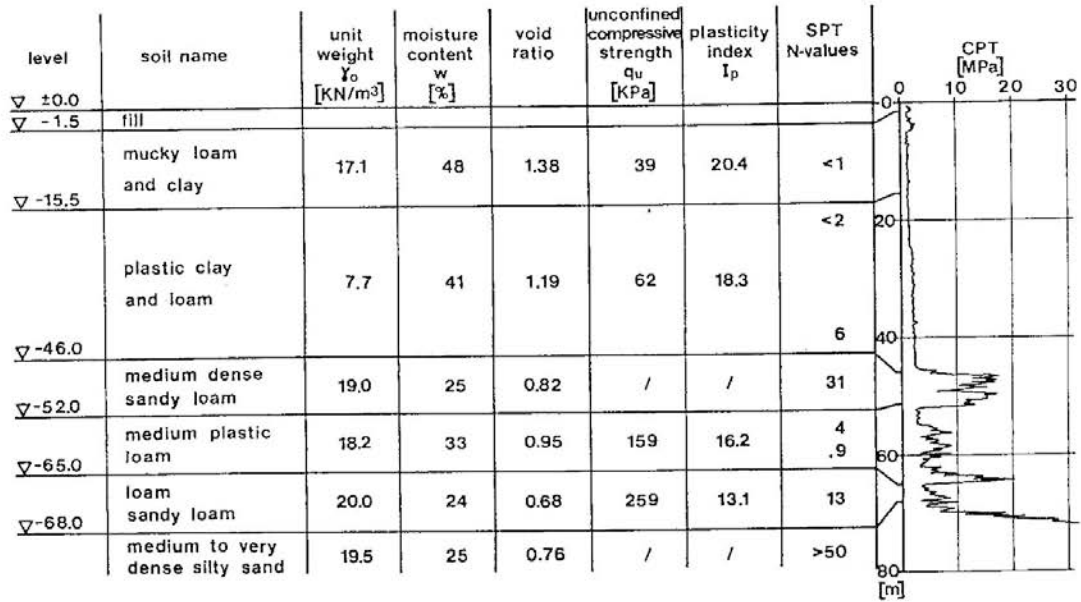| level	soil name	unit weight γ_o [KN/m³]	moisture content w [%]	void ratio	unconfined compressive strength q_u [KPa]	plasticity index I_p	SPT N-values	CPT [MPa]
▽ ±0.0								
▽ -1.5	fill							
	mucky loam and clay	17.1	48	1.38	39	20.4	<1	
▽ -15.5							<2	
	plastic clay and loam	7.7	41	1.19	62	18.3		
▽ -46.0							6	
	medium dense sandy loam	19.0	25	0.82	/	/	31	
▽ -52.0	medium plastic loam	18.2	33	0.95	159	16.2	4 .9	
▽ -65.0	loam sandy loam	20.0	24	0.68	259	13.1	13	
▽ -68.0	medium to very dense silty sand	19.5	25	0.76	/	/	>50	

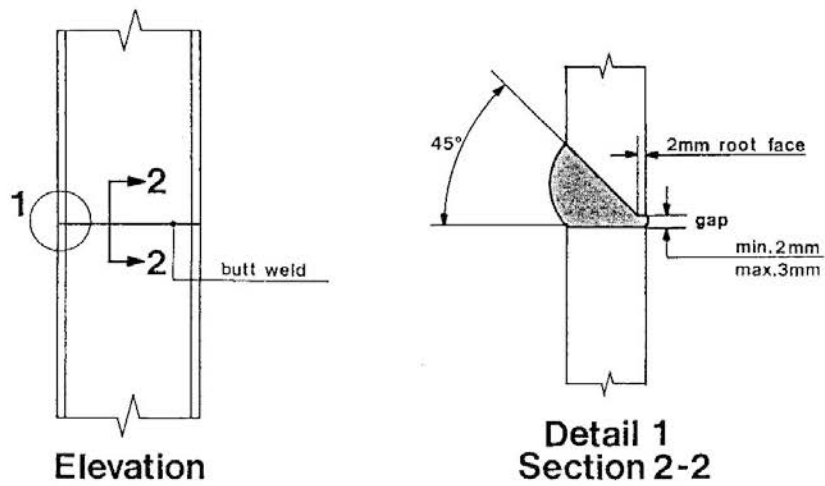**Figure 1 Project Lotus Mansion, Shanghai General soil conditions at site**

Figure 2 Typical details of butt welded joint for H-piles

87

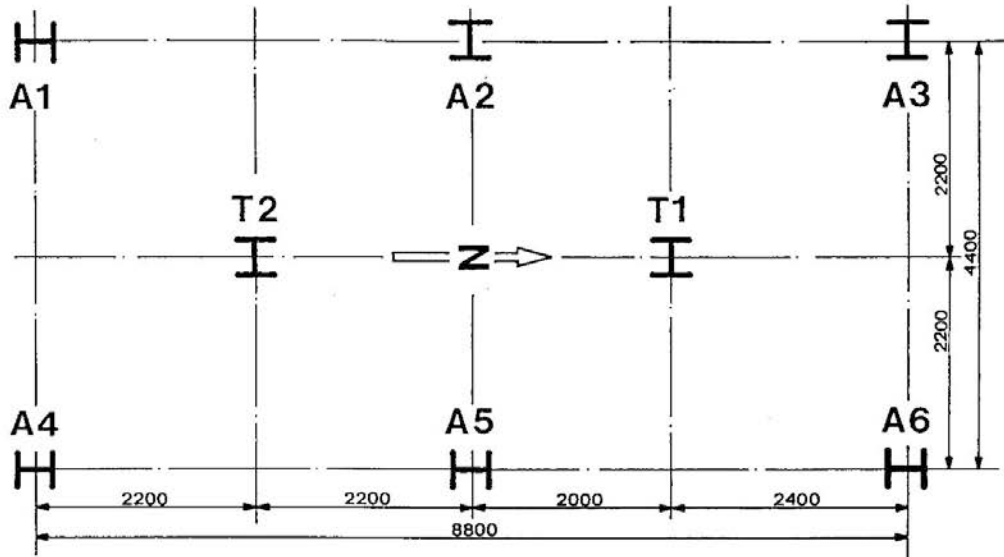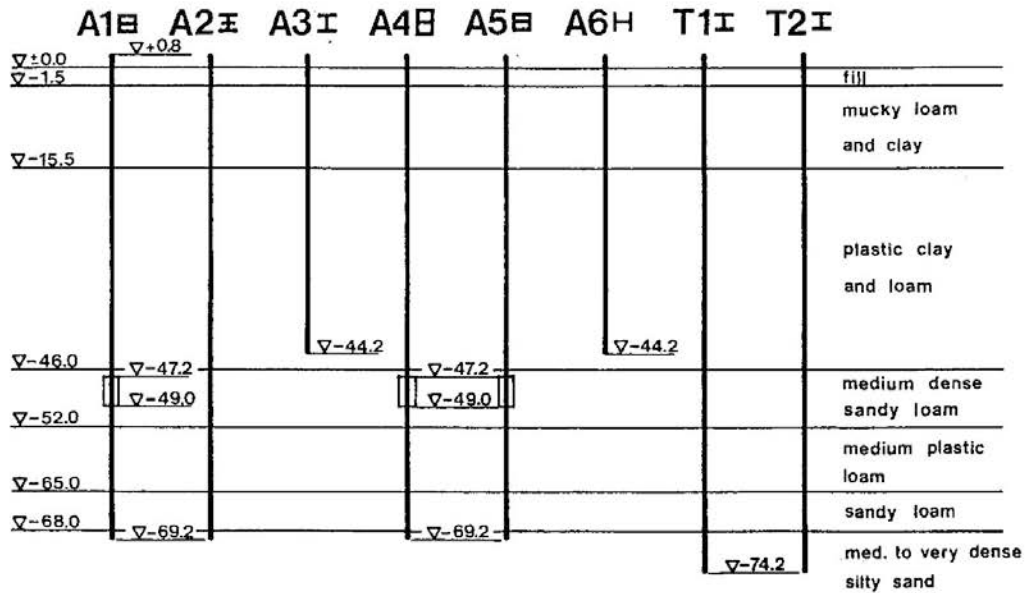**Figure 3 Pile arrangement at site**

Figure 4 Pile Levels and main soil layers

All pile sections: HP 360 x 410 x 176 in steel quality BS 4360 Gr. 50B

| steel plates 20mm | fillet welds 6mm | steel plates 20mm | fillet welds 8mm | channel 100x100 | fillet welds 10 mm |

Reinforcement of pile A4

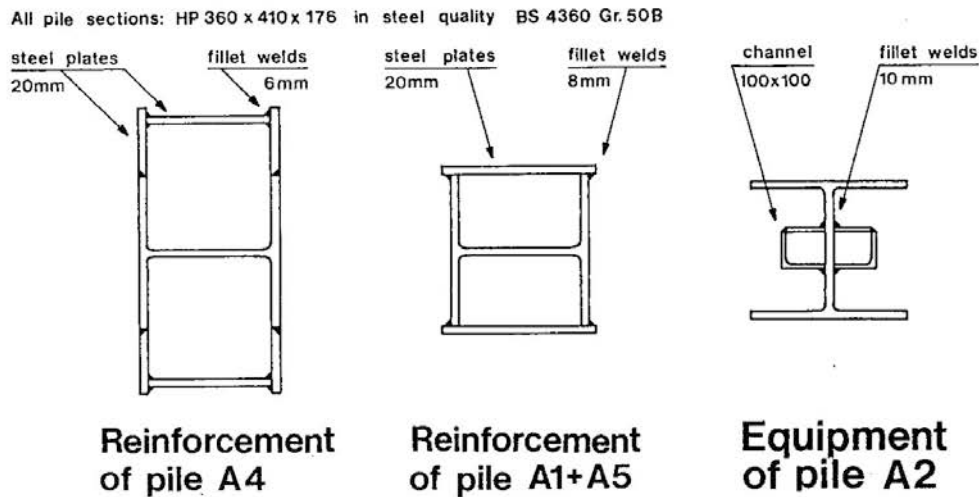Reinforcement of pile A1+A5

Equipment of pile A2

Figure 5 Details of reinforcement of piles A1, A2, A4, A5

The pile arrangement at site was done in such a manner that the loading installation can be attached to 4 reaction piles (see fig.3). The pile levels are shown on figure 4. The piles A1, 4, 5 were equipped with a special reinforcement between the depths of 47.2m and 49.2m in order to increase the bearing surface of the piles in the first sand layer, extending approx. between the depths of 46m and 52m. The pile A2 is equipped with 2 U-shapes, attached at both sides of the web. They will serve later for the vertically measurements of this pile. Details of the reinforcements are shown on figure 5.

Driving equipment

All piles were driven and restruck with a Kobe KB60 open end diesel hammer, provided by the Shanghai Foundation Engineering Corporation (SFEC). The weight of the piston is ≈60kN. At the maximum 2.67m stroke, this hammer is capable of developing an energy of ≈160kNm. The hammer cushion consists of wood, protected by a steel plate. The helmet consists mainly of a circular steel plate with 4 guiding elements for the H-section; the helmet is attached to the hammer by means of wire ropes. Only the hammer is guided by the lead; the pile is seized at the top by the helmet. At ground level there is a very weak attachment serving mainly for the vertical alignment of the first pile element prior to driving.

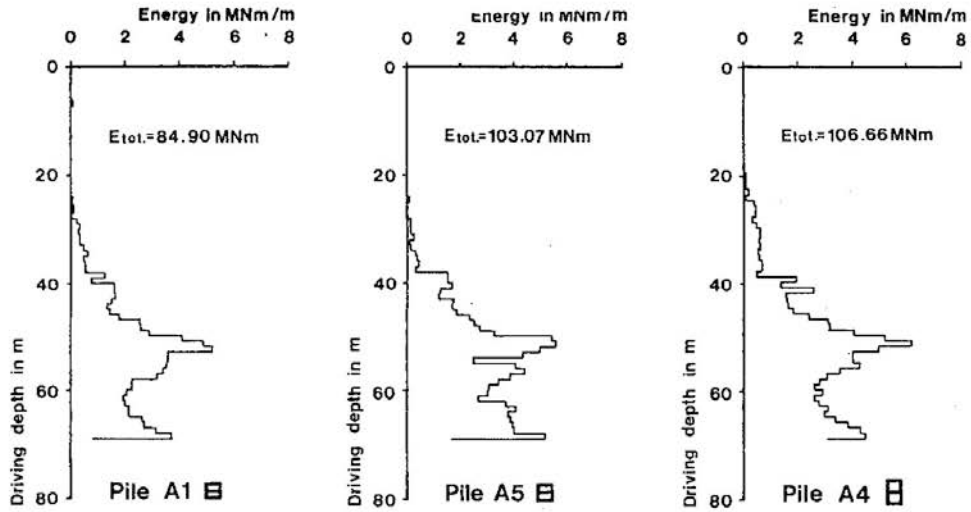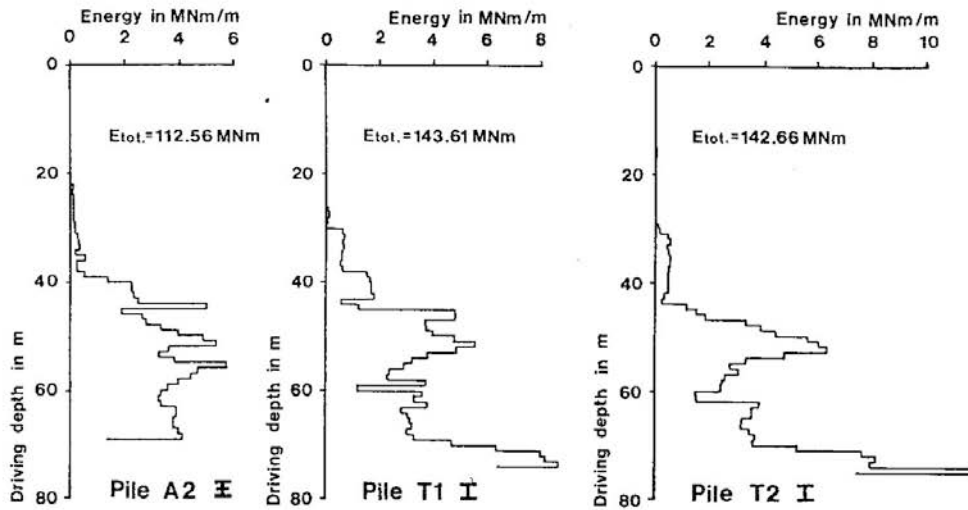**Figure 6 Diagram of delivered hammer energy versus depth**

Figure 7 Diagram of delivered hammer energy versus depth

90

Pile driving

All the piles were driven smoothly to the final depth. The driving was only interrupted by the pitching and welding operations of the individual pile segments.

Considering the diagrams of the developed hammer energy (°product of the number of blows and their corresponding stroke for a given penetration; see fig. 6/7), it can be seen in general that almost no driving energy was needed until the pile reached a depth of 20m. In fact, the pile was pushed into the ground by the hammer weight only. Down to a depth of 40m, the energy input was still very low; however, it started increasing from this level on to a first maximum at about 52m depth, corresponding to the full penetration of the pile tip into the upper sand layer. Below, the soil resistance drops again until a depth of ≈68m is reached, corresponding to the upper level of the compact sand layer. From here on, the driving resistance increased rapidly with depth. The 75m long test piles T1 and T2 penetrate approximately 7m into this second sand layer, showing that H-piles can be driven to the required grade without problems. The maximum blow count observed was 100 blows/m for pile T2 at the end of driving (EOD). No sign of pile buckling is observed.

The final position of the pile head is typically within 5cm of the theoretical position. Only the top of pile A5 displaced for over 20cm in the Y-direction of the section. This is mainly due to the absence of lateral support by the soil at the upper 10m. In fact, soil material had been extracted between the flanges of the first pile segment, when it had to be pulled out of the ground because of an incorrect installation sequence. A slight pile/hammer misalignment and the absence of a ground guide added to this displacement.

Approximately 40 hours after the initial driving, the piles A1, 4, 5 and T2 were restruck (BOR) for assessing the increase in bearing capacity by dynamic measurements.

DYNAMIC MEASUREMENTS

Testing procedure

During driving of the last pile segment and for restrike, two accelerometers and two strain transducers were bolted to the pile web approx. 0.8m from the top. The

signals were conditioned, amplified and calibrated by the Shanghai Municipal Institute of Architectural Design (SMIAD) pile driving analyzer as provided by Piling Development-Uppsala/Sweden (PiD).
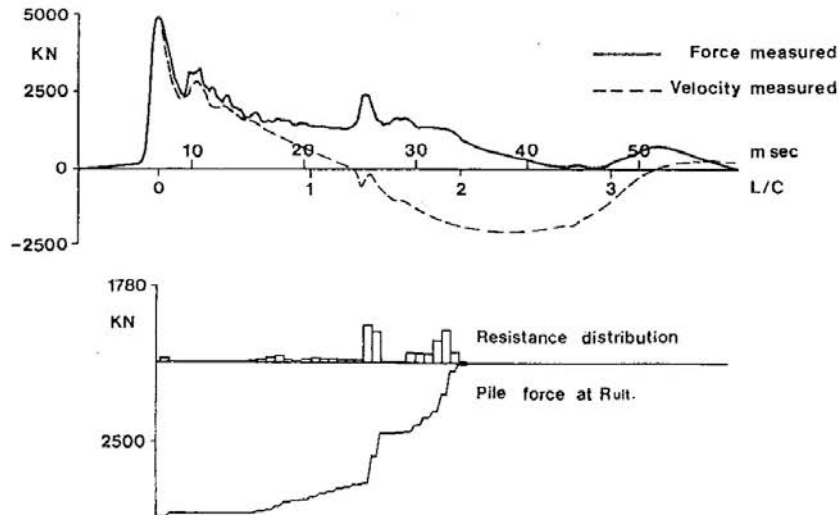

Figure 8 Dynamic force/velocity measurements and computed CAPWAP resistance distribution for pile A4 BOR blow No.3.

Laboratory processing

Data processing was accomplished by SMIAD, using the modified Case method, where different damping factors are applied to the toe and skin resistance. However, since the appropriate damping factors were unknown at the moment of testing, only a rough estimation in the bearing capacity prediction could be made. For more elaborate computations by the stress wave analysis program CAPWAP, SMIAD provided a diskette with EOD and BOR data of the piles A1, 4, 5, T1 (without BOR) and T2. These data were converted by the Swedish Geotechnical Institute for use with the CAPWAP program at ARBED.

Typical force/velocity curves of the piles A4 BOR and T2 BOR are shown in figures 8 and 9. The influence of the reinforcement on the dynamic record of pile A4 can be easily seen at the time 1.35L/C on figure 8. The reflection of the toe of pile T2 is visible at the time 2L/C in figure 9. In addition to these curves, the computed CAPWAP soil resistance distributions of the two piles are shown on figures 8/9.

92

Results of the dynamic measurements and computations: Hammer performance

The max. observed stroke for the KB 60 hammer was $\simeq 2.13$m, corresponding to a maximum potential energy of 128kNm (pile T2-E0D2). The maximum measured energy actually transferred to the pile top was 93.5kNm. From table 1, it can be seen that the energy transfer efficiency (see column "eff.") varies between 39.9% and 65.5%; these values may be considered as a good result.

Pile behavior during driving

The maximum measured dynamic pile force was 5049kN (pile A4-EOD), corresponding to a max. stress of 225Mpa. It has to be noted that this max. stress is due to the locally concentrated mass and resistance at the reinforcement, the down travelling input wave reflects and starts an upward travelling compression wave. The superposition of these upward and downward waves produces the stress concentration just above the reinforcement. The ratio of force just above the reinforcement to the measured pile top force was as high as 5049:4494 or 1.12:1.

The maximum dynamic stresses ranged typically at this site between 152-225MPa, which is well below the yield point of 345Mpa for a grade 50B steel. The maximum stress of the bare pile at EOD was 203MPa (T1-EOD2 at 74.2m depth).

Considering the force and velocity diagrams versus time, no abnormal reflections from the pile splices can be detected. This is to say that the full penetration welds behave well and without failure during the whole driving process. No additional steel plates were used to stiffen the splices; skillful workers are however required to execute good quality welds.

Pile bearing capacity from dynamic measurements

The bearing capacities of the dynamically tested piles were determined using the Case and CAPWAP methods (ARBED) and the modified Case method (SMIAD). The computation result of the 3 methods are shown in table 1. Of course, all capacities given in this table are indicative of their amount only at the time of testing, i.e. end of driving and $\simeq 40$ hours after driving. Additional wait time causes further capacity increase and maybe also changes in the resistance distribution. Details of the computed resistance distributions at EOD and BOR are shown on figure 10.

Table 1: Summary Table of Dynamic Measurements and Computations

pile data set	blow count EOD (bl/m)	stroke (m)	Er (kNm)	Et (kNm)	eff. (%)	top force (kN)	max. pile force (kN)	max. dyn. str. (MPa)	J=.0 (kN)	J=.4 (kN)	J=.5 (kN)	J=.6 (kN)	J=.7 (kN)	J=.8 (kN)	skin (kN)	toe (kN)	tot. (kN)	Jc	SMTAD Case result J1=.15 J2=.45 (kN)
A1-EOD-69.2m	32	1.95	117.0	65.9	56.3	3438	3625	162	3660	2301	1961	1622	1282	942	1286	62	1348	0.68	1400
A1-EOD-69.2m				61.5		3670	3709	166	4652	3565	3294	3022	2750	2479	2904	15	2919	0.64	2260
A4-EOD-69.2m	39	2.01	120.6	77.2	64.0	4494	5049	225	5324	3824	3449	3074	2699	2325	2340	13	2353	0.79	2500
A4-EOD-69.2m				93.5		4833	4851	217	6449	5067	4722	4376	4031	3685	4899	15	4914	0.45	2580
A5-EOD-69.2m	48	1.83	109.8	43.8	39.9	3259	3413	152	3484	2203	1883	1563	1243	923	1377	4	1381	0.66	1730
A5-BOR-69.2m				64.4		3942	3909	175	5020	3922	3648	3374	3099	2825	3503	50	3553	0.53	2030
T1-EOD1	100	2.13	127.8	65.4	65.5	4121	4121	184	4185	3799	3414	2643	1872	1101	3073	6	3079	0.42	2000
T1-EOD2-74.2m				83.7		4499	4541	203	4811	3147	2731	2315	1899	1483					
T2-EOD2	100	2.04	122.5	53.0	52.7	3388	3517	157	3445	3132	2820	2195	1570	945	2973	10	2983	0.48	2180
T2-EOD2-74.2m		1.86	111.6	64.6	65.1	4139	4029	185	4581	3252	2920	2588	2256	1924	4440	45	4485	0.38	2470
T2-BOR-74.2m				72.7		4254	4457	199	5625	4415	4112	3809	3507	3204					
A2-EOD-69.2m	37	1.92	115.2																
A3-EOD-44.2m	26	0.98	58.8																
A6-EOD-44.2m	34	/	/																

Notes: - E_r = delivered energy by the hammer
- E_t = transferred energy to the pile
- blow count and stroke values are given at EOD/BOR
- eff. = $(E_t/E_r)100$ = energy transfer efficiency of the driving system
- for the blows where CAPWAP has been performed, the values in the column "max pile force" are CAPWAP values
- elapsed time between EOD and BOR for pile A1 = 38 hours, A4 = 43 hours, A5 = 37 hours, T2 = 40 hours
- the values of the Jc column indicate the damping factor to be introduced in the Case method in order to get the CAPWAP capacities

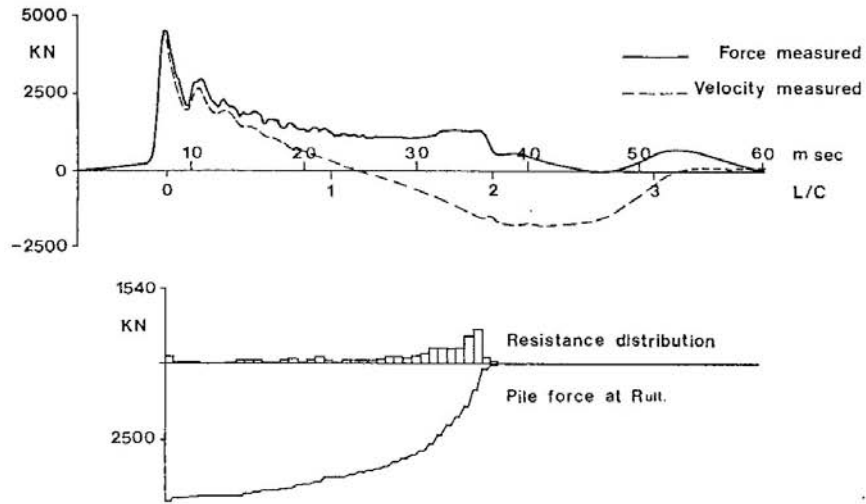**Figure 9** Dynamic force/velocity measurements and
computed CAPWAP resistance distribution for pile T2 BOR blow No.3.

Figure 10 Resistance distribution at EOD and BOR from CAPWAP computations.

INFLUENCE OF TIME ON BEARING CAPACITY

It is well known that bearing capacity increases with time in the Shanghai area. For the dynamically tested piles, a restrike was performed 37-43 hours after initial driving. The magnitude of set-up of the piles A1, 4, 5 and T2 can be seen for the different layers in figure 9. The first considered layer extends from ground level to the upper sand layer at approx. 46m depth, the second layer between 46m and 52m, the third between 52m and 66m and the fourth below 66m. These depths do not correspond exactly to the levels shown on figure 1; they are however in agreement with the pile element lengths from the CAPWAP computations. The average increase in friction resistance after approx. 40 hours of wait in the 4 layers is as follows, beginning at the ground level:

$$\text{layer } 1 = + \ \ 62\%$$
$$\text{layer } 2 = + \ \ 73\%$$
$$\text{layer } 3 = +206\%$$
$$\text{layer } 4 = + \ \ 12\%$$

It seems incorrect to consider an average set-up of the four piles A1, 4, 5 and T2 in layer 4, since the penetration in this layer is different for the T- and A-piles. We assume that the set-up of pile T2 (penetration of 8.2m in layer 4) gives the most probable value of $\simeq +12\%$ increase in bearing capacity after a wait time of 40 hours.

One may also argue that the average value of set-up in layer 1 is not correct since here, the soil is not disturbed during driving of pile T2, whereas it is for the A-piles due to the passage of the reinforcement through this layer. However, there is no uniform trend of set-up among the reinforced piles. It is obvious that, because of the lagging, the A-piles show at EOD less resistance in layer 1 than the T-piles. In spite of that fact, pile A4 with the largest lagging shows, in layer 1 and at BOR, approximately the same resistance as the unreinforced pile T2.

STATIC LOADING TESTS

Loading procedures

The static compression tests were performed following two different procedures, both in accordance with the Chinese code of practice.

96

* The quick loading procedure for the vertical test of pile T2 was as follows:
  - the load is applied in increments of 10% of the maximum expected load of 6000kN (=600kN increments)
  - the load is released in decrements of 2 times the applied load increments (=1200kN decrements)
  - the readings are taken at 0', 5', 10', 15', 30', 45', 60', after the application of each load increment and 0', 15', 30', after the removal of each load decrement
  - after the load is decreased to zero tons, final readings are taken after 0', 30', 60', 90' and 120'.

* The slow loading procedure for the test of pile T1 was as follows:
  - the load is applied in increments of 500kN up to 200% of the design load
  - the load is released in decrements of 2 times the applied load increments (=1000kN decrements)
  - the readings are taken at the same intervals as for pile T2 during the first hour and at every half hour thereafter until the rate of settlement is not greater than 0.05mm per half an hour for each loading increment.
  - the readings are taken at 0', 15', 30', 60' after the removal of each load decrement
  - after the load is decreased to zero tons, final readings are taken every half an hour up to 3 hours.

The horizontal loading procedures are carried out according to the ASTM standard D3966-81.

Vertical loading test results

Using the SFEC loading installation, the pile T2 was tested 32 days after EOD and the pile T1 was tested 40 days after EOD.

Following the original test program, the pile T1 was to be loaded to twice the working load (2×2300kN) and the pile T2 to failure. As can be seen on figure 11, the maximum test load for pile T1 was 4750kN; the time/settlment curves show no sign of failure after maintaining the max. load for 90 minutes. After unloading, the permanent settlement at the pile head was 5.3 mm versus a temporary settlement of 52.7mm under the maximum load; the difference is due to elastic shortening of the pile. For pile T2, the static test was stopped at a load of 6000kN, because some reaction piles were pulled out for ≈17mm. Although this value is quite normal and not at all critical for piles of such length, the Chinese code of practice is to stop the test when a given amount of displacement is reached by the reaction piles.
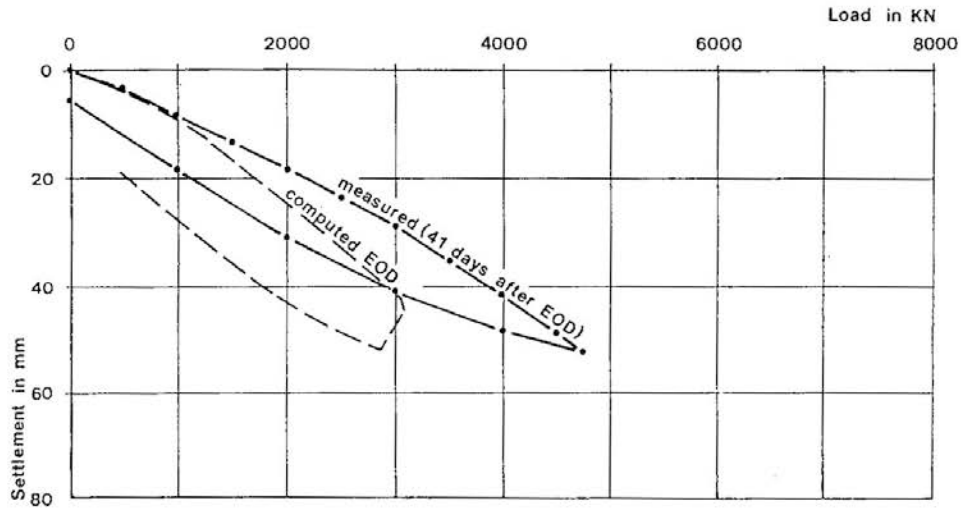
97

**Figure 11 Comparison between measured load/settlement behaviour of pile T1
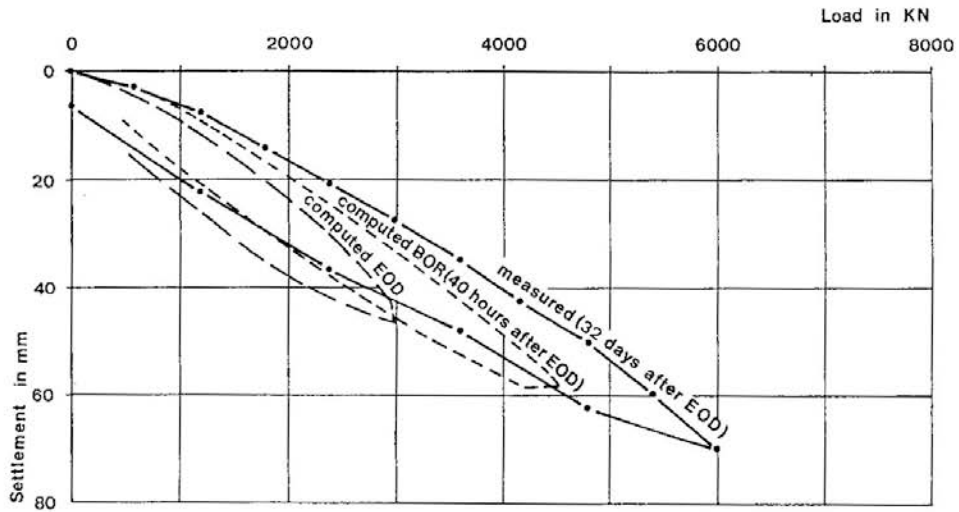and the computed load/settlement curve at EOD (CAPWAP).**

**Figure 12 Comparison between measured load/settlement behaviour of pile T2
and the computed load/settlement curves at EOD and BOR (CAPWAP).**
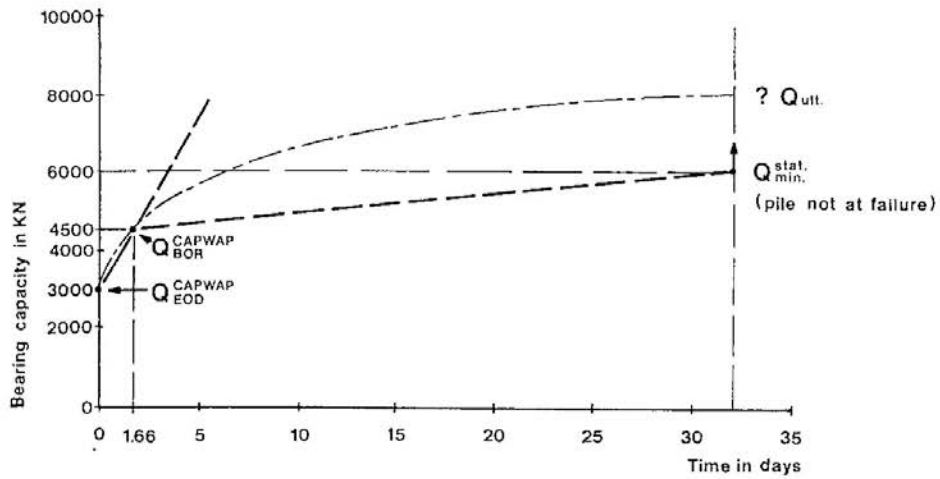
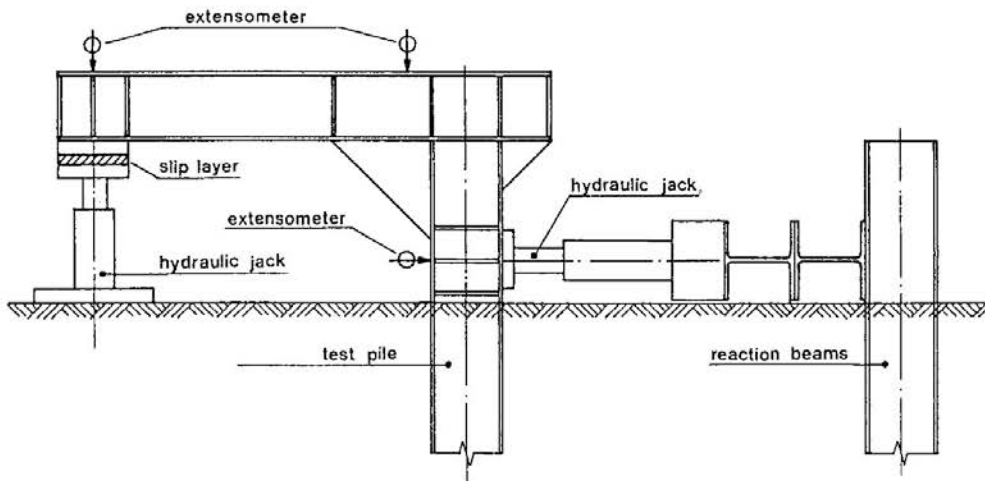**Figure 13 Variation of bearing capacity with time for pile T2.**

Figure 14 Horizontal loading installation. (not to scale)

As for pile T1, no sign of failure was seen in the time/settlement diagram and on the load/settlement diagram on figure 12; it can be stated that the long term static resistance of pile T2 is well above 6000kN. The permanent settlement at the pile head was 6.1mm versus a max. temporary settlement of 70.4mm under the final load.

Considering figure 13, the time dependent evolution of the bearing capacity was ≃3000kN at EOD (CAPWAP), ≃4500kN after 40 hours (CAPWAP) and >6000kN after a one month wait (static test after 32 days).

For comparison purposes, the calculated load/settlement curves at EOD for pile T1 and at EOD/BOR for pile T2 are plotted against the measured ones on figure 12. The effect of set-up is clearly visible here; however, the wait time of 40 hours is too short to get an idea about the permanent bearing capacity by the dynamic measurements. A restrike with dynamic measurements at the beginning of the main driving works will give precious information about the amount of permanent set-up in the different soil layers.

Horizontal loading test results

The horizontal tests have been performed with a fixed pile head, one on pile T1 against the X-axis and one on pile T2 against the Y-axis of the H-section. The typical arrangement is shown on figure 14.

Both tests are performed approx. one week after the execution of the compression tests.

The load/displacement diagrams for the horizontal loading tests are given in figure 15. The applied load is somewhat higher than twice the working load in order to consider the friction within the supporting system of the loading installation.

For the max. applied load of ≃87kN, the top displacement was 36.44mm for pile T2 (Y-axis) and 20.95mm for pile T1 (X-axis). For both piles, no obvious soil rupture occured; the pile head displacements are within the acceptable range determined by the Chinese Building Authorites.
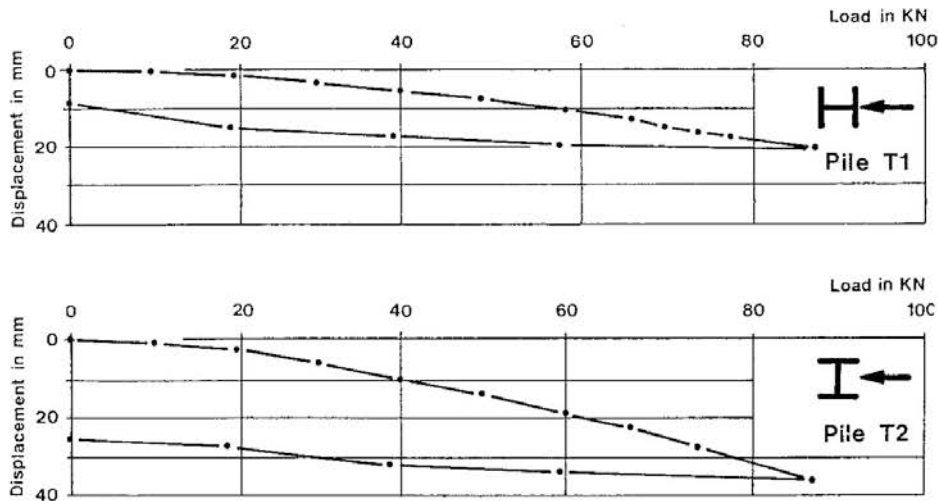
Figure 15 Load/displacement curves for horizontal tests of piles T1 and T2.

CONCLUSIONS OF THE DRIVING TESTS

By executing these tests, the following conclusions can be drawn:

- no pile buckling has been experienced during driving and loading of the HP 360×410×176 sections in the soil conditions at Shanghai
- the H-piles can be easily driven to the compact sand layer at 60-70m depth
- the splicing has no observable influence on the pile behavior
- the driving resistances are much lower than the final rupture load
- the amount of set-up is very important, especially in the soil layer between the depths of 52m and 68m
- the computed amount of point resistance is very small for all piles (CAPWAP)
- the failure load of the 75m long H-piles is well above twice the vertical working load; the real rupture load cannot be determined at this moment since the static test stopped at a load of 6000kN without any sign of failure and since the dynamic measurements have been performed too quickly after initial driving.
- the horizontal displacements of the pile top at twice the working load are within the acceptable range

101

RELATION BETWEEN PEAK DRIVING FORCE AND THE BEARING CAPACITY OF DRIVEN PILES

Y K Chow[1], C L Yu[2], K Y Wong[3] and S L Lee[4]

INTRODUCTION

The bearing capacity of driven piles is commonly evaluated using static and/or dynamic formulae. The static formula is generally used to estimate the approximate penetration depth of the pile while the dynamic or pile driving formula is used to establish driving criteria for construction control. Hence, the bearing capacity of piles in the field is generally determined by pile driving formula, the most popular in Singapore being Hiley's formula. The popularity of the pile driving formula is due to its simplicity, but the penalty for such a simplification is that the results are often unreliable. This inconsistency can be traced to the incorrect assumption of rigid body dynamics in the formulation.

The need to correctly simulate the propagation of the stress wave in the pile during driving has led to the development of one-dimensional wave equation models (Smith, 1960; Lee et al., 1988). If the driving system can be reasonably modelled, the wave equation method can give a reliable prediction of pile capacities using set measurements (Forehand & Reese, 1964; Chow et al., 1988a).

Developments in electronics technology in the last decade or so have made it possible to make reliable measurements of the stress wave in the pile during driving. These measurements essentially remove the uncertainty associated with the driving system. The stress-wave matching method (Goble et al., 1975; Chow et al., 1988b) and the Case-method (Goble et al., 1975), using these stress-wave measurements, have been successfully used to predict the bearing capacity of piles. The stress-wave matching technique is not suitable for field application since it requires repeated analyses using a wave equation computer program. The main assumption in the Case-method is that soil damping is concentrated at the pile toe. Recommendations on the choice of damping factor in some soil conditions are reported by Goble et al. (1975). If this damping factor can be correlated with the pile capacity from a load test

---

[1]Senior Lecturer, Department of Civil Engineering, National University of Singapore, Singapore.

[2]Manager, Dynamic Pile Testing Division, Maunsell Consultants (M) Sdn. Bhd, Malaysia.

[3]Executive Engineer, L & M Geotechnic Pte Ltd, Singapore.

[4]Professor, Department of Civil Engineering, National University of Singapore, Singapore.

or from the stress-wave matching method, the predictions of pile capacities at similar sites are more reliable.

Thompson & Thompson (1978) showed that for piles driven to practical refusal bearing in very dense granular soil and shale bedrock in Ontario, Canada, it is possible to correlate the bearing capacity of piles with the peak driving force determined from dynamic measurements. Since pile behaviour depends to a considerable extent on local soil conditions, a relation between the peak driving force and the bearing capacity of piles, if found also to be applicable to driven piles in Singapore, can form a useful basis for estblishing driving criteria for the determinaton of pile capacity in the field. This peak driving force obtained from strain measurements is not dependent of further assumptions.

FIELD RESULTS

A total of 63 driven piles, which were dynamically tested, were examined in this study. The types of piles include: precast reinforced concrete piles, prestressed concrete pipe piles, steel H piles and steel pipe piles. The penetration depths of piles varied between 11 m and 54 m. The piles were all driven to practical refusal, generally taken to be a set of less than 25 mm per 10 blows. Measurements of strains and accelerations near the pile heads during driving were carried out using a Pile Driving Analyser (PDA). The force- and velocity-time histories, which were obtained from these measurements, were used to estimate the bearing capacity of the piles using the Case-method. In addition to the Case-method, the capacities of 34 of the piles were also estimated using the stress-wave matching method using the CAPWAP computer program (Goble et al., 1975).

The driving system comprising the ram, capblock, pile cap and pile cushion (for concrete piles) would influence the shape of the stress wave (i.e. impact force-time history). In Singapore piling practice, the capblock and pile cushion are generally of plywood material. Hydraulic hammers in Singapore are generally single-acting. In principle, the operation of single-acting hammers and that of drop hammers is somewhat similar, differing only in the lifting mechanism of the ram. Hence, the stress wave in piles driven with either type of hammer would be expected to be of similar shape. The driving mechanism of diesel hammers is different.

Figure 1 shows some typical soil profiles in which the piles were installed. The piles were generally driven through less competent ground then to bearing in a hard stratum; this is a common feature of driven pile design in Singapore.
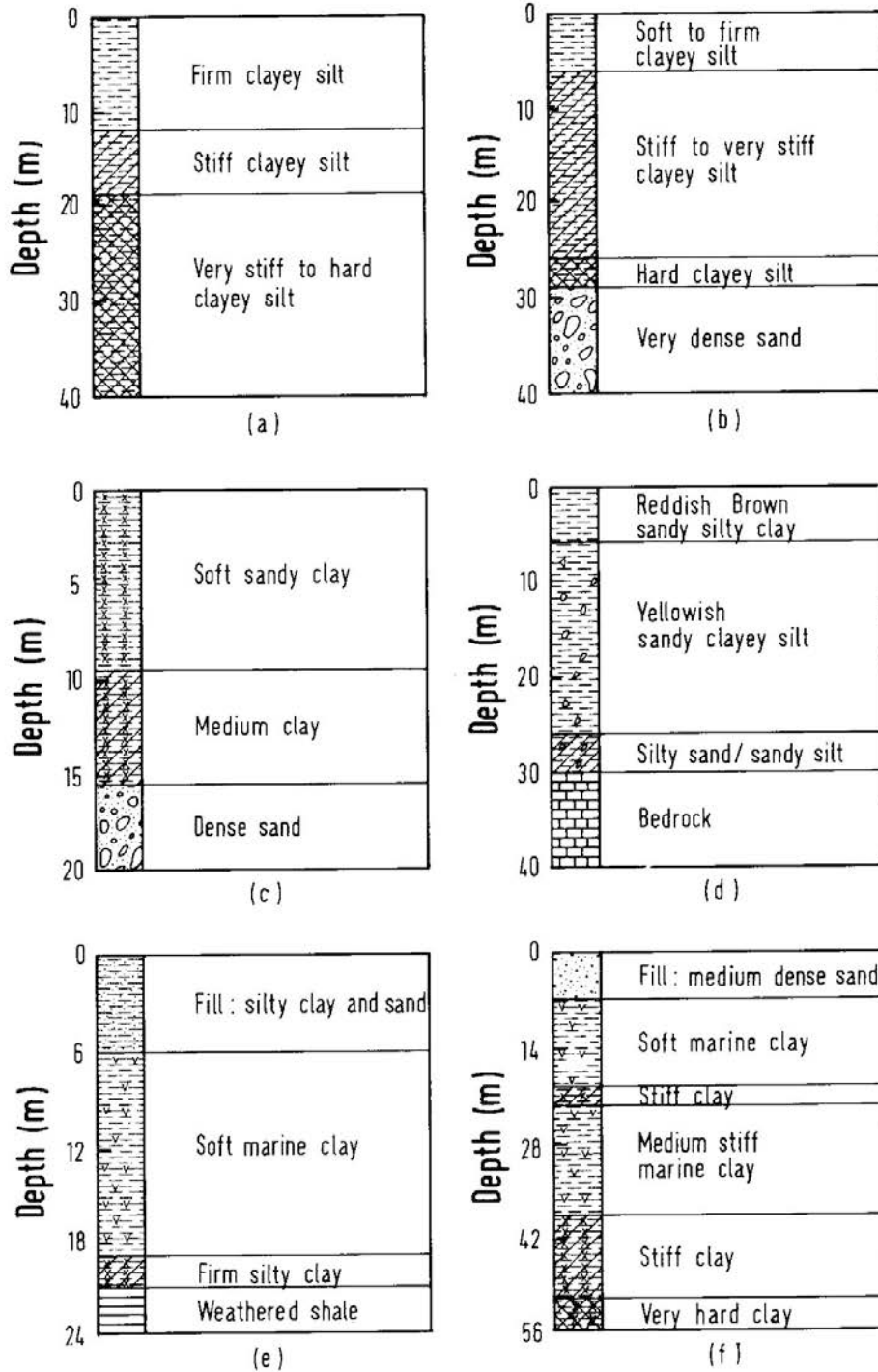
104

Fig. 1. Some typical soil profiles

The predicted capacities of the 34 piles using the CAPWAP computer program are plotted against the respective peak impact forces in Fig. 2. For the given data, the influence of the pile type (steel or concrete piles) and hammer type (diesel, hydraulic or drop hammers) does not appear to be significant. Statistical analysis was performed on the data as a single group. The mean of the ratio of the peak driving force (F_p) to the CAPWAP pile capacity (Q_a), and the standard deviaton of this ratio are tabulated in Table 1. It can be seen that this ratio is close to unity with a standard deviation of 0.18. The mean line relating the CAPWAP pile capacity to the peak impact force is given by

$$Q_a = 1.04 F_p \tag{1}$$

This is also shown in Fig. 2. If the relationship in Eqn(1) is applied to the values of F_p, then the statistical analysis yields a mean of unity with a standard deviation of 0.19 as tabulated in Table 1.

The Case-method pile capacities for all 63 piles are plotted against the respective peak driving forces in Fig. 3. Again, the influence of the pile type and hammer type does not appear to be significant. It may be noted that in these cases, the Case damping factors have been calibrated with results from CAPWAP analyses and also with previous experience in similar soil conditions. The mean of the ratio of the peak driving force (F_p) to the Case-method pile capacity (Q_c), and the standard deviation of this ratio are given in Table 2. The mean of F_p/Q_c is close to unity with a standard deviation of 0.14. The mean line is given by

$$Q_c = 1.07 F_p \tag{2}$$

This is also shown in Fig. 3. Applying this relationship in Eqn (2) to the measured peak driving forces (F_p) gives a mean of unity and a standard deviationof 0.15 as tabulated in Table 2. This scatter is at least comparable to the scatter obtained comparing the Case predictions to the measured pile capacities.

CONCLUSIONS

For piles driven to practical refusal, generally taken to be a set of less than 25mm per 10 blows, in soil conditions similar to those examined in this study, it is possible
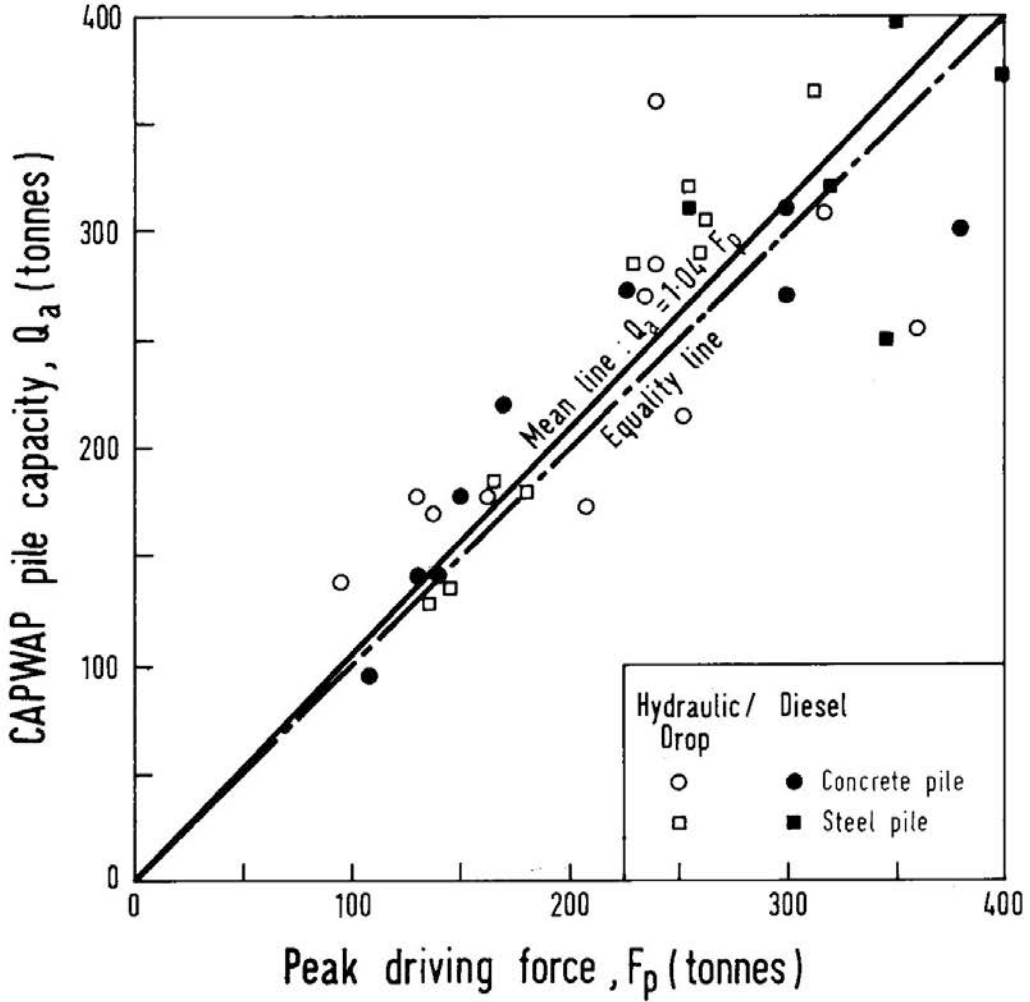
106

Fig. 2. Relation between CAPWAP pile capacity and peak driving force

Table 1. Relation between peak driving force (F_p) and CAPWAP pile capacity (Q_a)

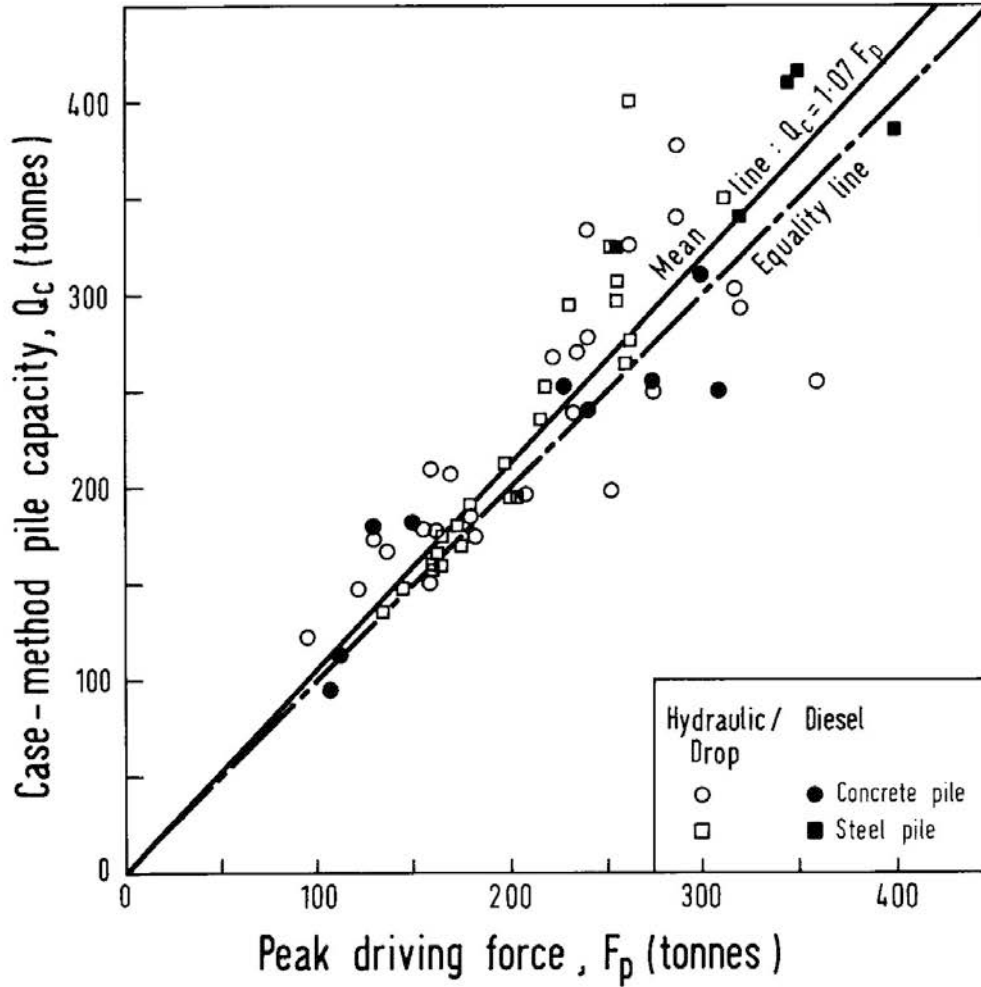|	Mean	Standard Deviation
F_p/Q_a	0.96	0.18
$1.04\,F_p/Q_a$	1.00	0.19

Fig. 3. Relation between Case-method pile capacity and peak driving force

Table 2. Relation between peak driving force (F_p) and Case-method pile capacity (Q_c)

	Mean	Standard deviation
F_p/Q_c	0.94	0.14
$1.07\,F_p/Q_c$	1.00	0.15

to relate the measured peak driving force to the bearing capacity of piles determined by the stress-wave matching method or the Case-method. Hence, the peak driving force may be used to estimate the bearing capacity of piles in the field under similar conditions. It is noted that this peak impact force is obtained directly from strain measurements near the pile head whereas the accuracy of the Case-method depends on a reliable estimate of the Case damping factor. It is necessary, however, to ensure that the peak driving stresses are within the permissible material stresses of the piles.

REFERENCES

CHOW, Y.K., KARUNARATNE, G.P., WONG, K.Y. & LEE, S.L. (1988a). "Prediction of load-carrying capacity of driven piles", *Canadian Geotechnical Journal*, Vol.25, No.1, 13-23.

CHOW, Y.K., WONG, K.Y., KARUNARATNE, G.P. & LEE, S.L. (1988b). "Prediction of pile capacity from stress-wave measurements: some numerical aspects", *International Journal for Numerical and Analytical Methods in Geomechanics*, Vol.12, No.4, 505-512.

FOREHAND, P.W. & REESE, J.L. (1964). "Prediction of pile capacity by the wave equation", *Journal of the Soil Mechanics and Foundations Division, ASCE*, Vol.90, No.SM2, 1-25.

GOBLE, G.G., LIKINS, G.E. & RAUSHE, F. (1975). *"Bearing capacity of piles from dynamic measurements"*, Final Report, Department of Civil Engineering, Case western Reserve University, Cleveland, OH.

LEE, S.L., CHOW, Y.K., KARUNARATNE, G.P. & WONG, K.Y. (1988). "Rational wave equation model for pile-driving analysis", *Journal of Geotechnical Engineering, ASCE*, Vol.114, No.3, 306-325.

SMITH, E.A.L. (1960). "Pile driving analysis by the wave equation", *Journal of Soil Mechanics and Foundations Division, ASCE*, Vol.86, No.4, 35-61.

THOMPSON, C.D. & THOMPSON, D.E. (1978). "Influence of driving stresses on the development of high pile capacities", *In Behavior of Deep Foundations*, ASTM STP670, 562-577.

DEFORMATION CHARACTERISTICS OF BANGKOK CLAY UNDER THREE DIMENSIONAL STRESS CONDITIONS

Jiro Kuwano* and Binaya Nath Bhattarai**

SYNOPSIS

A series of drained tests was carried out on soft Bangkok clay by using a true triaxial apparatus. The clay specimens were sheared along different radial stress paths on the octahedral plane to study anisotropic deformation characteristics of Bangkok clay. A significant role of the intermediate principal stress in the deformation characteristics of Bangkok clay was observed. With the increasing magnitude of b-value the stress-strain relationship became steeper, volumetric strain decreased and the strength increased. The angle of internal friction was lowest in the triaxial compression condition. The test results also showed the anisotropic deformation characteristics of Bangkok clay. The clay was found to be more deformable in the vertical direction than in the horizontal directions.

INTRODUCTION

The deformation characteristics of soils obtained from a conventional triaxial test pertain to axi-symmetrical conditions in which the intermediate principal stress equals the minor or major principal stress. The present design procedure is usually based on the data of this testing technique. In general, however, stress and strain conditions either equal a plain strain or conform to a general state with triaxial compression and extension as limits. Therefore, it is of fundamental interest to investigate the strength and deformation characteristics of soils for the whole range of stress states when the intermediate principal stress increases from the minor to the major principal stress.

The behaviour of sandy soils subjected to three dimensional stress conditions have been extensively studied by using true triaxial apparatus by investigators, e.g. Ko & Scott (1967), Lade & Duncan (1973) and Yamada & Ishihara (1979). The anisotropic deformability of sand specimens showed that the compressibility was lower in the direction of specimen deposition than in the direction perpendicular to

---

*Asst. Prof. and **graduate student, AIT Bangkok

it. It was also observed that the effect of inherent anisotropy in the sand specimen disappeared as the stress ratio became large to cause failure. The relative magnitude of the intermediate principal stress affected to some extent the deformations and the shear strengths. The failure surfaces shown on octahedral planes in the principal stress space were curved and circumscribed the Mohr-Coulomb failure surface. The plane strain condition was accompanied by a frictional angle which was larger than that obtained from the triaxial compression test. Similar studies were made on clays by Shibata & Karube (1965), Vaid & Campanella (1974), Nagaraj & Somashekar (1977), Lade & Musante (1978) and Lee et al. (1988). However, only a limited number of investigations have been performed on the behavior of undisturbed clays under three dimensional stress conditions especially on Bangkok clay. Therefore, this study aims to investigate the deformation and strength characteristics of the soft Bangkok clay under generalized stress conditions by using a true triaxial apparatus.

CUBICAL TRIAXIAL APPARATUS

The test apparatus used in this study was a true triaxial apparatus which permitted three principal stresses to be applied independently by means of three pairs of rubber pressure bags to a cubical specimen of 10cm×10cm×10cm. It is the same type of apparatus as that used by Yamada & Ishihara (1979). A vertical cross section is shown in Fig.1. The specimen is held in the cubical space formed by assembling six wall units face to face around the spacing frame.

Details of cross section of the top wall unit are shown in Fig.2. The wall unit has a pressure chamber enclosed by a rubber membrane at its front and covered by a rigid brass lid at the back having a inlet hole to supply water pressure. In the pressure chamber a perforated brass plate is placed just behind the rubber membrane. This brass plate can be displaced back and forth. After the sample preparation is completed, the brass plates are pulled back slightly as water pressure is applied in the chamber which supports the specimen thereafter. The stress is then applied to the specimen only through the flexible membranes.

In the top and bottom wall units, a small porous stone, 8mm in diameter, is centrally attached to the face of the rubber membrane to provide drainage. Behind the porous stone, brass tubing is installed, which is in turn connected to an electrical pressure transducer and a burette. The porous stone is designed so that it may move back and forth together with the surrounding rubber membrane. Three principal stresses can be controlled independently by connecting an air-water system to each

112

pair of pressure chambers. Each principal strain is measured by monitoring the amount of water flowing in and out of the pressure chamber using a volume change gauge.
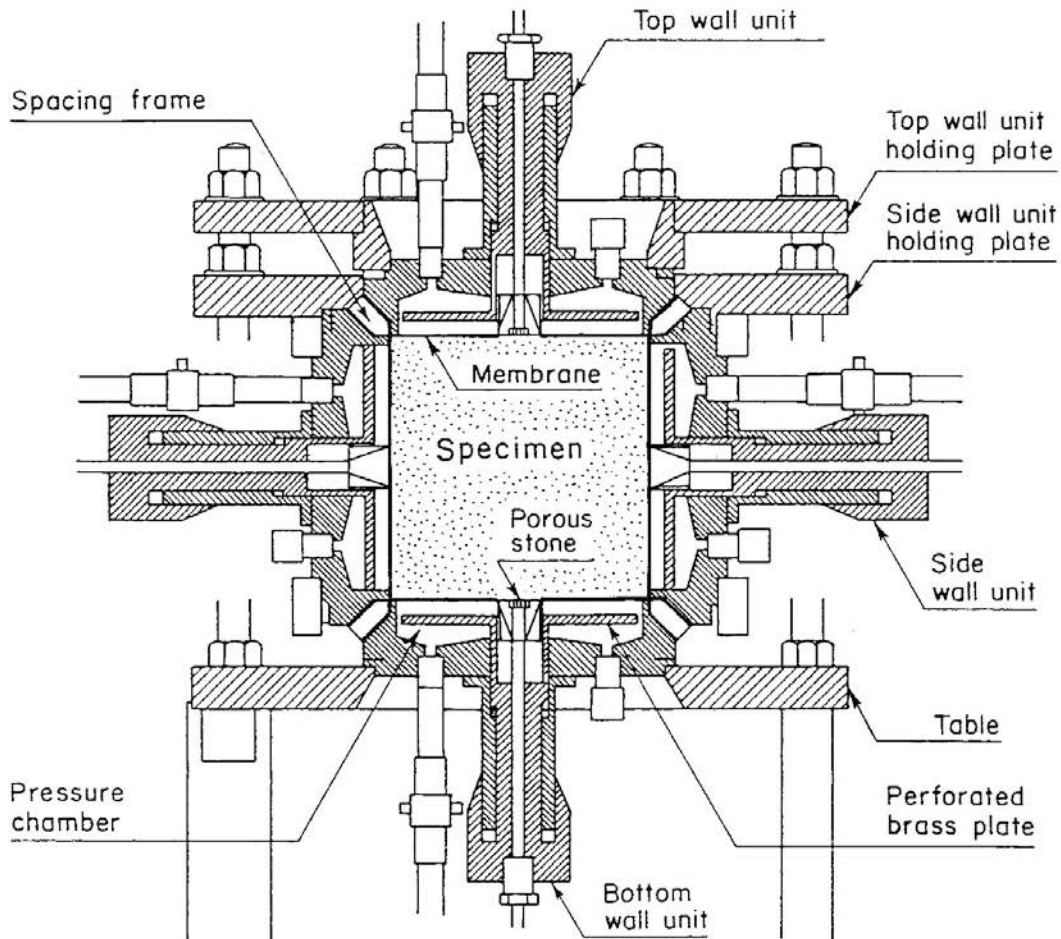

Fig.1 Cross section of the true triaxial cell (Yamada & Ishihara, 1979)

THREE DIMENSIONAL STRESS AND STRAIN SYSTEMS

In dealing with the three dimensional stress system the state of stress on an element can be conveniently expressed by the three principal stresses. A rectangular coordinate system in which σ'_z axis is vertical is selected as shown in Fig.3(a). In this coordinate system, the isotropic stress line defined by $\sigma'_x = \sigma'_y = \sigma'_z$ is called the space diagonal, and a plane normal to the space diagonal expressed by $\sigma'_x + \sigma'_y + \sigma'_z$ = const. is termed the octahedral plane. The three dimensional state of stress can be
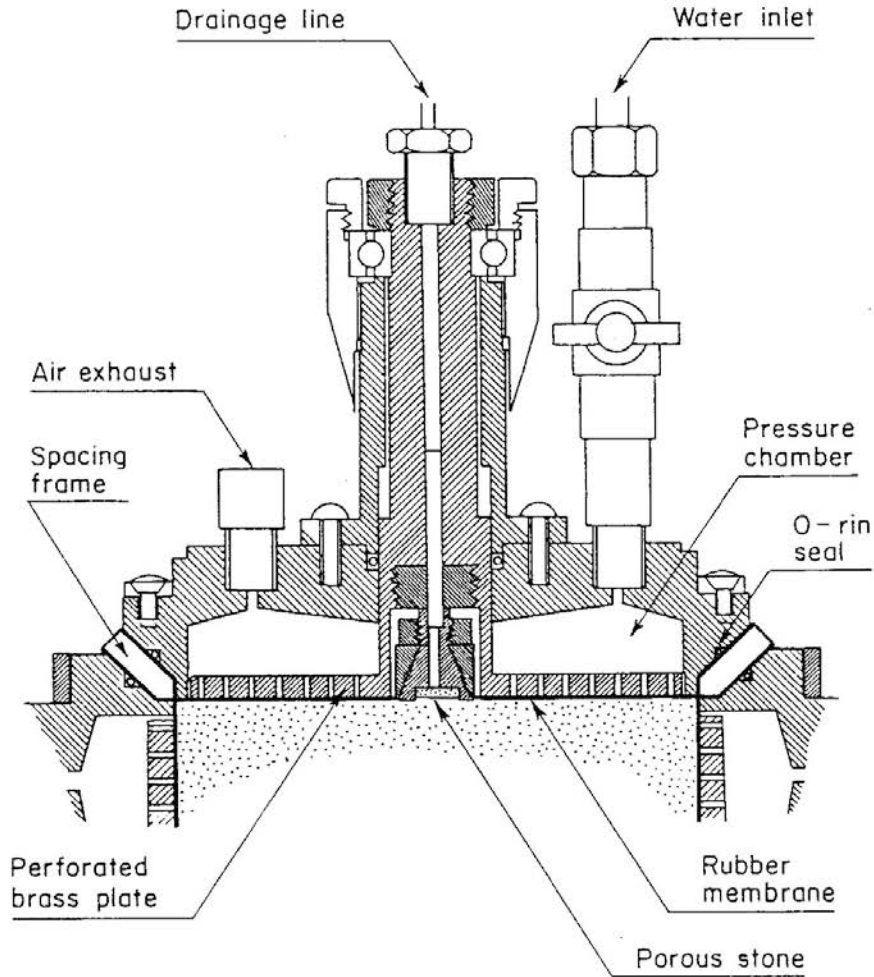
113

Fig.2   Details of cross section of the wall unit (Yamada & Ishihara, 1979)

converted into the normal and the tangential components of the stress acting on the octahedral plane. The normal component, p', and the tangential component, τ_{oct} are called the effective mean principal stress and octahedral shear stress respectively, and are given by the following equations.

$$p' = \frac{1}{3}(\sigma_x' + \sigma_y' + \sigma_z') \tag{1}$$

$$\tau_{\text{oct}} = \frac{1}{3}\sqrt{(\sigma_x' - \sigma_y')^2 + (\sigma_y' - \sigma_z')^2 + (\sigma_z' - \sigma_x')^2} \tag{2}$$

114

The quantities p' and $\tau_{ocт}$ are related to the length of the space diagonal from the origin to the octahedral plane, OO', and the length of $O'S$ respectively. Since the coordinates of the points O' and S are (p', p', p') and $(\sigma_x', \sigma_y', \sigma_z')$, the length of OO' and $O'S$ are

$$OO' = \sqrt{3}\, p' \tag{3}$$

$$O'S = \sqrt{3}\, \tau_{ocт} \tag{4}$$

The direction of shear stress on the octahedral plane is determined by a variable θ which is expressed as a function of principal stresses.

$$\tan \theta = \frac{\sqrt{3}\,(\sigma_y' - \sigma_x')}{2\sigma_z' - \sigma_x' - \sigma_y'} \tag{5}$$

The relative magnitude of the intermediate principal stress between the major and minor principal stresses is expressed by the parameter

$$b = \frac{\sigma_2' - \sigma_3'}{\sigma_1' - \sigma_3'} \tag{6}$$

The volumetric strain, v, and the octahedral shear strain, $\gamma_{ocт}'$ are defined as follows

$$v = \varepsilon_x + \varepsilon_y + \varepsilon_z \tag{7}$$

$$\gamma_{ocт} = \frac{2}{3}\sqrt{(\varepsilon_x - \varepsilon_y)^2 + (\varepsilon_y - \varepsilon_z)^2 + (\varepsilon_z - \varepsilon_x)^2} \tag{8}$$

where ε_x, ε_y and ε_z are principal strains in the X, Y and Z directions respectively.
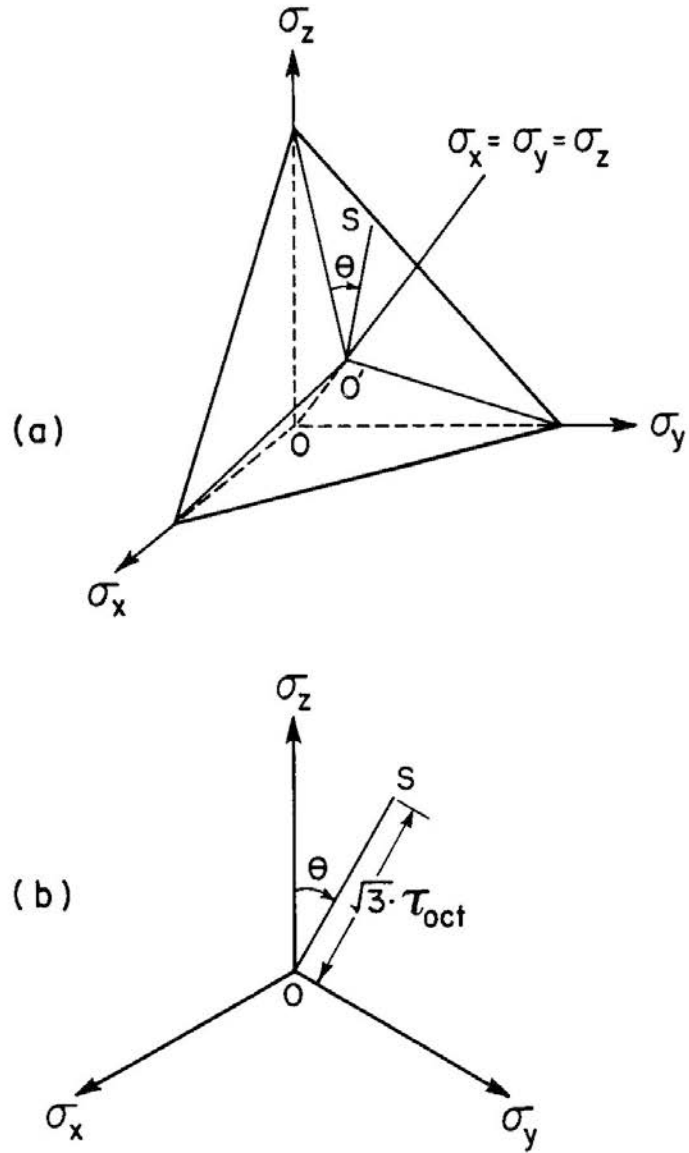
115

Fig.3   Representation of the octahedral plane

TEST SCHEME

In this investigation, all the specimens were first consolidated isotropically to an effective pressure of 98kPa and were then subjected to shear stresses along some straight stress path in radial directions on the octahedral plane as shown in Fig.4 while keeping the effective mean principal stress constant. The stress path is termed the radial shear stress path. Tests were performed for each of the radial stress paths on the octahedral plane at an angle interval of 15 degrees, though tests along the paths with θ equal to 135° and 165° could not be performed due to the limited number of samples. As illustrated in Fig.4, the radial shear stress path having a clockwise-angle of θ degrees is referred to as the RSθ° stress path.

Since the constant value of θ corresponds to the constant value of b, the radial stress paths have constant b-values. The RSθ° stress path having a b-value of 0 is similar to the conventional triaxial compression test and this path is called the ZC stress path. The RS 120° stress path has the same stress condition as the ZC test except that the major principal stress is oriented horizontally in the y direction. This test is called the YC test. The RS 180° stress path having a b-value of 1.0 is similar to the conventional triaxial extension test, in which the minor principal stress is applied vertically in the z direction and this path is called and ZE stress path. The RS 60° stress path is identical to the ZE test except that the direction of the minor principal stress path is changed from z to x. This type of test is called the XE test. The stress paths of RS 15°, RS 105° and RS 135° have b-values of 0.268. The only difference is that the directions of the major, the intermediate and the minor principal stresses are different. The RS 30°, RS 90° and RS 150° stress paths have b-values of 0.5. The RS 45°, RS 75° and RS 165° stress paths have b-values of 0.732.

SAMPLES

Samples used in this investigation were extracted using a thin-walled sampler of 254mm in diameter and 560mm in length from a depth of 3 to 3.5 meters at the western side of AIT campus in the suburb of Bangkok. The general soil properties of the clay are given in Table 1. As seen in the table the soft clay is highly plastic with a water content closer to the liquid limit. Because of the limited stress range in the true triaxial apparatus used in this study the soil specimens had to be consolidated at a stress level of 98 kPa. The samples, however, were normally consolidated, since the maximum past pressure was known to be 60.8 kPa from the oedometer test as shown in Fig.5.

Table 1. General properties of Bangkok Clay

General soil properties	
Natural water content, %	79
Plastic limit, %	28
Liquid limit, %	95
Plasticity index, %	67
Specific gravity	2.63
Total density, g/cm^3	1.534
Dry density, g/cm^3	0.857
Initial void ratio	2.07
Degree of saturation, %	100

RESULTS AND DISCUSSIONS

Soil samples were sheared along different radial stress paths on the octahedral plane with constant effective mean principal stress of 98 kPa. Measured values of the three principal strains, ε_x, ε_y and ε_z, obtained in the shear tests under drained conditions are plotted versus stress ratio, τ_{oct}/p', in Fig.6 through Fig.16.

In the ZC test the soil specimen was sheared by increasing the vertical principal stress while decreasing the two horizontal principal stresses by the same amount simultaneously. The tensile strains in both X and Y directions were almost identical as shown in Fig.6. It shows that the sample deformed isotropically in the two horizontal directions. Similar isotropic deformation properties in the two horizontal directions were also obtained for loose sands by Yamada & Ishihara (1979) using the similar type of apparatus.
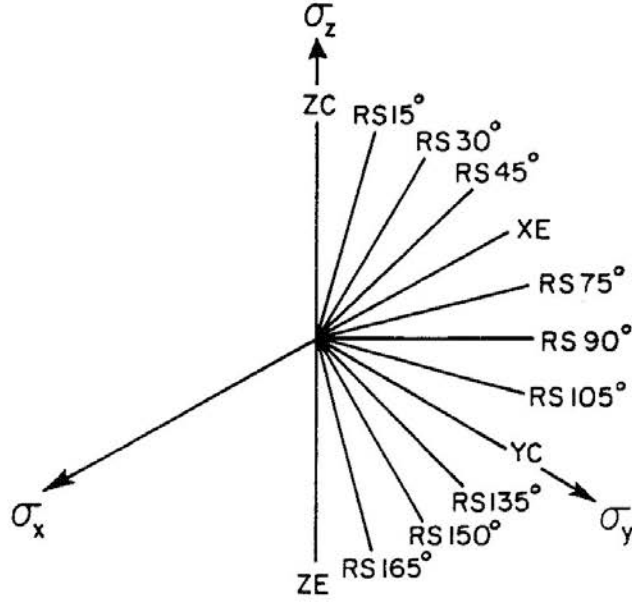
118

Fig.4   Radial stress paths on the octahedral plane
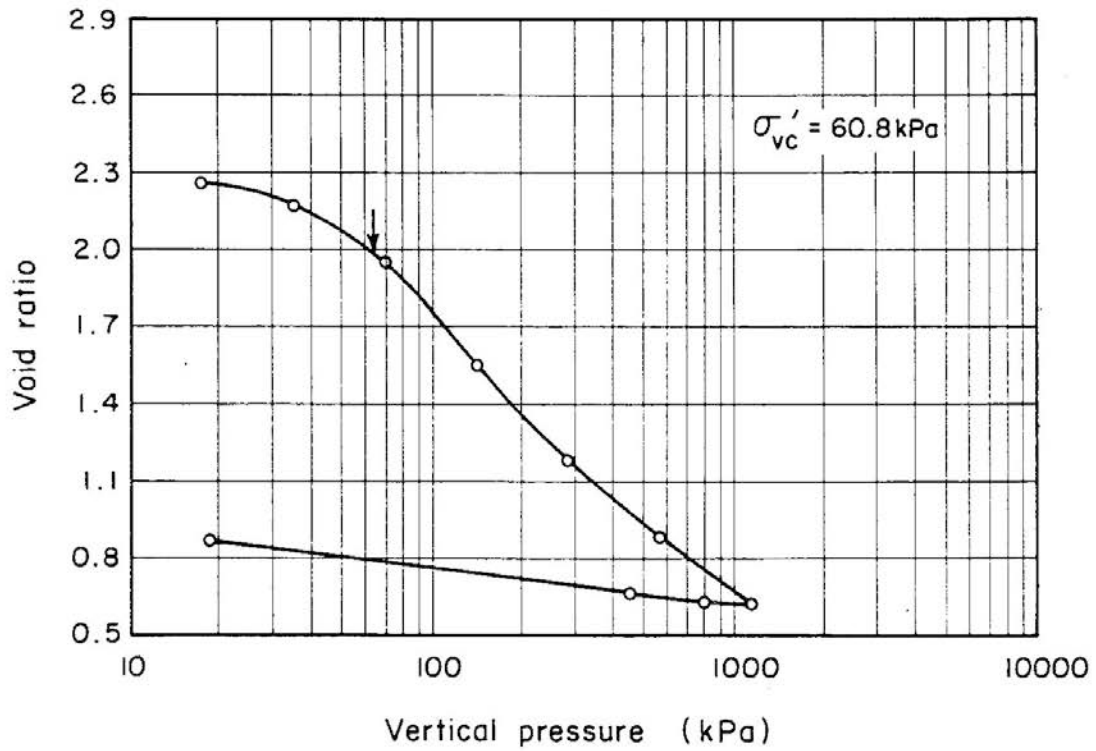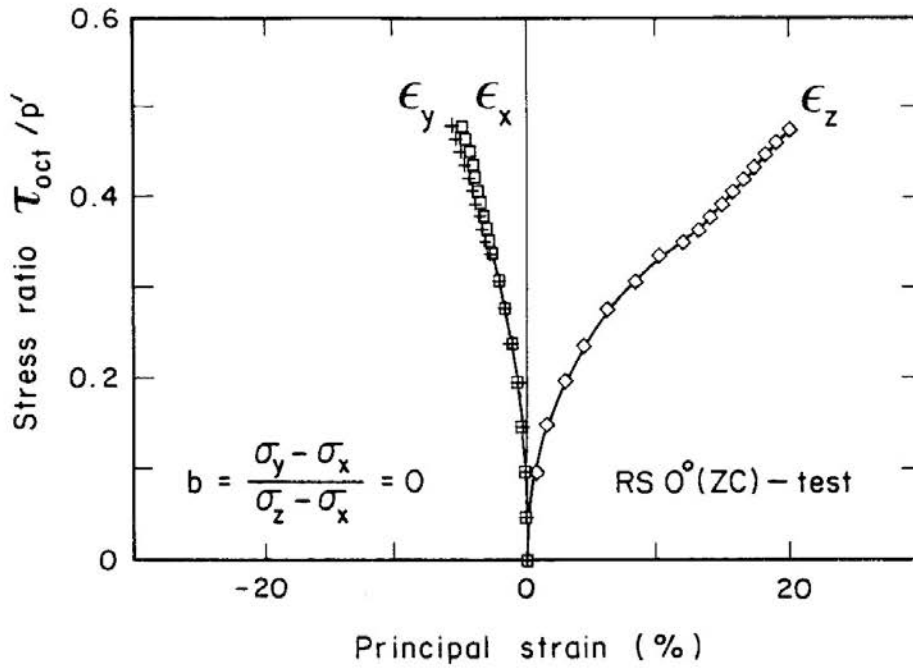

Fig.5   Oedometer test result

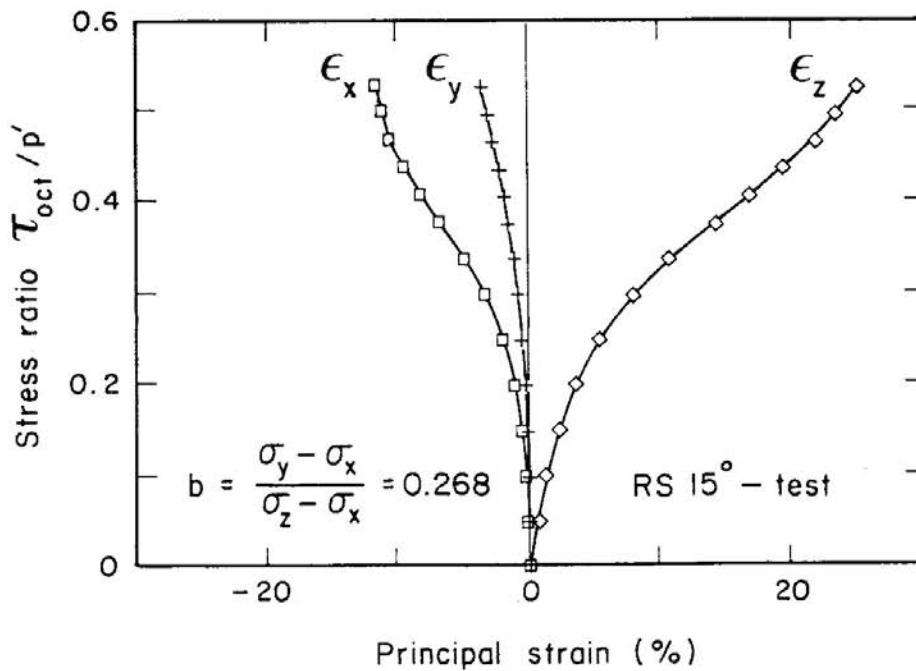**Fig.7   Principal strains versus stress ratio of RS 15° test**

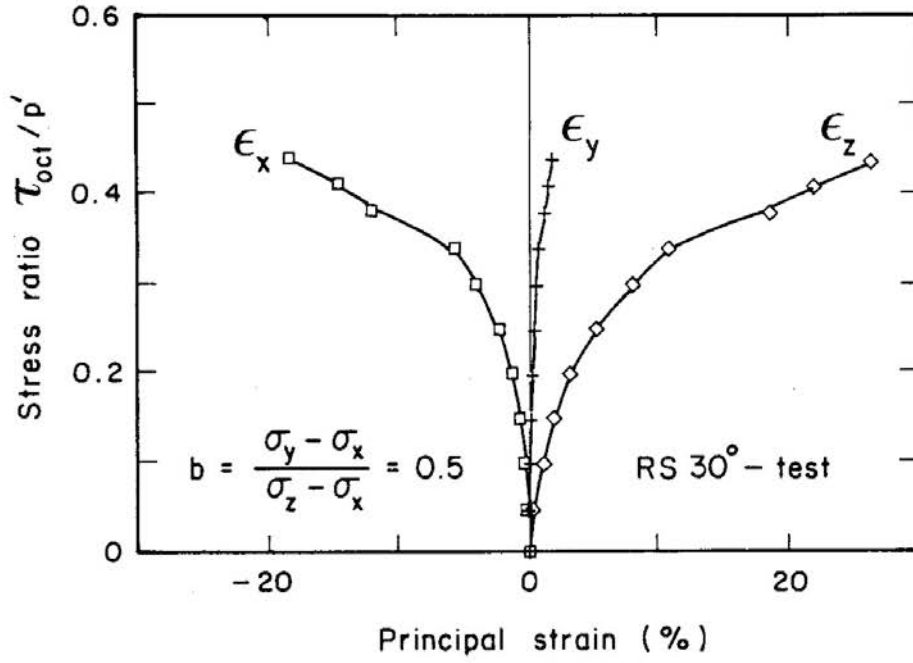**Fig.6   Principal strains versus stress ratio of RS 0° test (ZC test)**

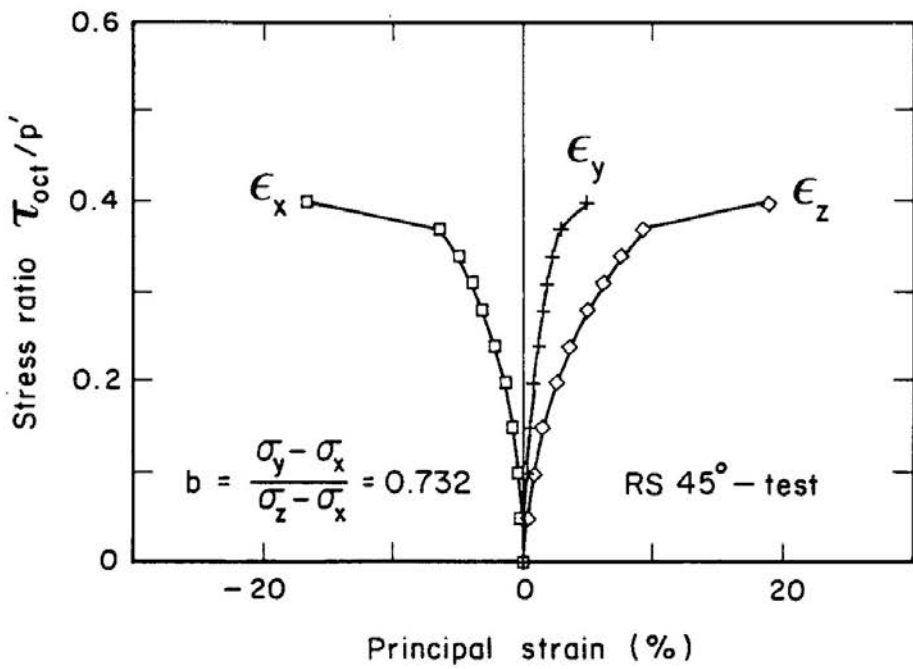Fig.8   Principal strains versus stress ratio of RS 30° test
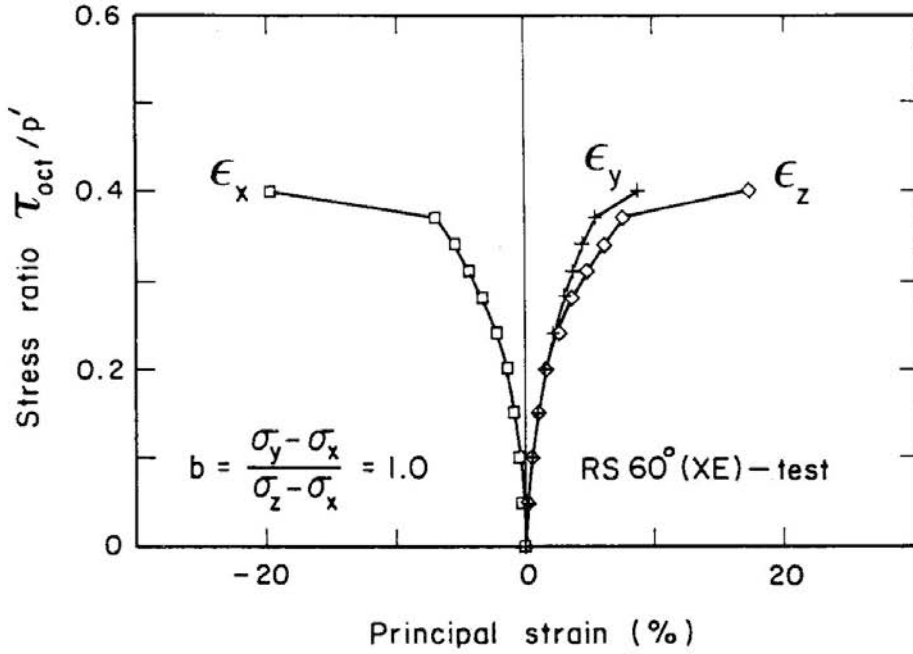

Fig.9   Principal strains versus stress ratio of RS 45° test

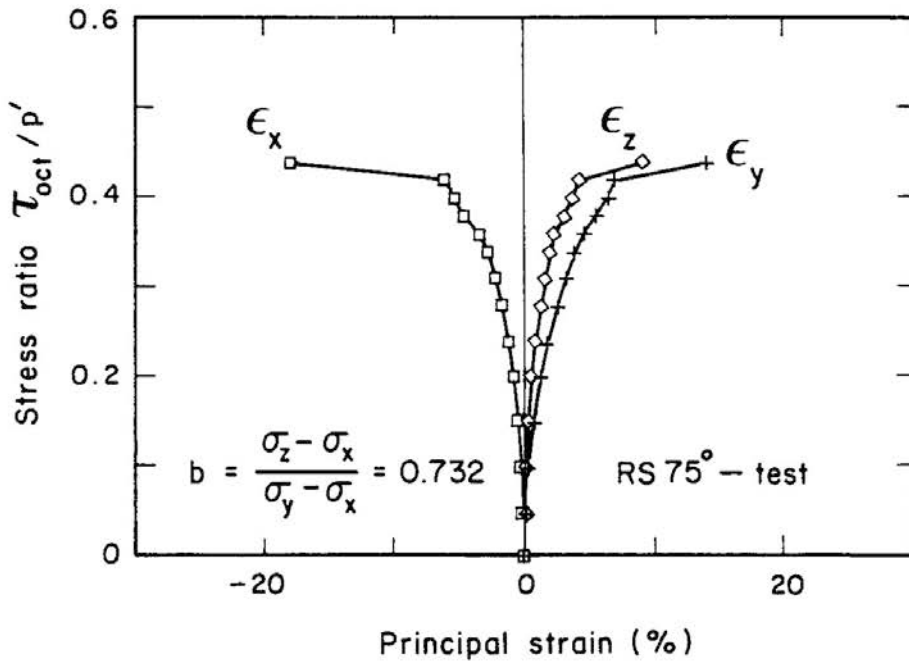Fig.10   Principal strains·versus stress ratio of RS 60° test (XE test)

Fig.11   Principal strains versus stress ratio of RS 75° test
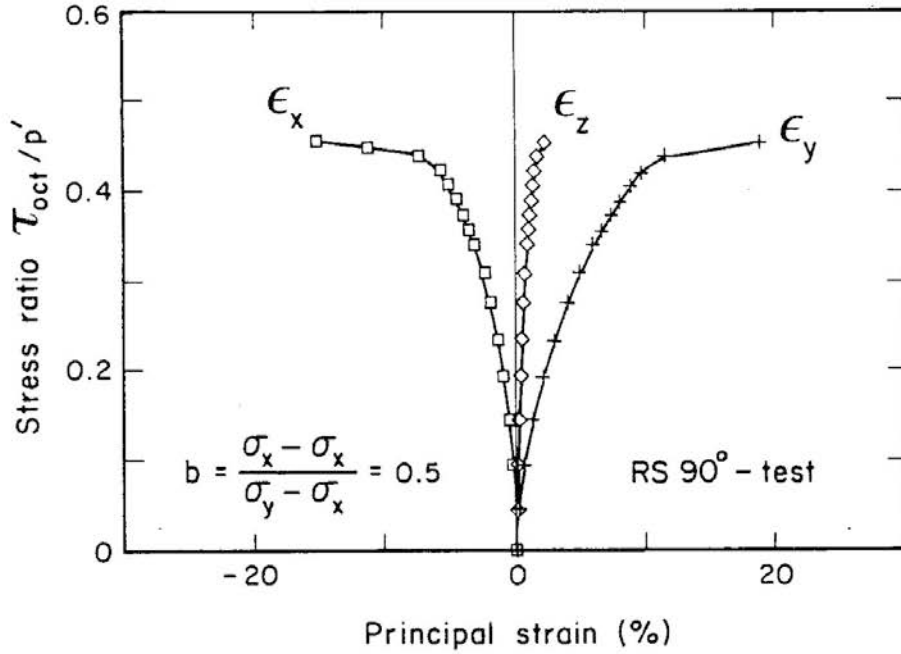
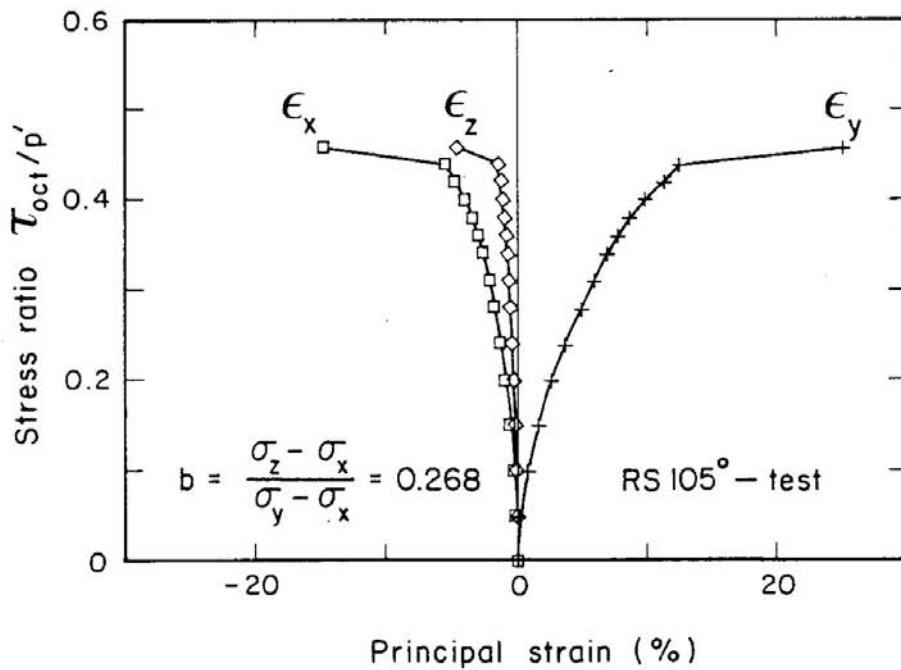Fig.12   Principal strains versus stress ratio of RS 90° test
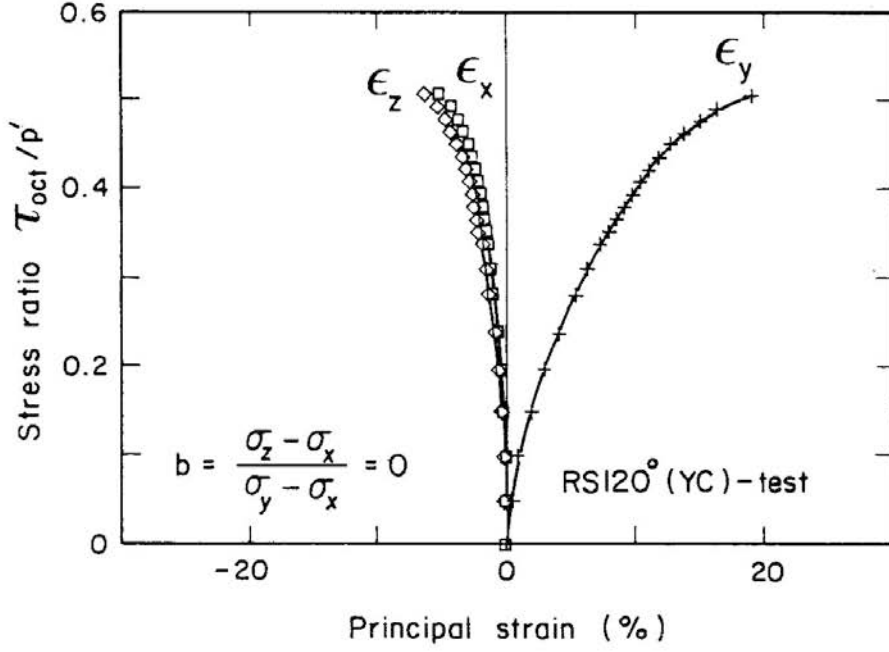

Fig.13   Principal strains versus stress ratio of RS 105° test

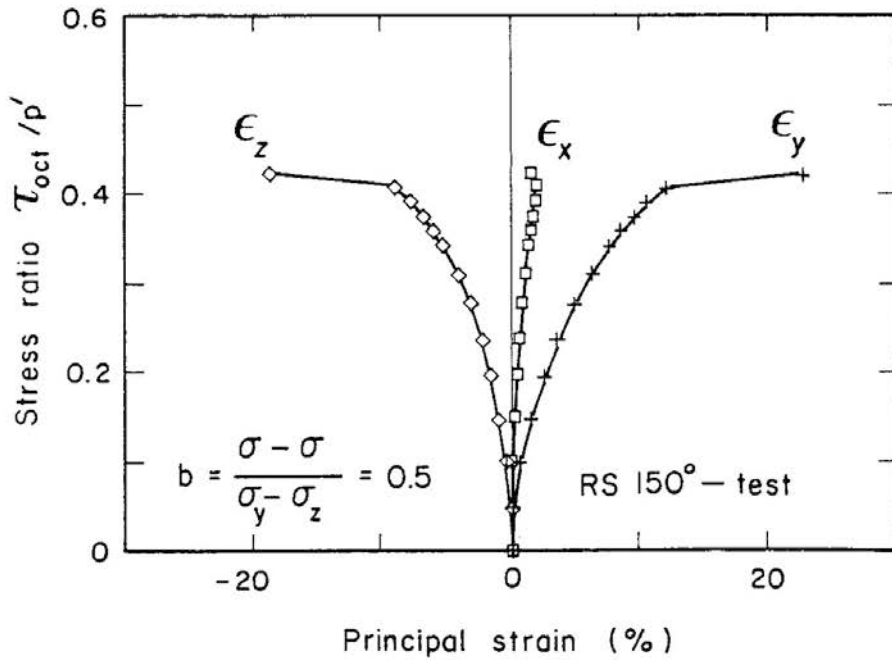**Fig.14 Principal strains versus stress ratio of RS 120° test (YC test)**

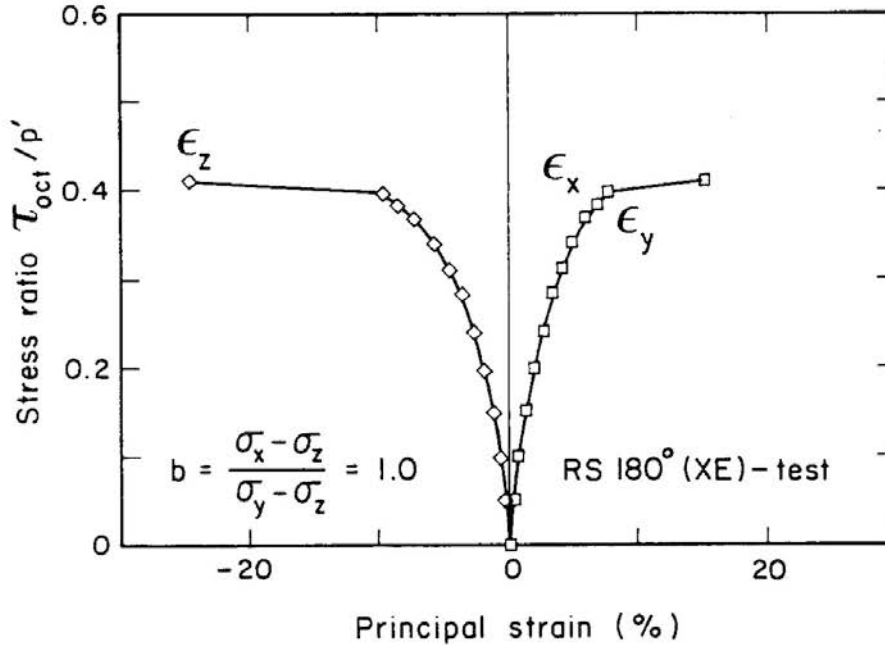**Fig.15 Principal strains versus stress ratio of RS 150° test**

124

Fig.16 Principal strains versus stress ratio of RS 180° test (ZE test)

The stress conditions for ZC (RS 0°) and YC (RS 120°) tests were the same except for the direction of the major principal stresses. There were some differences, however, in the deformation characteristics between these two tests. Comparing the major principal strains in these two tests it was observed that the sample was more compressible in Z direction than in Y direction. Similar observations were made by Taesiri (1976) in studying the consolidation characteristics of Bangkok clay. This characteristic is different from the test results on one dimensionally consolidated kaolin by Kirkpatrick & Rennie (1972) which showed higher compressibility in the horizontal direction. In addition, results of YC test given in Fig.14 showed that expansive strain in the vertical direction was slightly larger than that in the horizontal direction. These observations indicate that the specimen can be compressed and expanded more easily in the direction of its natural deposition than in the direction perpendicular to it.

Similar anisotropic behaviour could also be observed in the deformation characteristics of the specimens in XE (RS 60°) and ZE (RS 180°) tests as shown in Fig.10 and Fig.16 respectively. These two tests were performed under identical stress conditions where specimens were sheared by increasing simultaneously the two major principal stresses while decreasing the minor principal stress. The compressive strain

125

ε_z in the vertical direction was greater than the compressive strain ε_y in the horizontal direction in XE test whereas compressive strains ε_x and ε_y in the two horizontal directions were equal in ZE test.

Comparing principal strain plots in Fig.8 (RS 30°), Fig.12 (RS 90°) and Fig.15 (RS 150°) of the stress paths having an equal b-value of 0.5, it was found that ε_z of RS 30° had the largest magnitude at certain stress ratio among three major principal strains which were compressive. Similarly comparing the minor principal strains which were negative, ε_z of RS 150° was slightly higher at the initial stages of the test. These observations further confirm the fact that the magnitude of compressive strain in the vertical direction is higher whereas the difference in tensile strains are not obvious. This behaviour is different from loose sand. Loose sand is more resistant when compressed in the vertical direction, whereas it becomes less resistant to deformation in the vertical direction than in the horizontal directions while undergoing tensile strains.

Fig.6 to Fig.10 are arranged in the increasing order of b-value. When the stress-strain curves of the RS 15° and RS 30° are compared, it can be seen that the strain in the direction of the intermediate principal stress changed from a tensile strain to a compressive strain. Hence between these two stress conditions there is a plane strain condition in which ε_y was zero.

As θ increased from 0° to 60° (i.e. b increased from 0 to 1.0) the absolute magnitude of the major principal strain at a particular stress ratio decreased monotonically. The intermediate principal strain which was a tensile strain when $\theta = 0°$ became a compressive strain, which was nearly equal to the major principal strain at $\theta = 60°$. The transition from a tensile strain to a compressive strain occurred between 15° and 30°. The absolute magnitude of the minor principal strain increased with the increasing b-value.

With the increasing b-value the strain level required to cause a large strain increment decreased. For b=0 to b=0.5 a failure point as marked by the peak in the stress-strain relationship, was not observed. Though the stress ratio increased until the termination of tests along these stress paths, higher strains were to be induced for specimens having higher b-values at higher stress level despite the initial steepness in the stress-strain curve. It is seen from the test results along RS 45° (b=0.732) and RS 60° (b=1.0) that the samples showed a rapid increase in the major strains after 9% and 8% respectively. This indicates that the failure strain depends on the

magnitude of the intermediate principal stress. Similar observations were made by Lade & Musante (1978) in studying the behaviour of remoulded clay under three dimensional stress conditions.

Fig.10 to Fig.14 show the stress-strain behaviour observed in the tests where the intermediate principal stress, σ_z', decreased from the major principal stress to the minor principal stress, giving decreasing b-values from 1.0 to 0. In this test series, the intermediate principal strain changed its sign with b-values between 0.268 and 0.5, as in the case observed in the first series.

Relationships between stress strain ratio and volumetric strain for different b-values are shown in Fig.17 through Fig.21. Volumetric strain decreased as b-value increased from 0 to 1.0. A comparison of the observed volumetric strains in the ZC and YC tests shown in Fig.17 indicates that the volumetric strain in the ZC test was higher than the corresponding volumetric strain in the YC test despite the same stress conditions. This difference is due to the inherent anisotropy in that the specimens were more compressible in the vertical direction as discussed earlier. The volumetric strains obtained in the XE and ZE tests shown in Fig.21 were almost same at the beginning of the test and towards the end, slightly higher values were obtained for the XE test. The volumetric strains obtained for stress paths having equal b-value of 0.5 took maximum, intermediate and minimum values in RS 30°, RS 90° and RS 150° stress paths in which the vertical direction was the direction of the major, intermediate and minor principal stress respectively. Similar observations were made for the different b-values of 0.268 and 0.732.

Octahedral stress-strain curves are plotted for the specimens sheared along different radial stress paths in Fig.22 through Fig.26. With the increase in b-value the stress-strain curve became steeper. The anisotropic behaviour can be visualized in the plots as well. The octahedral stress-strain relationships of the samples sheared along the ZC and YC stress paths are shown in Fig.22. It is indicated that the sample deformed more in the vertical direction. Similarly comparing the shear strains obtained from two extension tests shown in Fig.26, it can be found that this anisotropic behaviour is more pronounced in compression than in extension.

The mobilized angles of internal friction, ϕ_{mob}, determined by the following equation at different strain levels are shown in Fig.27 for samples sheared along different stress paths.

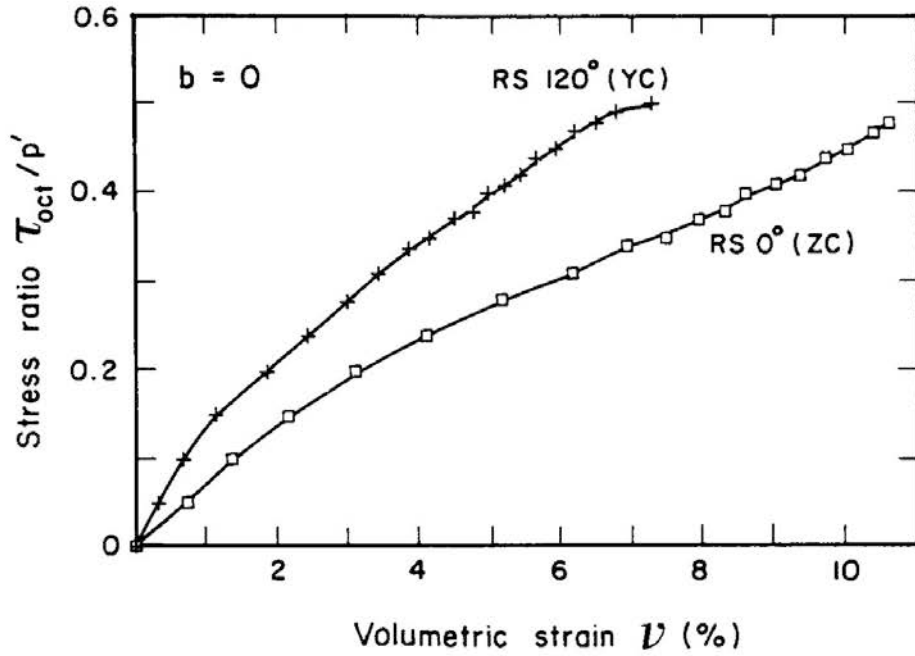$$\phi_{mob} = \sin^{-1} \frac{\sigma_1' - \sigma_3'}{\sigma_1' + \sigma_3'} \qquad (9)$$

127

Fig.17 Volumetric strains versus stress ratio of ZC and YC tests

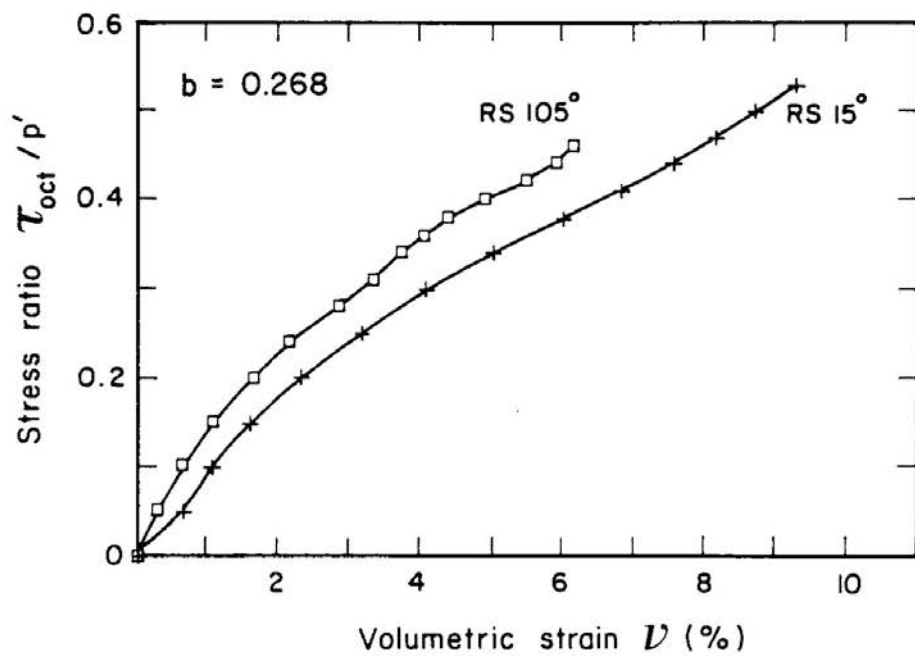

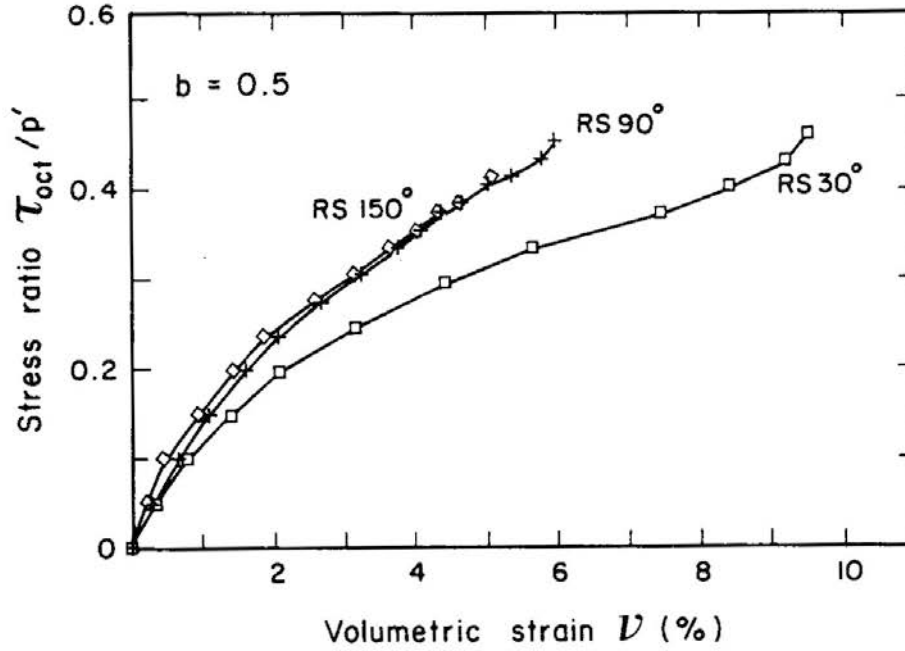**Fig.18 Volumetric strains versus stress ratio of RS 15° and RS 105° tests**

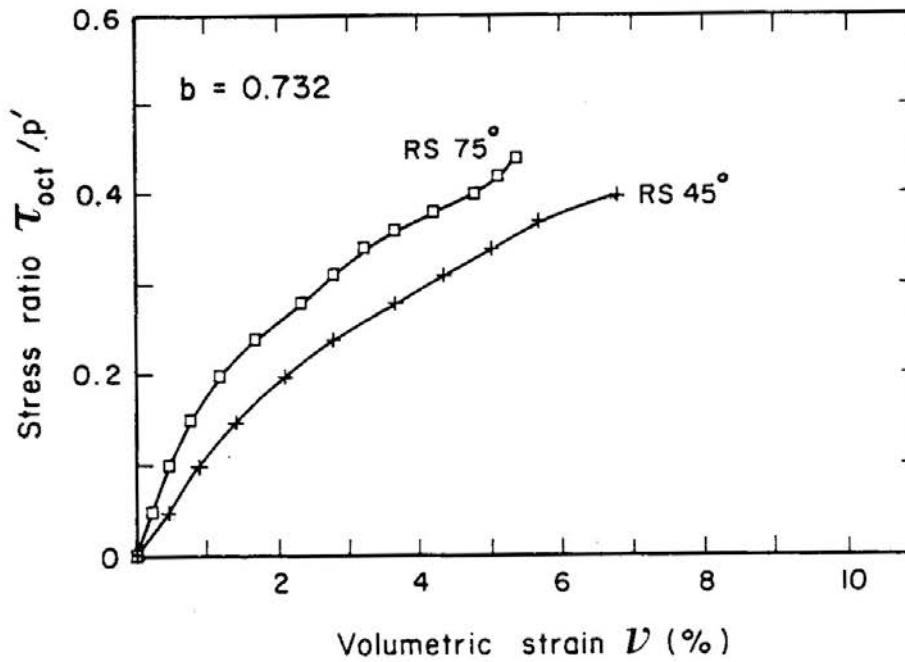**Fig.19 Volumetric strains versus stress ratio of RS 30°, RS 90° and RS 150° tests.**

Fig.20 Volumetric strains versus stress ratio of RS 45° and RS 75° tests
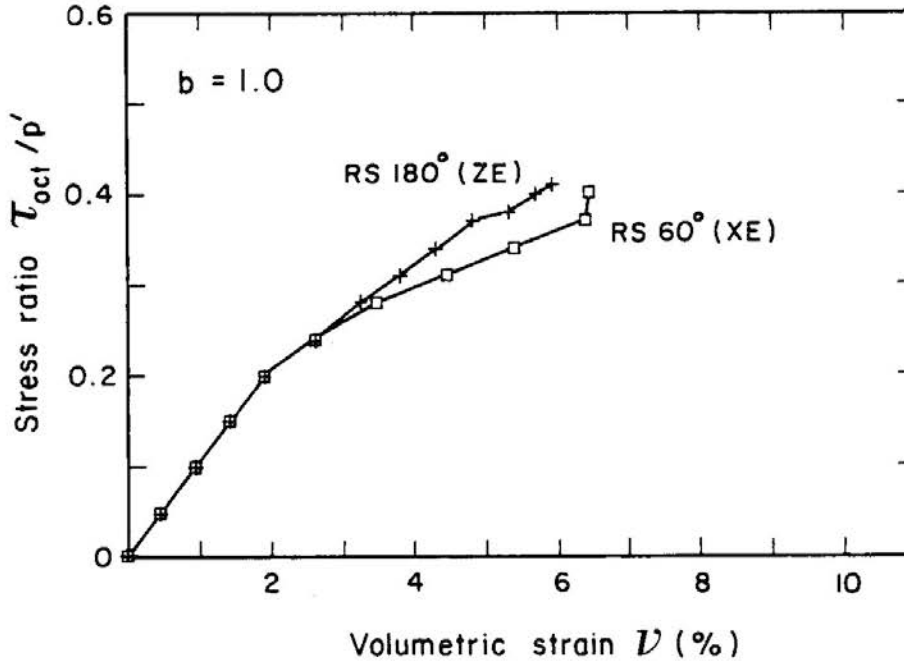
Fig.21 Volumetric strains versus stress ratio of XE and ZE tests

The figure shows that ϕ_{mob} increased with b-value in the range of b=0 to 0.732 and dropped gently at b=1.0 for all the strain levels. This behaviour is compatible with the test results on sand specimens using the three flexible boundaries type of true triaxial apparatus. The difference between ϕ_d in compression and extension tests at γ_{oct}=20% was 4.9°. A difference of 2.2° at failure was reported from drained loading tests on Bangkok clay by Li (1975) using a conventional type of triaxial test apparatus.

Fig.28 is the representation of the measured shear strains on the octahedral plane. Considering homogeneous deformation in the horizontal plane it can be seen that there was some discontinuity in shear stain contour in the vertical direction at smaller strain levels. However, such unusual behaviour disappeared at higher strain levels. Shear stress ratios required to cause different strain levels are plotted in Fig.29. It can be observed that the stress ratio is smaller in the ZC path as compared with other stress conditions.
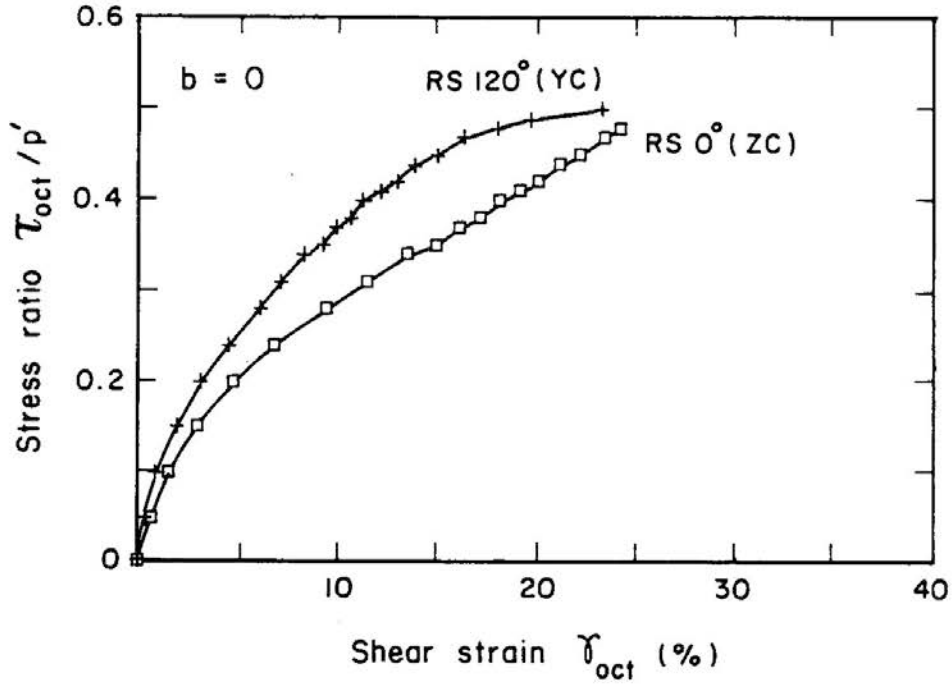
Fig.22 Octahedral shear strains versus stress ratio of ZC and YC tests
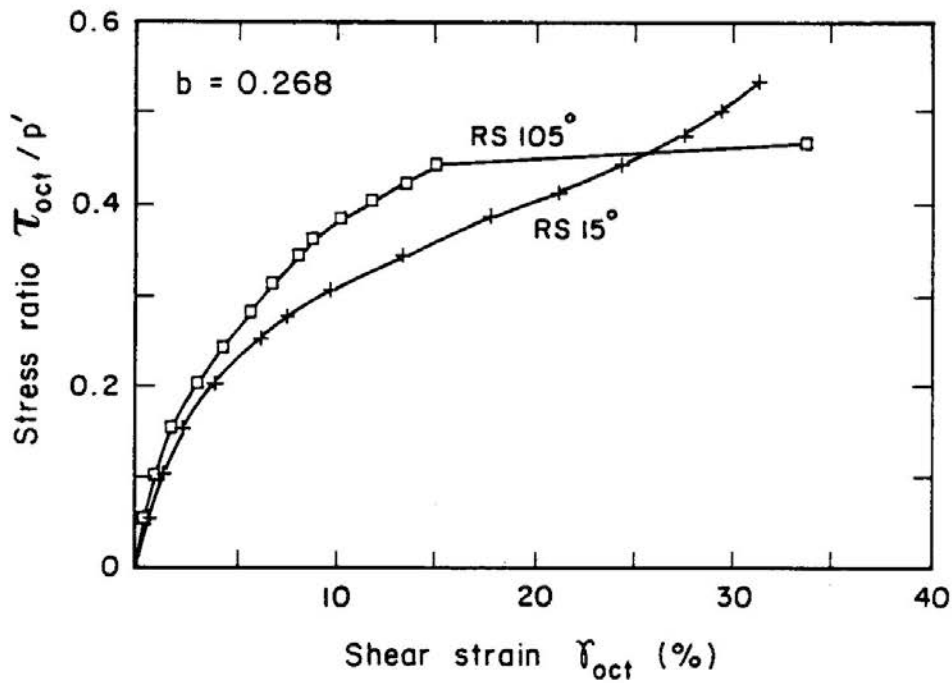
Fig.23 Octahedral shear strains versus stress ratio of RS 15° and RS 105° tests
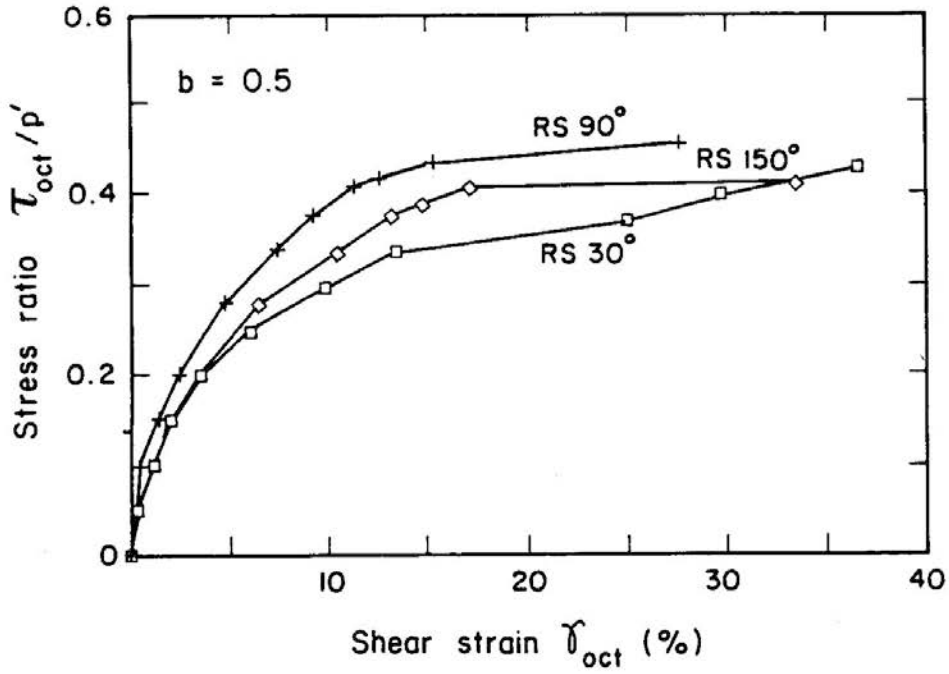
Fig.24 Octahedral shear strains versus stress ratio of RS 30°, RS 90° and RS 150° tests.
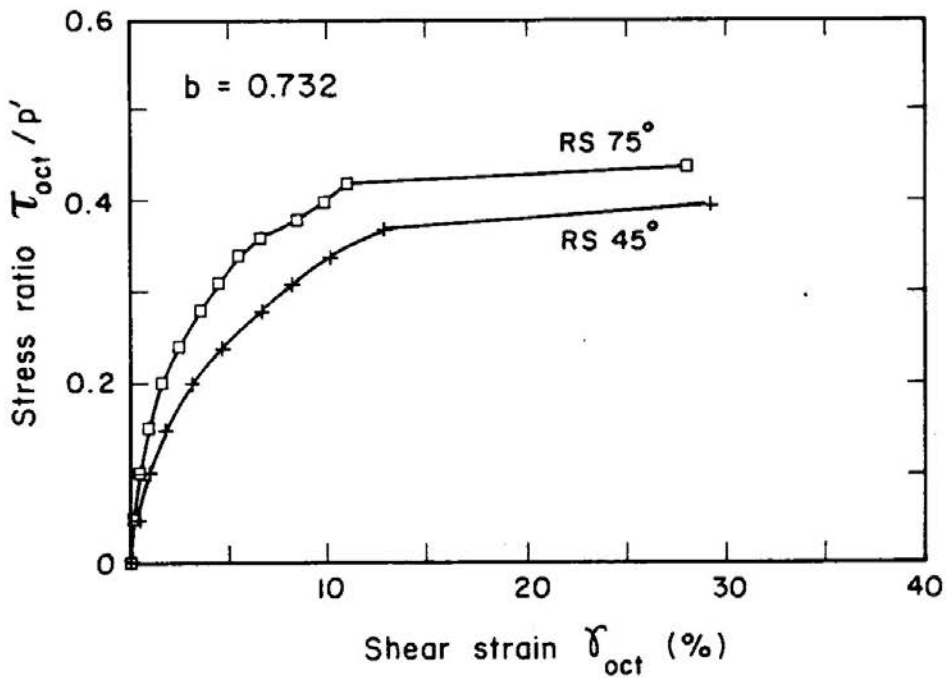
**Fig.25 Octahedral shear strains versus stress ratio of RS 45° and RS 75° tests.**
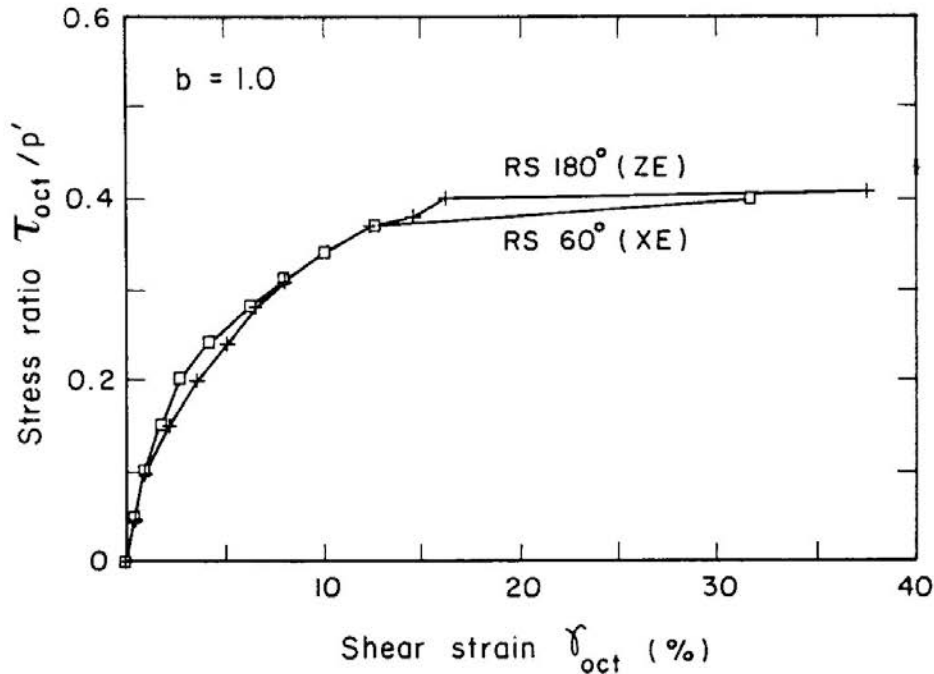
Fig.26 Octahedral shear strains versus stress ratio of XE and ZE tests

CONCLUSIONS

A series of drained tests was carried out on soft Bangkok clay by using a true triaxial apparatus. The undisturbed Bangkok clay showed anisotropic deformation characteristics. The sample was more compressible in the vertical direction than in the horizontal direction, whereas it deformed isotropically in the horizontal plane. Deformation characteristics changed with the relative magnitude of the intermediate principal stress. A higher b-value gave a steeper stress-strain relationship. The plane strain condition lay between b=0.268 and b=0.5. Volumetric strain and the strain to failure decreased with the increase in b-value.

ACKNOWLEDGEMENTS

133
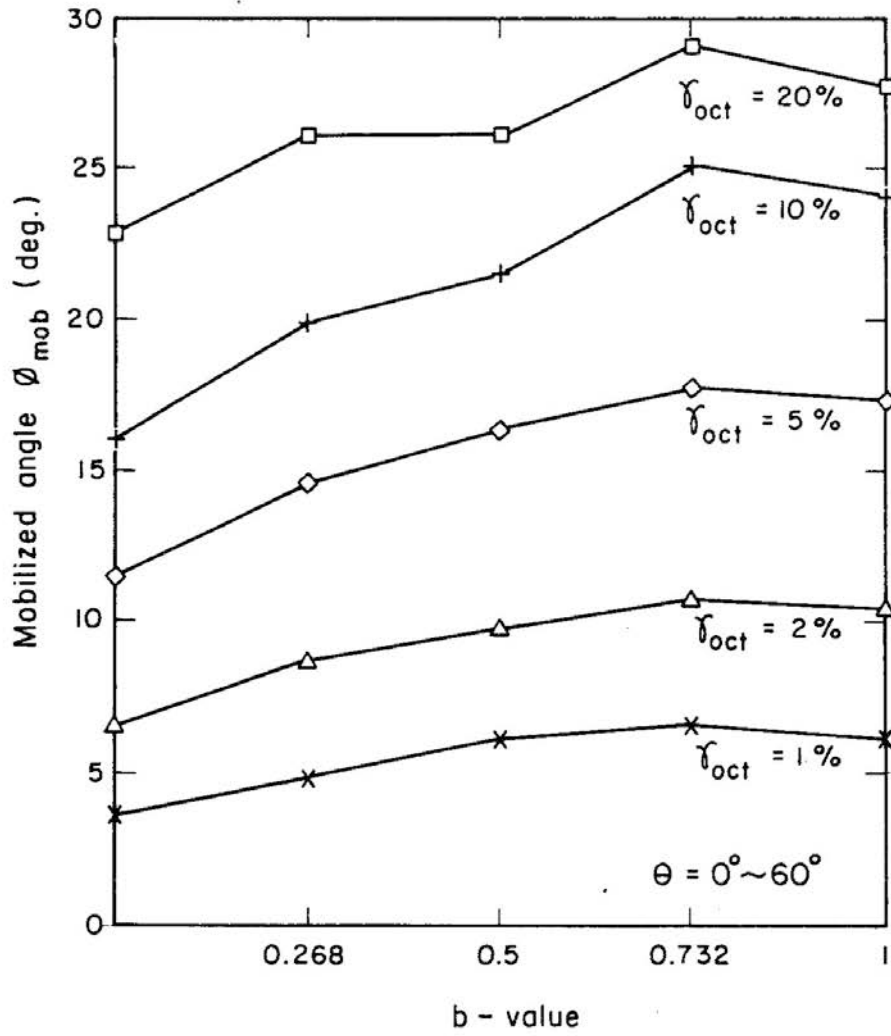
Fig.27 Mobilized angle versus b-value at different strain levels
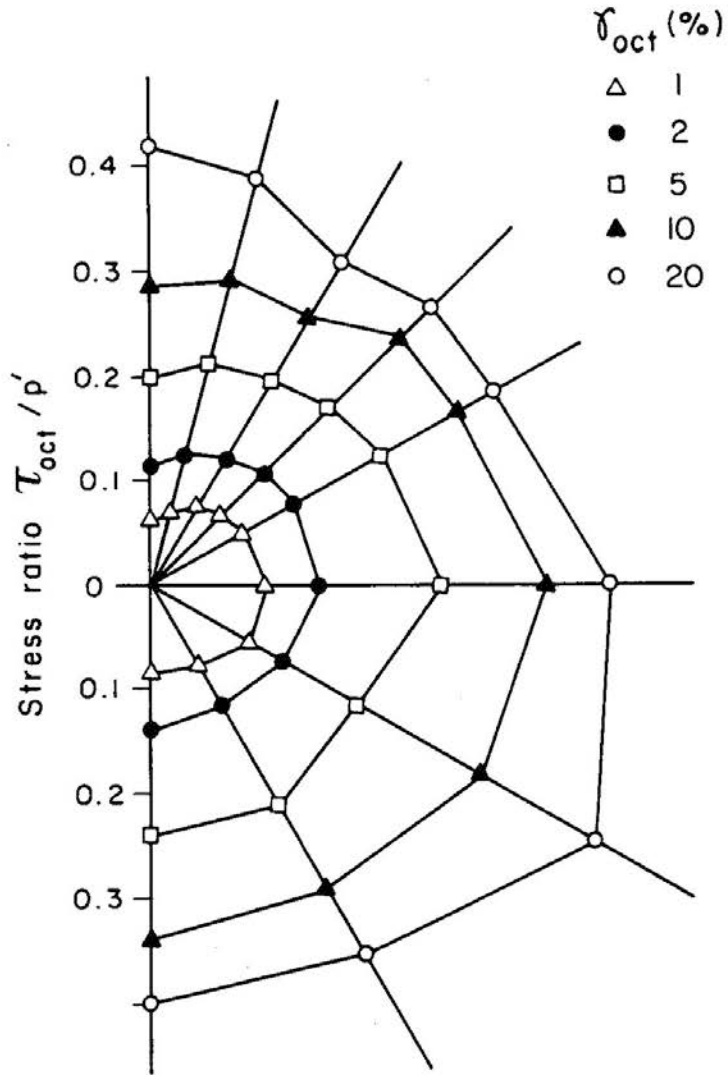
Fig.28 Measured shear strains on the octahedral plane
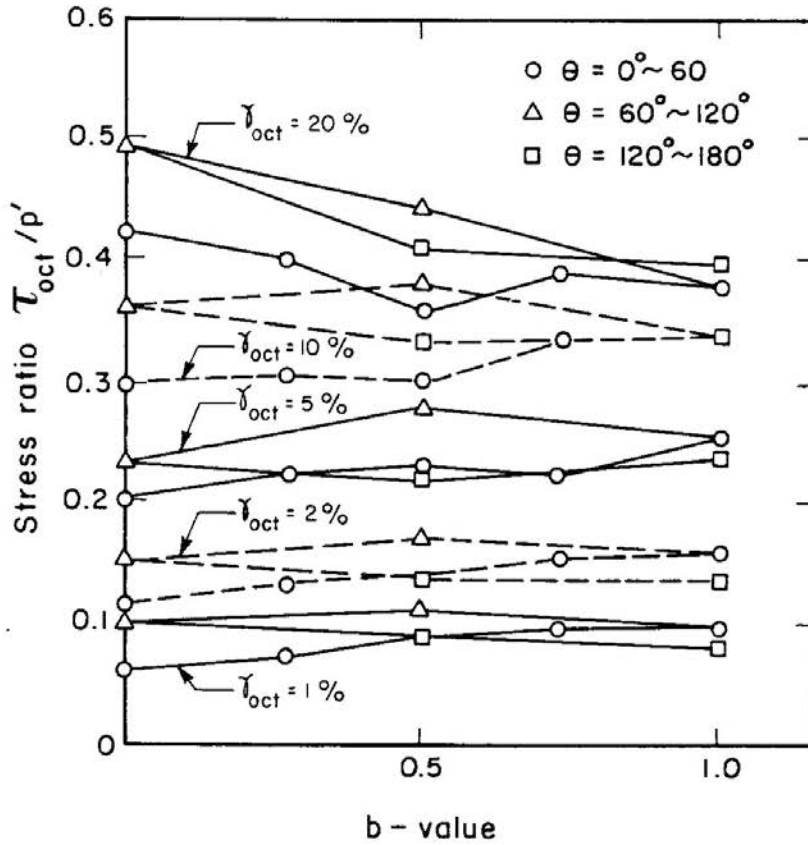
Fig.29   Stress ratio required to cause some strains in the specimen

REFERENCES

KIRKPATRICK, W.M. & RENNIE, I.A. (1972), "Directional Properties of Consolidated Kaolin", *Géotechnique*, Vol.22, No.1, pp.166-169.

KO, H.Y. & SCOTT, R.F. (1967), "A New Soil Testing Apparatus", *Géotechnique*, Vol.17, No.1, pp.283-310.

LADE, P.V. & DUNCAN, J.M. (1973), "Cubical Triaxial Tests on Cohesionless Soils", *Journal of Soil Mechanics and Foundation Engineering Division, ASCE*, Vol.99, No.SM10, pp.793-812.

LADE, P.V. & MUSANTE, H.M. (1978), "Three Dimensional Behaviour of Remoulded Clay", *Journal of Geotechnical Engineering Division, ASCE*, Vol.104, No.GT2, pp.193-209.

LEE, I.K., ZHAO, X., LO, S-C.R., YANG, WEI, X. & WU, X. (1988), "The Response of Shanghai Clay in Multi-Axial Tests", *Proceedings of Fifth Australia-New Zealand Conference on Geomechanics,* Sydney, pp.153-158.

LI, Y.G. (1975), *"Stress-Strain Behaviour and Strength Characteristics of Soft Nong Ngoo Hao Clay under Extension Conditions",* Master of Engineering Thesis, No.767, Asian Institute of Technology, Bangkok.

NAGARAJ, T.S. & SOMASHEKAR, B.V. (1977), "Shear Strength of Soils under General Stress Field", *Proceedings of the 9th International Conference on Soil Mechanics and Foundation Engineering,* Tokyo, Vol.1, pp.225-228.

SHIBATA, T. & KARUBE, D. (1965), "Influence of the Variation of the Intermediate Principal Stress on the Mechanical Properties of Clays" *Proceedings of the 6th International Conference on Soil Mechanics and Foundation Engineering,* Montreal, Vol.1, pp.359-363.

TAESIRI, Y. (1976), *"Consolidation Characteristics of Rangsit Clay",* Master of Engineering Thesis, No.918, Asian Institute of Technology, Bangkok.

VAID, Y.P. & CAMPANELLA, R.G. (1974), "Triaxial and Plane Strain Behaviour of Natural Clay", *Journal of Geotechnical Engineering Division, ASCE,* Vol.100, No.GT3, pp.207-224.

YAMADA, Y. & ISHIHARA, K. (1979), "Anisotropic Deformation Characteristics of Loose Sand under Three Dimensional Stress Conditions", *Soils and Foundations,* Vol.19, No.2,pp.79-94.

UPLIFT CAPACITY OF SCREW PILE ANCHORS

S. Narasimha Rao*, Y.V.S.N. Prasad**, M.D. Shetty*** and V.V. Joshi***

SYNOPSIS

Anchors are extensively used in a number of foundations subject to uplift forces. Screw piles used to resist both uplift and compressive forces proved to be quite successful in several soft clayey deposits. In this paper, the results obtained from the experimental programme carried out on model screw pile anchors are reported and the utility of such anchors has been brought out. These anchors used are of shaft diameters of 44mm and 60mm and helical plates of diameters 100mm and 150mm respectively. The pull out tests have been conducted in two silty clayey soils and at different moisture contents. These piles are screwed into the clayey soil bed prepared in the test tank using a standard torque wrench. The results indicate that the uplift capacities improve with consistency index and sizes of piles. The torque used to install the anchors can be correlated to the capacity. Further, the results indicate that with the spacing ratios (spacing of the helical plates to diameter of the helical plate) approaching about 1.5, very nearly cylindrical failure surfaces are formed and it is possible to make some good prediction of the capacities for such cases.

INTRODUCTION

Anchors are used in a number of instances to strengthen the foundations subjected to uplift forces and overturning moments. They are also used in berthing structures to provide stability against horizontal pulls. The common types of anchors in use are pile anchors, gravity anchors, plate anchors etc. The present study deals with the behaviour of screw pile anchors in clayey type of soils. These are made out of helical shaped circular steel plates welded to a steel shaft at a given spacing. They are installed into soil by applying a torque to the upper end of the shaft and this torque can be effected either manually or by mechanical means. The screw pile anchors foundation has a number of advantages over conventional types of foundations and are installed quickly using minimal equipment in comparison to the conventional foundation types. Especially in the case of marshy soil conditions and in the field situations with a high ground water table, the use of screw type anchors is found to

*Professor, Ocean Engineering Centre, Indian Institute of Technology, Madras

**Research Scholar, Ocean Engineering Centre, Indian Institute of Technology, Madras.

***Formerly graduate student, Dept. of Civil Engineering, Indian Institute of Technology, Madras 600 036, India.

be very convenient and economical. In this paper, some important aspects of screw pile anchors, the variation of ultimate pull out capacity with the spacing ratio (l/d) and consistency index of soil are studied by conducting the experiments on model screw pile anchors in soft to medium stiff clays. And also an attempt has been made to correlate the torque required to install the anchor with the ultimate pull out capacity.

BRIEF LITERATURE REVIEW

In the recent past, there are some studies made on the use of screw type of foundations. Wilson (1950) tried to correlate the torque required to install the screw pile and its bearing capacity and a relationship has been developed between penetrative effort and the bearing capacity of screw piles. In the recent years, screw piles are in use for mast and tower foundations in the U.S.S.R. and Canada. In the U.S.S.R. during 1961-64 many communication masts up to 254m high have been erected quite economically using these piles (Trofimenkov & Mariupolskii, 1965). About two hundred piles were tested to develop reliable methods of determining the capacity of these piles both in compression and tension. Robinson & Taylor (1969) reported the use of power installed helical anchors in two guyed transmission lines. In each of these projects which extended over a length of about 869km in British Columbia, helical anchors were investigated for possible use in mainly clayey deposits. Some anchors were tested and resistance to pull out was correlated with the installing torque.

A field testing program was carried out in northern Manitoba to evaluate the creep behaviour and load capacity of power installed screw anchors embedded in Permafrost by Johnston & Ladanyi (1974). The test results indicated that the anchors under uplift loads behaved in a similar was to the behaviour of deep footings. The linear relationship between installation torque for the lasat few inches of anchor penetration and uplift capacity has been stated in the design chart developed by the Chance Manufacturing company (1983), a manufacturer of steel helical anchors. Clemence & Pepe (1984) reported the results of helical anchors installed in sandy soils. A design method for the determination of uplift capacity of helical anchors in both sandy and clayey type of soils was developed based on extensive field and laboratory testing by Bobbitt & Clemence (1987). Results of these tests were compared with the results of the previous researchers and found to be in good agreement.

From the aforementioned review, it is clear that this type of screw pile is used to resist uplift forces. A number of model screw piles were tested for different condi-

tions in this experimental study. All these details of the experimental work and the methods followed are presented in the next section.

EXPERIMENTAL WORK

Scope Of The Investigation

In this experimental study, an attempt has been made to correlate the ultimate uplift capacity of screw pile anchor with its installation torque. And also the various other aspects like the variation of uplift capacity with the spacing ratio (l/d) and the influence of consistency index of soil on uplift capacity are studied.
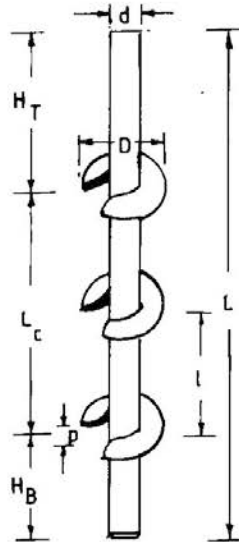
Fig.1: Typical screw pile used

Model Screw Piles

The investigations were conducted on the model screw pile anchors made with galvanished iron pipes welded with 3mm thick mild steel helical plates. Two different sets of anchors were fabricated for this investigation. One such typical anchor fabricated is shown in Fig.1. In the first set, there were 3 Nos. of anchors used to study the influence of spacings of helical plates. Different number of plates (2, 3, and 4 Nos.) were placed over a length of 457.5mm. The diameter of the shaft was 44mm and the diameter of the helical plate was 100mm in this set. Similar to first set, there

141

were 3 Nos. of anchors in the second set. To study the influence of the spacing of helical plates, different number of plates (2, 3 and 4 Nos.) were placed over a length of 457.5mm in this set also. But the diameter of the shaft was 60mm and the diameter of the helical plate was 150mm in this case. The total length of anchor in both the sets was 640mm and for all the anchors, the bottom of the shaft is closed. All the details of anchors used are given in Table 1.

Table 1: Details of Screw Pile Anchors Fabricated

S. No.	Set No.	Screw pile anchor Designation	Diameter of pile shaft, d in mm	Diameter of helical plate, D in mm	No. of helical plates	Pitch of helical plates, p in mm	Spacing of helical plates, 1 in mm	Distance between top and bottom helical plates, L_c in mm	Distance between shaft top and top helical plate, H_T in mm	Distance between shaft bottom and bottom helical plate, H_B in mm	Total length of screw pile anchor $L(L_C + H_T + H_B)$ in mm
1	1	P1	44	100	2	58	457.5	457.5	98.5	94.0	640.0
2	1	P2	44	100	3	58	229.0	457.5	98.5	84.0	640.0
3	1	P3	44	100	4	58	152.5	457.5	98.5	84.0	640.0
4	11	P4	60	150	2	58	457.5	457.5	98.5	84.0	640.0
5	11	P5	60	150	3	58	229.0	457.5	98.5	84.0	640.0
6	11	P6	60	150	4	58	152.5	457.5	98.5	84.0	640.0

General Experimental Set Up

Fig.2 shows the general experimental set up for carrying out pull-out tests. The test tank used was of inner dimensions, 800mm × 800mm × 1300mm and was made out of 5mm thick mild steel plates. The steel plates used for the test tank were sufficiently thick and rigid enough. The size of the tank was considerably large enough so as not to interface with the failure zones.

As shown in the Fig.2 the pull out has been effected with the help of wire rope passing over two pulleys and the wire rope has been subjected to tension with the

help of cast iron weights. The upward movement of the anchor has been measured with the help of two dial gauges of least count 0.01mm.

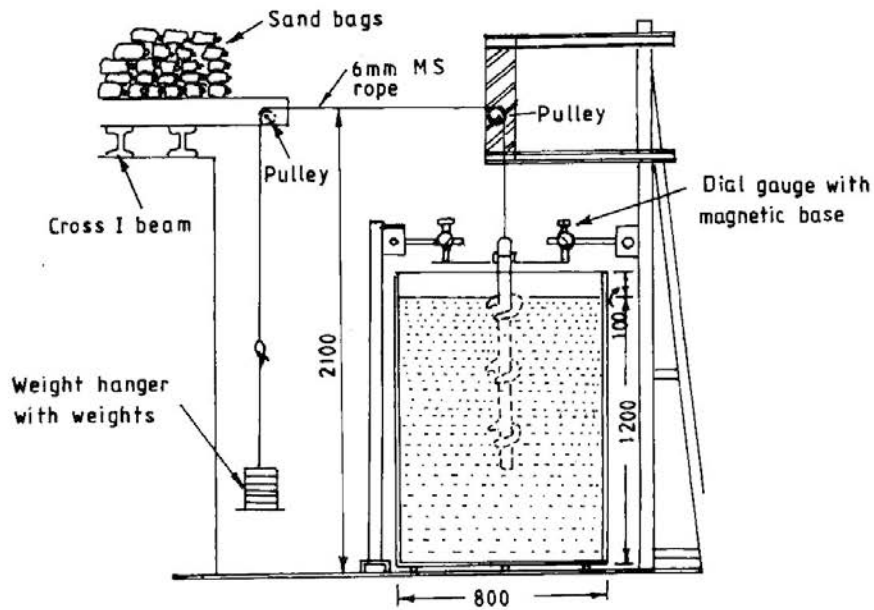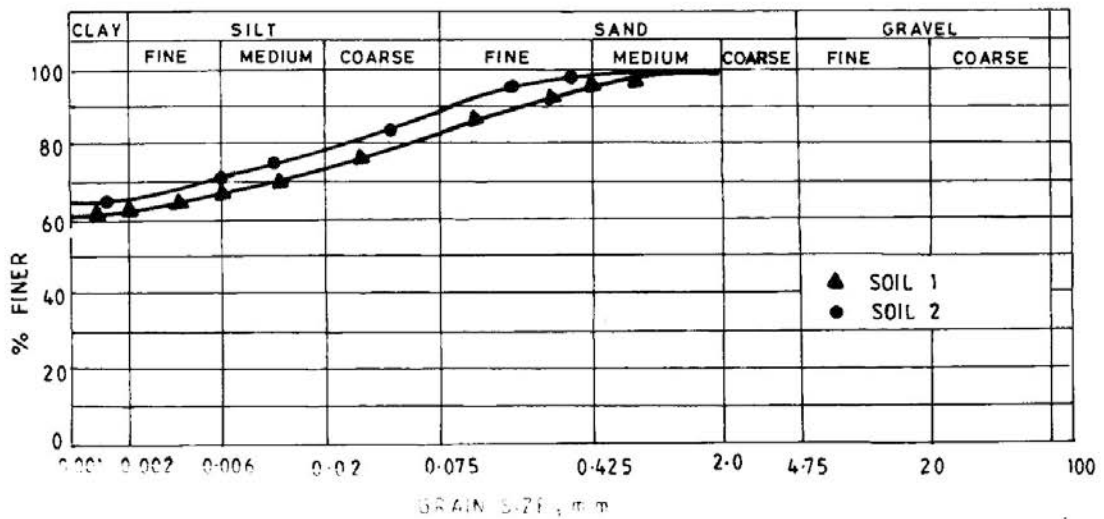**Fig.2: Experimental set-up for pull-out test**

Fig.3: Grain size distribution curves of soils used

Table 2: Soils – Index Properties

S. No.	Soil de-signation	Liquid limit (%)	Plastic limit (%)	Plasticity index (%)	Grain size distribution		
					Clay (%)	Silt (%)	Fine sand (%)
1	Soil 1	75	25	50	62	20	15
2	Soil 2	89	24	65	65	24	10

Soils Used For The Test

Two types of clayey soil were used for the testing and their index properties are given in Table 2 and their grain size distribution curves are given in Fig.3.

Testing Programme And Procedure

(a) First Set Of Screw Pile Anchors

The pull out tests were conducted on the first set of anchors (3 nos.) in both the soils. In soil 1, each of the anchor was tested at three different moisture contents, viz. 40.2%, 45.2%, 50.4%. In soil 2, they were tested at two different moisture contents, viz. 57.6%, 78.3%.

(b) Second Set Of Screw Pile Anchors

Having brought out the influence of moisture content, further testing has been limited to one moisture content only. The pull out tests were conducted on the second set of anchors (3 nos.) in the soil 1 at a moisture content of 45.2%.

Method of Filling up the Tank

The soil was placed in layers of 50mm thickness. Because of high moisture content (conforming either to soft or medium stiff consistency), there was no difficulty in placing the soil and a fairly homogeneous soil deposit could be formed around the anchor. After the clay bed was formed, anchor was installed by rotating the torque wrench which is connected to the top of the anchor shaft by means of a suitable adopter. In addition to the torque, enough downward force was also applied to the anchor shaft. The downward force was applied in such a way that rate of advancement of the anchor was equal to the pitch of the helical plate per rotation. Care was taken to apply the same amount of downward force in all the anchors installed. All the anchors were installed in the same way till the top helical plate coincided with the

144

top level of the soil (relative depth, H/D = 0) and the torque required to install each anchor was measured with help of torque wrench. In order to equilibriate the pore water pressures developed, there was a wait of 2 days before the test was started. The tank was covered with a polythene sheet to prevent the moisture content variation. At random, a few samples were taken out and checked for full saturation, homogeneity and for pore pressures.

Procedure Used in Conducting Pull Out Test

In the set-up shown in the Fig.2, the cast iron weights were used as the loads. Loads were continuously placed on the pan and the upward movement of anchor was noted down with the help of dial gauges. Loads were increased until the anchor came out of the soil bed. The load at which the anchor came out suddenly was considered as the ultimate uplift capacity of the screw pile anchor.

Measurement Of in Situ Shear Strength

The insitu strength was measured with the help of standard vane shear apparatus. These tests were conducted periodically and at different depth locations. It may be mentioned that the insitu vane shear strength measured for both the soils indicated very low values of strength varying between 0.0048 and 0.0093 N/sq.mm for soil 1 and from 0.002 to 0.005 N/sq.mm for soil 2. The strengths measured can be considered as remoulded strengths. These soils were obtained from coastal deposits in the east coast of India. The insitu strength tests made in the field and the strength obtained from a thoroughly disturbed or remoulded soil samples indicated the apparent sensitivity values between 5 and 6.

RESULTS AND DISCUSSIONS

The behaviour of these screw pile anchors can better be assessed with the help of results obtained from pullout tests. A number of pull out tests have been conducted and these results are presented and analysed critically. The pull out load vs upward movement of anchors obtained from the first set of anchors in soil 1 are presented in Figs.4 to 6. These tests were conducted at three different moisture contents, viz. 40.2%, 45.2%, 50.4% and these moisture contents cover a range of consistency index of 0.49 to 0.70. Fig.4 refers to the test results obtained from the screw pile anchor with 2 Nos. of helical plates and in Figs.5 and 6 the results obtained from the anchor with 3 and 4 helical plates respectively are presented. From these curves, it is clear that there is a similar load – movement (upward) behaviour in all these tests. From these Figs.4 to 6, it can be seen that the capacities are considerably decreased
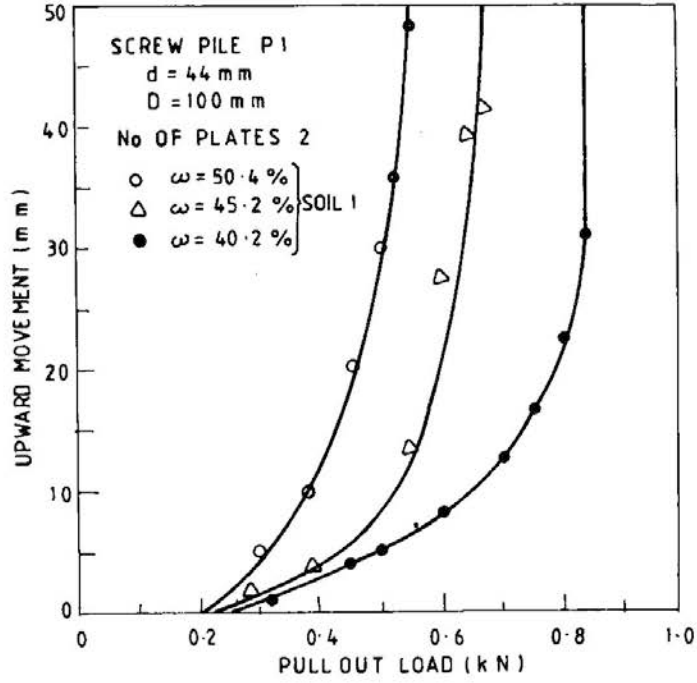
Fig.4: Pull-out load Vs upward movement curves
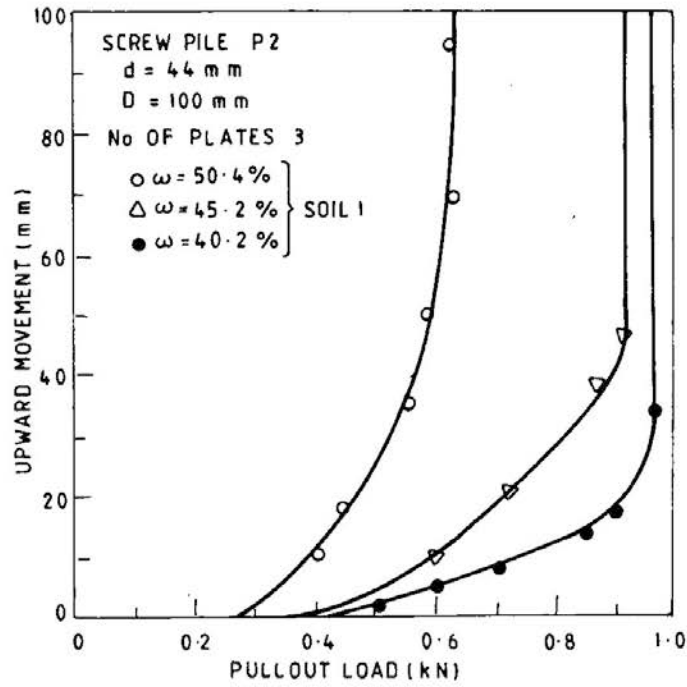
Fig.5: Pull-out load Vs upward movement curves
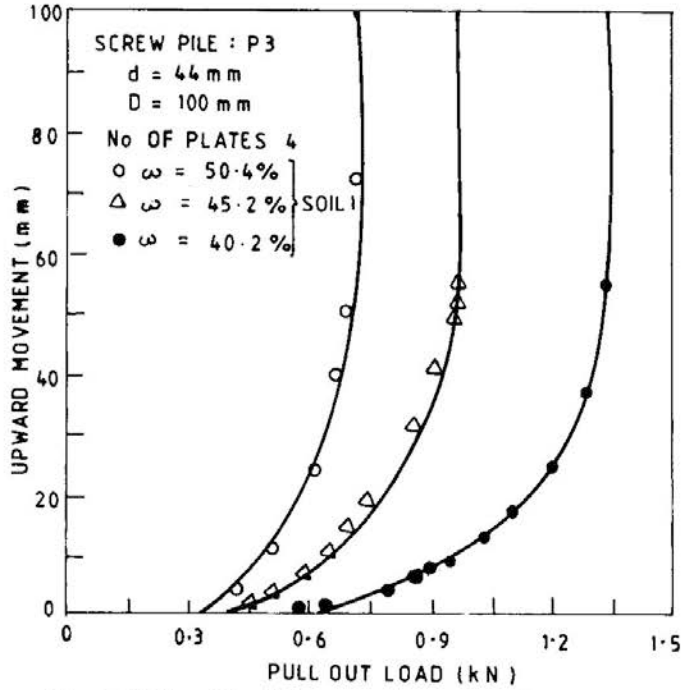
Fig.6: Pull-out load Vs upward movement curves

with increasing moisture contents and this is quite obvious because of the decrease in the strength with increase in moisture content in clayey soils. Also it can be observed that increase in the number of helical plates results in an increase in uplift capacities.

All the results of tests mentioned above are summarized in Table 3. The torques required to install the anchors were carefully measured and these values are also presented in the same Table. From Table 3, it can be observed that the increase in the number of plates resulted in a decrease in the torque required for the installation of anchors. The cause for this could be that with more plates the anchor cuts the soil at more points and hence easy driving is possible. Also from this Table it is clear that both the uplift capacities and installation torques increased with the decrease in moisture content of soil for the same anchor. Fig.7 refers to the relationship between installing torque and uplift capacities of the tests (i.e. first set, soil 1). These results indicate that it is possible to establish relationships between the torque and the uplift capacity. From this Figure it can also be said that relationships exist between (a) uplift capacities of the same anchor at different moisture contents of soil and the installing torque (b) uplift capacities of anchors with a different number of helical plates and the installation torque at the same moisture content. The pull out load versus upward movement of the first set of anchors in soil 2 are presented in Figs.8 and 9. These tests were conducted in soil 2 at two moisture contents, viz. 57.6% and

147

Table 3: Uplift Capacities
(Set I; Soil 1)

S.No.	Screw pile anchor Designation	No. of helical plates	Placement moisture content (%)	Consistency Index	Installation Torque, T in N.mm	Ultimate uplift capacity, P_{tu} in N
1	P1	2	40.2	0.696	28938.4	840
2	P2	3	40.2	0.696	24970.0	965
3	P3	4	40.2	0.696	23020.0	1340
4	P1	2	45.2	0.596	24779.0	665
5	P2	3	45.2	0.596	20848.8	910
6	P3	4	45.2	0.596	17207.4	965
7	P1	2	50.4	0.492	19296.0	550
8	P2	3	50.4	0.492	15142.5	625
9	P3	4	50.4	0.492	13077.6	725
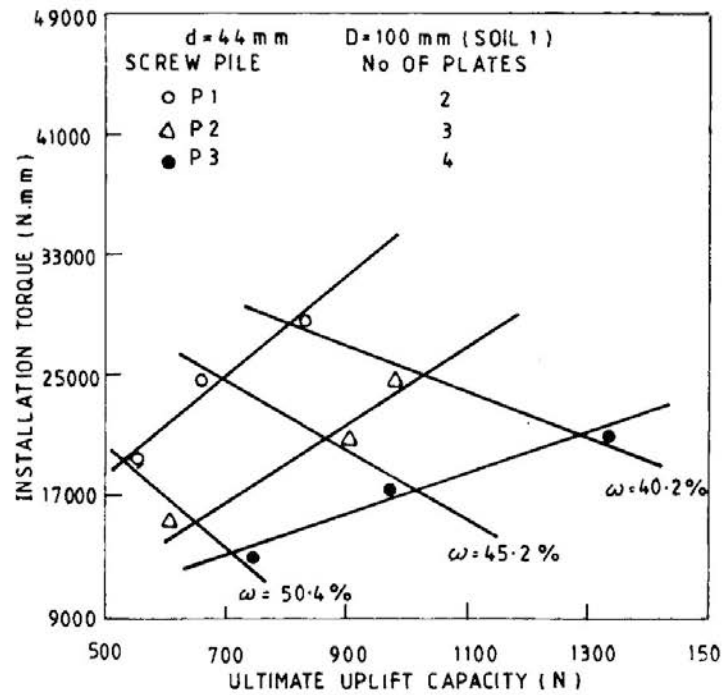
Fig.7: Relationship between ultimate uplift capacity and installation torque

Fig.8: Pull-out load Vs upward movement curves

Fig.9: Pull-out load Vs upward movement curves

149

Table 4: Uplift Capacities
(Set I; Soil 2)
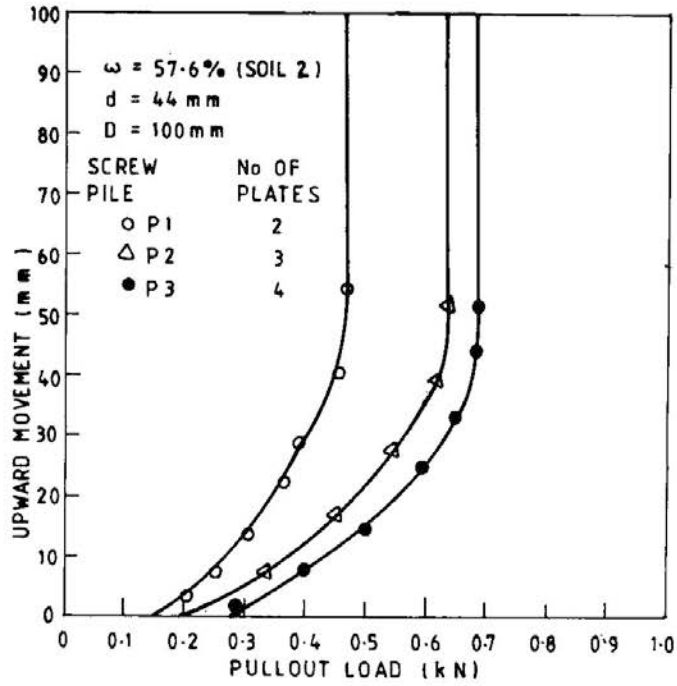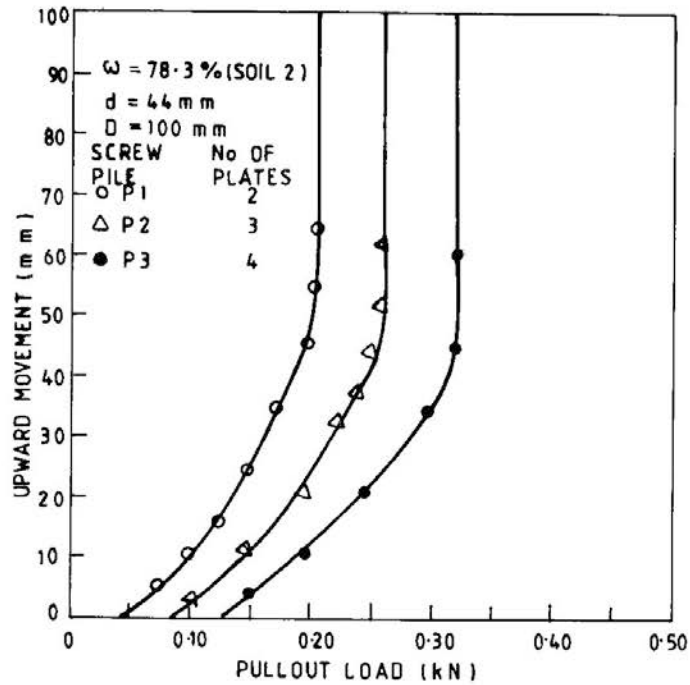
S.No.	Screw pile anchor Designation	No. of helical plates	Placement moisture content (%)	Conistency Index	Installation Torque, T in N.mm	Ultimate uplift capacity, P_{tu} in N
1	P1	2	57.6	0.483	16982.0	465
2	P2	3	57.6	0.483	14423.0	631
2	P3	4	57.6	0.483	12845.0	685
4	P1	2	78.3	0.165	6512.0	205
5	P2	3	78.3	0.165	5200.0	260
6	P3	4	78.3	0.165	4611.0	320

78.3%. These tests were conducted to confirm the effect of consistency index of the soil and the number of helical plates on uplift capacity and installation torque. Almost the same behaviour has been observed in this soil also as in soil 1. It can also be seen that the capacities of these anchors in soil 2 at a moisture content of 78.3% are very low because of the soft consistency of soil (consistency index = 0.165). All the test results in soil 2 i.e. uplift capacities and installing torques are presented in Table 4. Fig.10 refers to the relationship between the installing torque and uplift capacities of the tests. The conclusions drawn for soil 1 also apply to soil 2, i.e. the relationship between installing torque and uplift capacity of anchors with a different number of helical plates (but at the same moisture content); increase in uplift capacity and decrease in installing torque with the increase in the number of plates; increase in uplift capacity and installing torque with the increase in consistency index of soil for the same anchor, Fig.10.

Having confirmed the various aspects mentioned above in the first set of anchors, in the second set a limited number of tests were carried out on screw pile anchors with the increased diameters. These anchors are made with a shaft diameter of 60mm and plate diameter of 150mm. The same length has been kept. The pull out tests were conducted in the soil 1 at a moisture content of 45.2% and the curves are presented in Fig.11. the uplift capacities and installing torques are presented in Table 5 and in Fig.12. A comparison of these results with the results obtained in previous set but at the same moisture content (45.2%) in the same soil (soil 1) indicates that for the changes in the diameters in the anchor with 2 helical plates the uplift capacity is increased from 0.665kN to 1.480kN and the installing torque is increased from 24.779kN mm to 65.880kN mm. Similarly, in anchors with 3 and 4 helical plates, the increase in uplift capacities were from 0.910kN to 1.675kN and from 0.965kN to 1.720kN respectively and the increases in installing torques were from 20.849kN mm to 57.440kN mm and from 17.207kN mm to 53.088kN mm respectively.
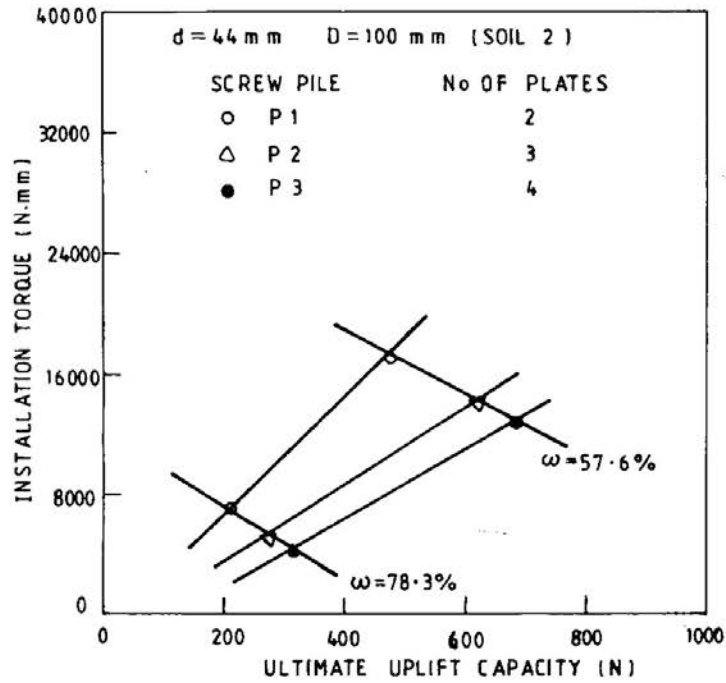
Fig.10: Relationship between ultimate uplift capacity and installing torque
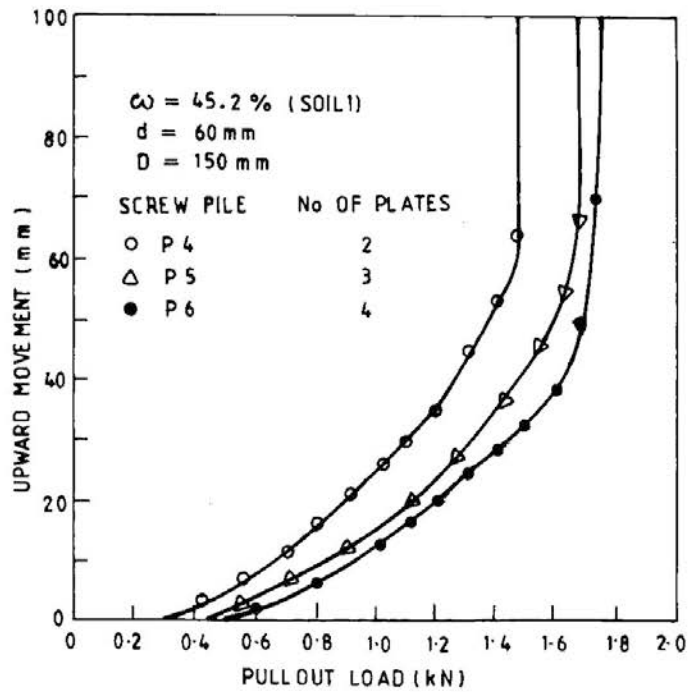
Fig.11: Pull-out load Vs. upward movement curves

151
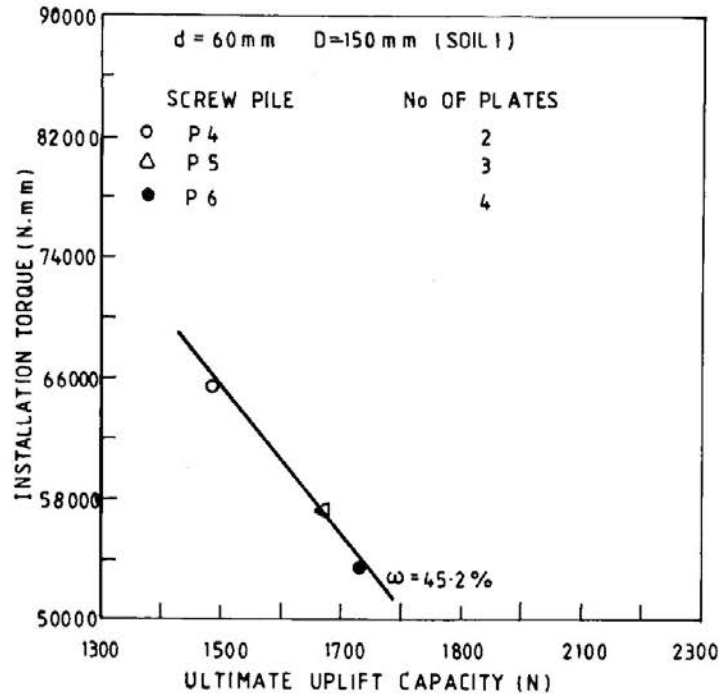
Fig.12: Relationship between ultimate uplift capacity and installing torque

Table 5: Uplift Capacities
(Set II, Soil 1)

S.No.	Screw pile anchor designation	No. of helical plates	Placement moisture content (%)	Conistency Index	Installation Torque, T in N.mm	Ultimate uplift capacity, P_{tu} in N
1	P4	2	45.2	0.596	65880.0	1480
2	P5	3	45.2	0.596	57440.0	1675
3	P6	4	45.2	0.596	53088.0	1720

COMPUTED CAPACITIES FROM THE MEASURED STRENGTH

The main components contributing to the uplift resistance of an anchor are (1) weight of anchor system (2) weight of soil mass bounded by an appropriate failure surface (3) friction and/or adhesion resistance along the failure surface and (4) suction developed under anchor plates. Even though the main components contributing to the uplift resistance are known, still there some difficulties experienced in successfully predicting the capacities. The differences in the measured and computed capacities can be because of (1) the use of an improper mechanism of failure and (2)

152

the inability to describe and allow for the stress history existing within the soil mass as well as volume change effects and progressive failure (Hanna, et al, 1972). However, in this present case of screw pile anchors, cylindrical failure surface are assumed between the top and bottom helical plates and the ultimate capacity P_{tu} (explained in Fig.13) is calculated by

$$P_{tu} = A_a N_{cu} c_t + c'_a A'_s + \alpha c_a A_s \tag{1}$$

where
P_{tu} = ultimate uplift capacity of screw pile
A_a = Area of cross section of the helical plate = $\frac{\pi}{4} (D^2 - d^2)$
D = diameter of the helical plate
d = diameter of the pile shaft
N_{cu} = uplift capacity factor
c_t = cohesion of soil above the top helical plate
c'_a = average cohesion of soil around cylinder of soil between top and bottom
  helical plates
A'_s = Surface area of cylinder between top and bottom plates = $\pi D L_c$
L_c = Distance between top and bottom helical plates
α = adhesion factor
c_a = average cohesion of soil along the pile shaft
A_S = surface area of pile shaft

In the equation (1), as a first approximation, the cohesion parameters are
equated because the same soil is compacted to form a more or less homogeneous deposit (i.e. $c_a = c_t = c'_a = c$). The adhesion factor α equal to unity has been used, as the soil condition mainly conforms to remoulded conditions in soft to medium stiff clays. The uplift capacity factor N_{cu} has to be estimated using some appropriate methods. Bobbitt & Clemence (1987) reported a relationship between the uplift capacity factor (N_{cu}) and relative depth (H/D) for helical anchors. In this present study, the top plate coincides with the top surface of the soil and hence there is no additional contribution due to uplift resistance on the top helical plate (i.e. $N_{cu} = 0$). So based on the above considerations, the ultimate uplift capacities were computed and compared with the experimental values from pull out tests as given in Table 6. From the Table, it is clear that there is a good agreement in these values. In general, for anchors with helical plates at close intervals, the agreement seems to be better. The spacing of these helical plates is expressed in terms of spacing ratio (l/d) which is a ratio between spacing of helical plates to diameter of helical plate. So from the

153

table, it is clear that when the spacing ratios approach a value of 1.5, the experimental values are almost in agreement with the computed values. This aspect is further examined from the photographs of pulled out anchors after pull out tests. The photographs of the pulled out anchors are presented in Figs.14 and 15 which correspond to the first set and second set of anchors respectively. So from the photographs, the nearly cylindrical failure surfaces can be observed for anchors with a spacing ratio of 1.5. It can also be stated that in the screw pile anchors with a spacing ratio of 1.5, the nearly cylindrical failure takes place between top and bottom helical plates in soft to medium stiff clays.

(NOTE: IN THIS PRESENT STUDY, $N_{cu}=0$ BECAUSE $H=0$)
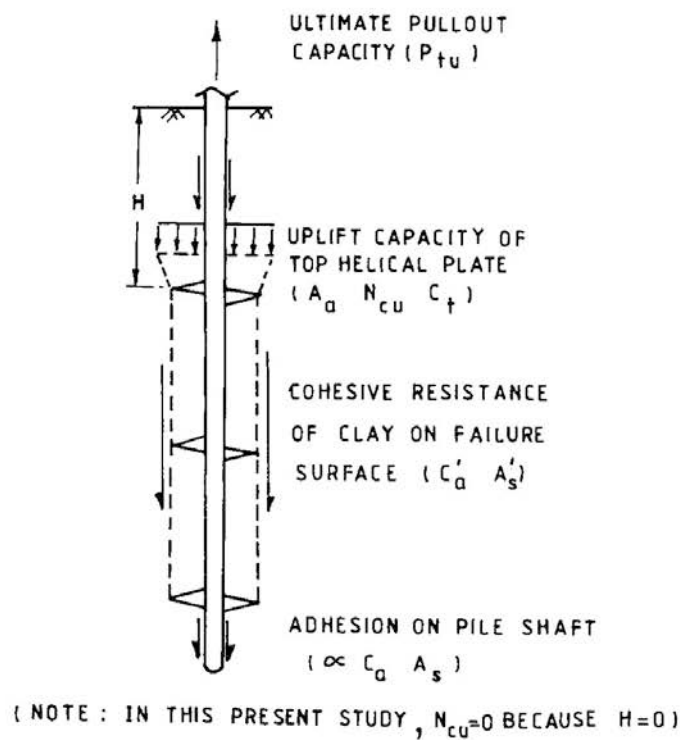
Fig.13: Screw pile in tension – forces acting

154
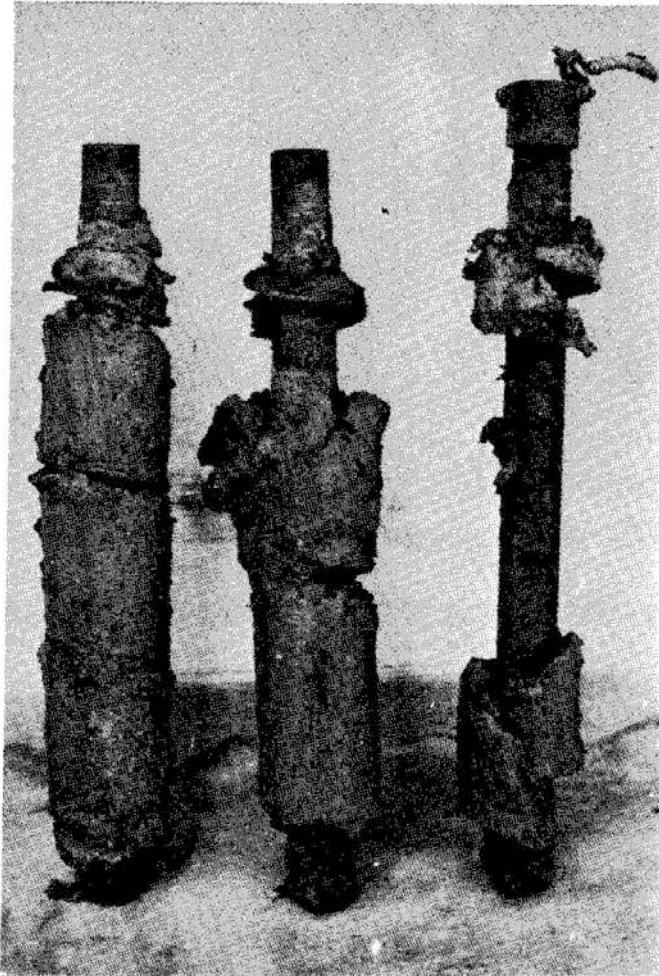
Fig.14: Photograph of pulled out piles after Pull-out tests (Set I, Soil 1)
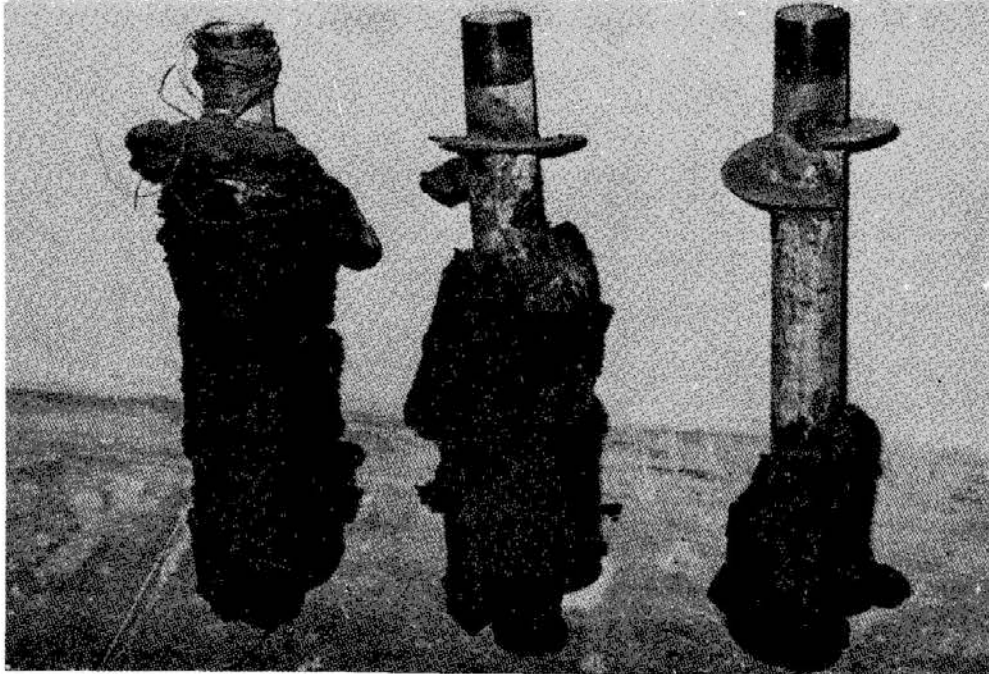
Fig.15: Photograph of pulled out piles after Pull-out tests (Set II, Soil 1)

COMPUTED CAPACITIES FROM MEASURED TORQUE

From the above discussion, it is clear that there exists some relationship between ultimate uplift capacity and installing torque. So in this limited experimental study, the field vane shear formulae is used to determine the strength S_r. The equation is,

$$T = 2\pi r^2 S_r (1 + 2r/3) \tag{2}$$

where

T = installing torque
r = radius of the helical plate = $D/2$
S_r = shear strength of soil
l = spacing of helical plate

From the equation 2, the value of S_r is determined and is used in place of C. The equation used for determining the P_{tu} is,

$$P_{tu} = S_r A_s' + \alpha S_r A_s \tag{3}$$

From the equation 3, ultimate uplift capacities are calculated and are presented in Table 7. For comparison purposes the experimental values are also presented in this Table. From the table, it is clear that there is a good agreement in these values. Especially in the anchors with 3 and 4 helical plates, the agreement seems to be better.

Table 6: Comparison between experimental values and computed values of the uplift capacities from the measured strength

Sl. No.	Screw pile anchor designation	No. of helical plates	Consistency index	Cohesive strength, C in N/mm²	Spacing ratio, I/D	Experimental value in N	Computed value in N	Experimental value Computer value
				Set I; Soil 1				
1	P1	2	0.696	0.0093	4.6	840	1450	0.58
2	P2	3	0.696	0.0093	2.3	965	1450	0.67
3	P3	4	0.696	0.0093	1.5	1340	1450	0.92
4	P1	2	0.596	0.0070	4.6	665	1090	0.61
5	P2	3	0.596	0.0070	2.3	910	1090	0.83
6	P3	4	0.596	0.0070	1.5	965	1090	0.89
7	P1	2	0.492	0.0048	4.6	550	750	0.73
8	P2	3	0.492	0.0048	2.3	625	750	0.83
9	P3	4	0.492	0.0048	1.5	725	750	0.97
				Set I; Soil 2				
10	P1	2	0.483	0.0050	4.6	465	780	0.60
11	P2	3	0.483	0.0050	2.3	631	780	0.81
12	P3	4	0.483	0.0050	1.5	685	780	0.88
13	P1	2	0.165	0.0020	4.6	205	310	0.66
14	P2	3	0.165	0.0020	1.5	320	310	1.08
				Set II; Soil 1				
16	P4	2	0.596	0.0070	3.1	1480	1620	0.91
17	P5	3	0.596	0.0070	1.5	1675	1620	1.03
18	P6	4	0.596	0.0070	1.0	1720	1620	1.06

CONCLUSIONS

Based on the experimental results the following conclusions can be drawn.

The screw piles can be conveniently installed and used as anchors to resist considerable uplift forces in soft to medium stiff clays. The installation torques can be conveniently correlated to the uplift capacities.

Table 7: Comparison between Experimental Values and Computed values of the uplift capacities from the measured torque

S.No.	Designation of screw pile anchor	No. of helical plates	Consistency Index of soil	Installation torque T in N.mm	Computed shear strength from measured torque in N/mm^2	Spacing ratio, I/D	Experimental value in N	Computed value in N	$\dfrac{\text{Experimental value}}{\text{Computed value}}$
				Set I; Soil 1					
1	P1	2	0.696	28938.4	0.0038	4.6	840	590	1.42
2	P2	3	0.696	24970.0	0.0061	2.3	965	948	1.02
3	P3	4	0.696	23020.0	0.0079	1.5	1340	1227	1.09
4	P1	2	0.596	24779.0	0.0032	4.6	665	497	1.34
5	P2	3	0.596	20840.8	0.0051	2.3	910	792	1.15
6	P3	4	0.596	17207.4	0.0059	1.5	965	917	1.05
7	P1	2	0.492	19296.0	0.0025	4.6	550	383	1.42
8	P2	3	0.492	15142.5	0.0037	2.3	625	575	1.09
9	P3	4	0.492	13077.6	0.0045	1.5	725	699	1.04
				Set I, Soil 2					
10	P1	2	0.483	16982.0	0.0022	4.6	465	342	1.36
11	P2	3	0.483	14423.0	0.0035	2.3	631	544	1.16
12	P3	4	0.483	12845.0	0.0044	1.5	685	683	1.01
13	P1	2	0.165	6512.0	0.0009	4.6	205	140	1.46
14	P2	3	0.165	5200.0	0.0013	2.3	260	202	1.29
15	P3	4	0.165	4611.0	0.0016	1.5	320	249	1.29
				Set II, Soil 1					
16	P4	2	0.596	65880.0	0.0037	3.1	1480	856	1.73
17	P5	3	0.596	57440.0	0.0058	1.5	1675	1342	1.25
18	P6	4	0.596	53088.0	0.0074	1.0	1720	1713	1.01

The capacities are significantly improved with the consistency index (with a decrease in moisture content) and with increases in sizes of piles. With the spacing ratios (spacing of the helical plates to the diameter of the helical plate) approaching about 1.5, the pull out tests indicated very nearly cylindrical failure surfaces.

It is possible to make theoretical predictions of the load capacities based on the shear strength of the soil and these predictions are quite satisfactory for the spacing ratios of 1.5.

REFERENCES

A.B. CHANCE COMPANY (1983), *Chance Earth Anchors,* Centralia, pp 1-28.

BOBBITT, D.E. & CLEMENCE, S.P. (1987), Helical Anchors: Application and design criteria, *Proc. 9th Southeast Asian Geotechnical Conference,* Bangkok, Thailand, pp 6-105 to 6-120.

CLEMENCE, S.P. & PEPE, F.D. (1984), Measurement of lateral stress around multihelix anchors in sand, *Geotechnical Testing Journal,* Vol7, No.3, pp 145-152.

HANNA, T.H., SPARKS, R. & YILMAZ, M. (1972), Anchor behaviour in sand, *Journal of the Soil Mechanics and Foundations Division, ASCE,* Vol.98, No.SM11, pp 1187-1208.

JOHNSTON, G.H. & LADANYI, B. (1974), Field tests of deep-installed screw anchors in permafrost, *Canadian Geotechnical Journal,* Vol.11, No.3, pp 348-358.

ROBINSON, K.E. & TAYLOR, H. (1969), Selection and performance of anchors for guyed transmission towers, *Canadian Geotechnical Journal,* Vol.6, No.2, pp 119-137.

TROFIMENKOV, J.G. & MARIUPOLSKII, L.G. (1965), Screw piles used for Mast and Tower foundations, *Proc. of sixth international conference on SM & FE,* Vol.11, pp 328-332.

WILSON, G. (1950), The bearing capacity of screw piles and screwcrete cylinders, *Journal of Institution of Civil Engineers,* Vol.34, pp 4-93.

MANUFACTURE AND MECHANICAL TESTING OF AN ARTIFICIALLY CEMENTED CARBONATE SOIL

C.F. Boey* and J.P. Carter**

SYNOPSIS

Unconfined compression tests were carried out on 55mm diameter, cylindrical samples of artificially cemented carbonate soil. The process used to manufacture this artificially cemented carbonate soil is described and the results of the compression testing are presented.

During manufacturing, a stress was applied for a selected duration of time to compact the mixture of carbonate soil, cement and water, and then each sample was left for the cement to cure. The effects of the manufacturing variables (i.e. magnitude of compaction stress, duration of compaction and curing time) and the material variables (i.e. cement and moisture contents and unit weight) on the soil behaviour are discussed.

INTRODUCTION

Foundations for offshore structures which are to be placed in a seabed consisting of weak calcareous sediments pose some significant difficulties for foundation designers. These weak calcareous sediments are known to undergo large volume reductions when subjected to relatively moderate loads. This reduction is due to the crushing of the calcareous sediments and due to the fact that they naturally have quite large initial voids ratios (e.g. Datta et al., 1979; Nauroy and Le Tirant, 1983; Semple, 1988). The tendency to compress may result in excessive foundation movements and may also reduce significantly the ultimate load capacity of the foundations. Recently there have been numerous field and laboratory tests carried out to investigate the material properties of, and the behaviour of foundations in this type of material (e.g. Angemeer et al., 1975; Poulos et al., 1982; Chua, 1983; Puyuelo et al., 1983; Ping et al., 1984; Poulos, 1984; Nauroy and Le Tirant, 1985; Dutt et al., 1985; Chan, 1986; Lu, 1986; Lee, 1988; Allman, 1988; Hull et al., 1988).

The cost involved in extracting 'undisturbed' core samples from offshore for laboratory testing is extremely high and this has limited the scope of previous investigations into the behaviour of these natural materials. Although recently there have

---

*Research Student and **Reader in civil engineering, University of Sydney.

been a number of investigations carried out on naturally cemented calcareous soils (e.g. Fahey & Jewell, 1988; Ripley et al., 1988; Williams & van der Zwagg, 1988; Johnston et al., 1988; Carter et al., 1988), there exists a need to understand better the behaviour of this type of material when it is subjected to different types of loadings and under varying test conditions.

The difficulties involved in obtaining good quality undisturbed samples of naturally cemented soil from the field are well known (e.g. Sangrey, 1977; Saxena & Lastrico, 1978; Frydman et al., 1980; Clough & Bachus, 1981). Even if the soil can be obtained in a sample tube, there is a distinct possibility that it may be damaged in the process of extruding it from the tube because the structure of the material is reasonably fragile. For these reasons, there may be doubts about whether a conventional investigation of cemented soils will result in a realistic evaluation of the soil properties (Iwabuchi, 1986). Because of the problems associated with sampling and testing of undisturbed samples of naturally cemented soils, it is often preferable to perform in situ testing to ascertain the material and mechanical properties. Unfortunately, the cost involved in performing this sort of test, especially offshore, is also extremely high (Iwabuchi, 1986).

The variability in properties of the natural material also presents an additional and difficult challenge to the interpretation of field and laboratory test results. It is possible to derive 'average' material and mechanical properties and design parameters from the field and laboratory test data by statistical applications (e.g. Mostyn, 1988). Of course, some of the finer detail of the actual physical behaviour may be lost in this averaging process.

In the present study an attempt was made to gain a clearer picture of the behaviour of cemented calcareous soils by eliminating the high degree of material variability. To do this a process for artificially cementing the soil was developed. As a first stage in understanding the mechanical behaviour of the material a series of 73 unconfined compression tests was carried out. Future testing will include triaxial compression and direct shearing under constant normal stress and constant normal stiffness.

SAMPLE MANUFACTURE

The major advantage in using an artificially prepared material in the study of calcareous sediments is that some degree of control can be exercised over material parameters, such as the amount of cement, the unit weight and the moisture content. In particular, the significant variations in strength and consistency of the naturally cemented material can be avoided.
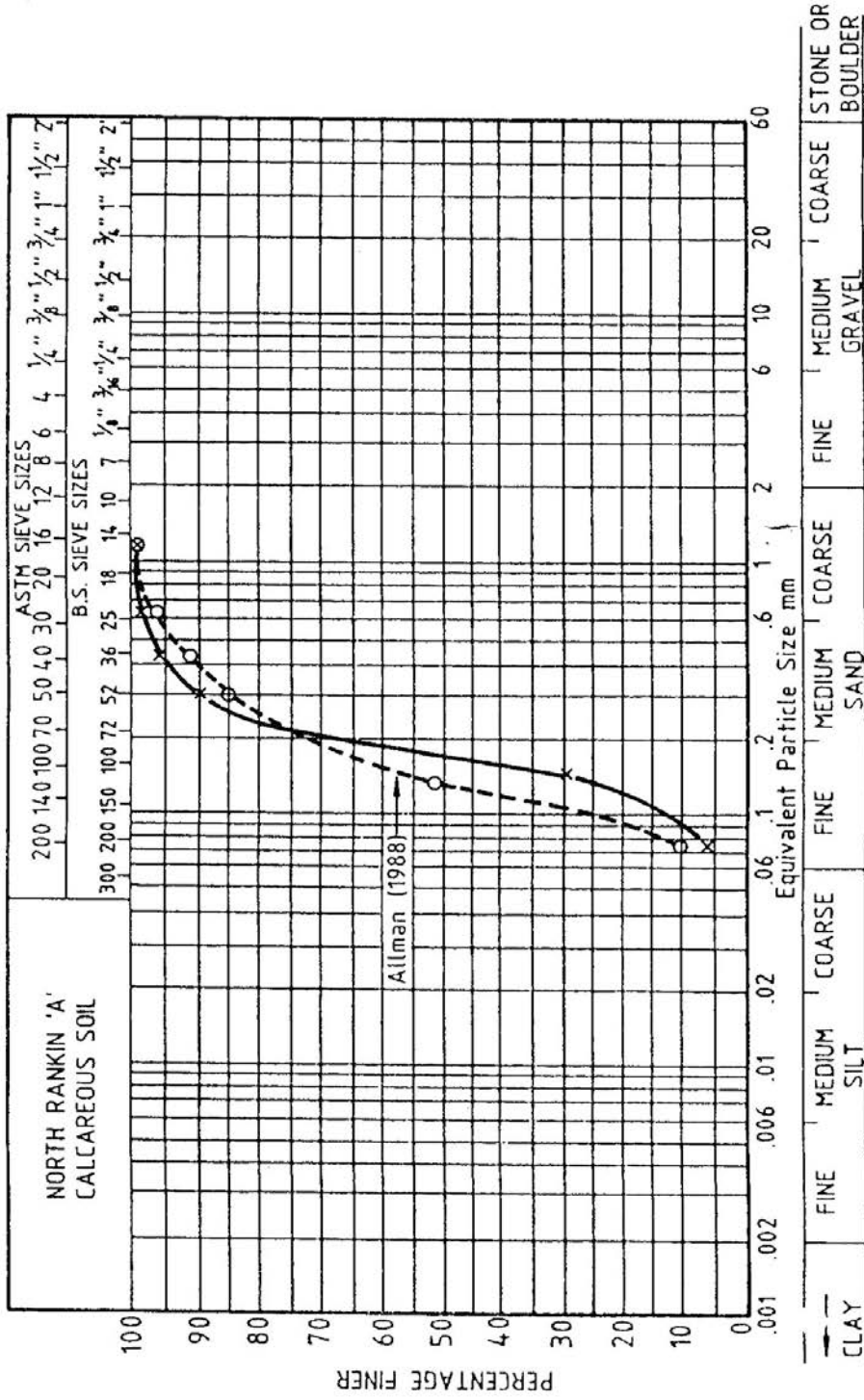
162

Fig.1   Grading curve of the carbonate soil from North Rankin 'A' site

In this study test samples were prepared from a natural calcareous soil and "hydrostone" cement (plaster). The calcareous soil was obtained from the North-West Shelf region of Australia. Allman (1988) has given a detailed description of its constituents, but it is worth noting here that it is composed predominantly of calcium carbonate (greater than 90%). The grading curve for this calcareous soil is shown in Fig. 1. The major mineral component of the cementing agent was gypsum, which has a compressive strength when dry of 76 MPa and a linear expansion of 0.002mm per mm. This cement has a setting time of approximately 25 minutes.

Naturally cemented calcareous materials are formed by compaction and consolidation of marine sediments over long periods of time. The engineering properties of these materials are largely related to the cement and moisture content, the degree of homogeneity of the material and the degree of compaction. Importantly, they are also controlled by the stress history and voids ratio. In the present study it was found that an appropriate model material could be produced conveniently using the technique described below. The advantage of this is that it renders a larger turnover of samples for the laboratory testing. This facilitates the possibility of parametric studies into the material behaviour in response to different loadings and conditions, and studies of the mechanisms of failure.

In the manufacturing process, the soil was first oven-dried and sieved using different mesh sizes (from mesh size 75 to 2400 microns). The cement was also sieved with a mesh size of 75 microns. The oven-dried soil and cement were mixed together thoroughly. Water was later added and the mixture was given another thorough mix. Typically, the amount of cement added was 20% of the weight of the oven-dried soil. The amount of water added for all samples was 40% of the combined weight of the oven-dried soil and cement. The soil-cement-water mixture was placed into a 55mm diameter PVC cylindrical mould. The inside wall of the mould was greased lightly to prevent the sample from binding to it and also to minimize the skin friction between the sample and mould. Once in the mould, the sample was subjected to a selected, statically applied, total vertical stress for a period of approximately 15 minutes. The external stress was then removed. While the sample was still in the mould but not subjected to external stress, it was allowed to harden for a further 15 minutes. (The plaster alone sets in an average time of 25 minutes). The sample was then taken out of the mould and wrapped with plastic film and placed into a thick plastic bag to cure for a period of between 3 and 20 days. To keep the air moist, some water was sprinkled into the bag and it was kept in a location where the humidity was relatively constant.

The manufacturing procedure is simple and economical in terms of time, cost and labour. Numerous tests were carried out to investigate the repeatability of the response of the artificially cemented soil in the unconfined compression test. The results indicate that the preparation procedure developed is capable of producing consistent samples having reproducible strength and behaviour. It was also found that the properties of the artificial material were similar to those of at least one naturally cemented material, as described below.

TEST PROCEDURE

The samples manufactured were generally 135mm in length and 55mm in diameter, thus having a length to diameter ratio of approximately 2.5. Most of the samples tested were only partially saturated. The samples were trimmed to right circular cylinders with both ends smooth and flat. Each sample was then seated on a steel platen, and another platen was placed on top of the sample. The top steel platen had a spherical seat incorporated in it. The axial load was applied using a rate of axial displacement equal to 0.2mm/minute (1.5×10^{-3} strain/minute) to ensure that the sample would fail between 10 to 15 minutes from the commencement of loading. The test was stopped when the sample had reached an axial strain of about 2.5% or when the sample had reached its "residual" strength, whichever came first.

TEST RESULTS

Manufacturing parameters

A typical set of results from the unconfined compression tests is presented in Fig.2, which shows curves of axial stress versus axial strain for samples with various cement contents in the range 5-30%, and an average moisture content of 35%. The results presented in the figure have not been corrected for seating error. Due to the fact that some water and cement (and possibly some soil fines) were squeezed out of the sample and lost during the compaction process, the stated cement contents are only nominal. The amount of cement lost is difficult to quantify.

In all cases, except for the sample with a nominal 5% cement content, a pronounced peak strength was observed followed by a post-peak softening response. The behaviour of the various samples shows that cementation influences the peak strength and the point of departure from a linear stress-axial strain response. As the degree of cementation increases the peak strength increases. The variation of peak
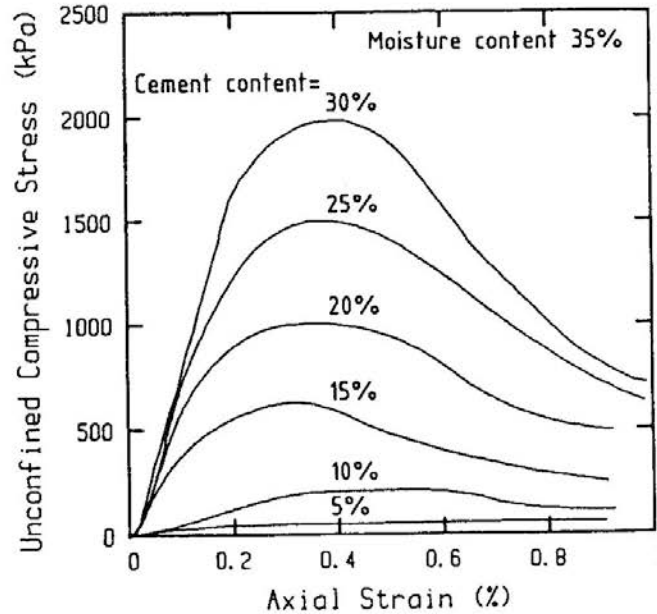
Fig.2   Variation with cement content of the behaviour in unconfined compression

strength with cement content is plotted in Fig.3, where it can be seen that the strength increases almost linearly with cement content over the range 10-30%. Samples with a moisture content of zero (oven-dried) show similar behaviour but the peak strengths are significantly higher than those of the samples with the same cement content but 35% moisture content. Under the Nyland classification for naturally cemented soils (Nyland, 1988), the artificially cemented material with a cement content of 20% having a peak strength of 1.0MPa, would be described as a moderately cemented.

The effects of compaction stress and duration of compaction on the unconfined compressive strength are shown in Fig.4 and 5, respectively. It can be seen that the strength varies with the degree of compaction. The samples that were not compacted had the least strength. This may be due to their large void space. Fig.4 indicates that the compressive strength increases with compaction stress up to about 200kPa but remains fairly constant for higher compaction stress. This reduced dependence of the strength on the magnitude of the compaction stress may be due to the higher stresses causing proportionally less reduction in voids ratio in the sample before the cement sets. However, the development of shear stresses between the soil and the mould during compaction may also be a contributing factor. The use of very high compaction stress (greater than 200kPa) may also cause some crushing of the soil particles during compaction, thus eventually forming a sample with a different distribution of particle sizes.
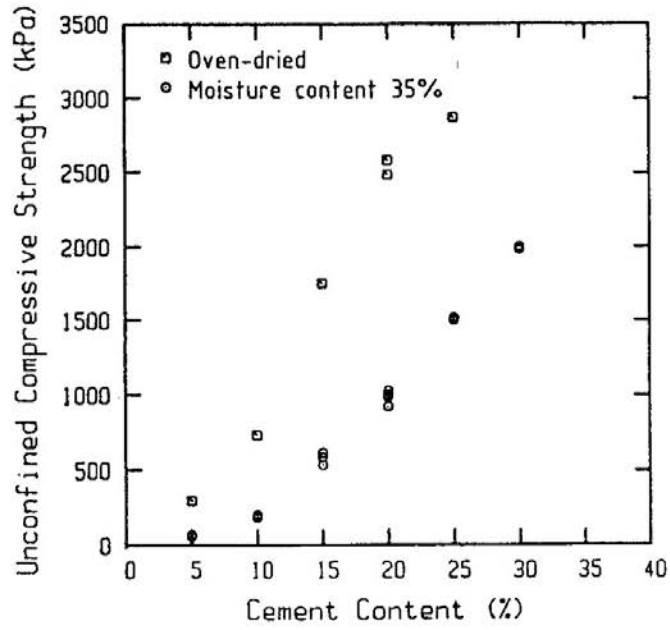
166

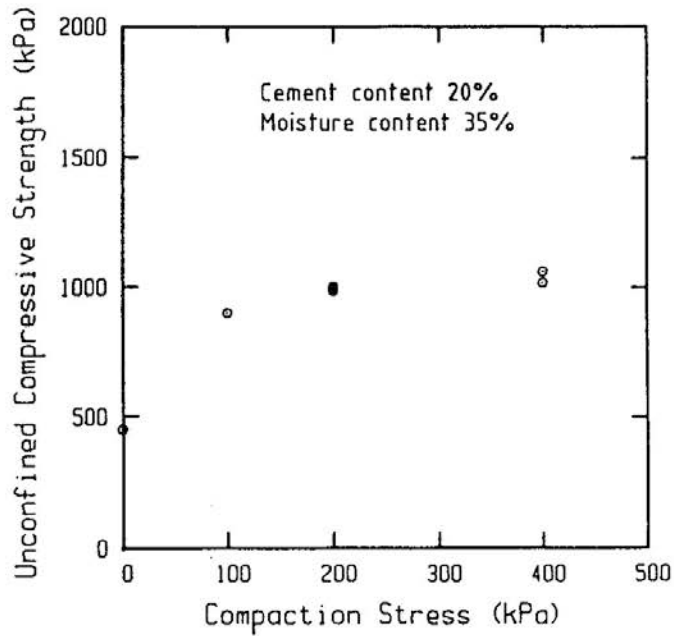**Fig.3   Effect of cement content on the unconfined compressive strength**

Fig.4   Effect of compaction stress on the unconfined compressive strength
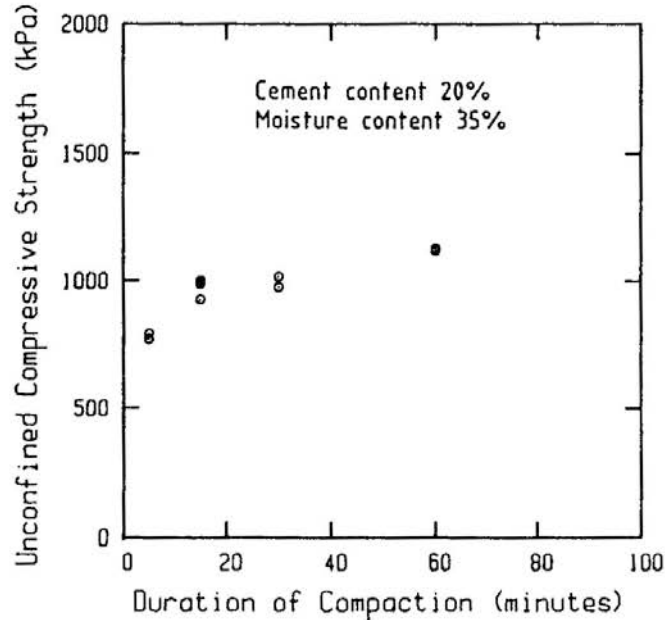
Fig.5   Effect of duration of compaction on the unconfined compressive strength

Fig.5 indicates that the duration of compaction also seems to increase the compressive strength of the sample up to a certain period of time, after which the strength is not significantly affected. An axial total stress of 200kPa was applied to all the samples represented in Fig.5. The duration of compaction at which there is no significant change in peak strength is about 60 minutes. It is clear that the cement would have fully set and hardened in this time period and under this applied stress (200kPa). In some tests the variation with time of the settlement under the compaction stress was measured. It was found that almost all of the overall settlement occurred in a relatively short interval, typically less than 5 minutes, possibly due to consolidation of the soil mixture. This implies that all of the time-dependent compaction movement occurs before the cement is fully hardened. No discernible changes in length of the samples were measured after one hour.

Tests were also carried out to determine if the duration of curing of the sample after manufacturing was an important parameter to consider. Fig.6 shows the effect of the duration of curing on the peak strength of the sample. Since the cement sets and hardens within 60 minutes and gains much of its strength within this time, there is little likelihood that a curing time of more than three days will affect the sample strength significantly. The fast setting cement and its early gain in strength renders a large turnover of samples for testing within a short period of time. It also allows the
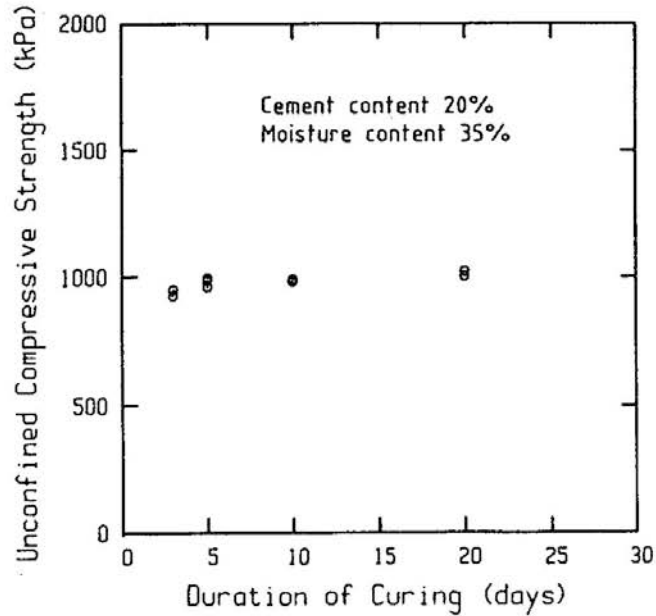
168

Fig.6   Effect of duration of curing on the unconfined compressive strength

sample to be handled without much disturbance to its cementation after this period of time. This explains the consistency and reproducibility in strength and behaviour of the samples.

Techniques for manufacturing the artificial material in blocks and then coring cylindrical samples were not employed because it was felt that coring may inadvertently disturb the sample thus affecting its subsequent strength and mechanical behaviour.

Repeatability of the manufacturing process

Fig.7 shows that the sample preparation procedure is capable of producing consistent samples and reproducible properties at the different cement contents. Fig.8 shows the degree of reproducibility of behaviour for samples with 20% cement content.

Material parameters

Three of the important material parameters, i.e. cement content, unit weight and moisture content, and their influence on the material strength will be discussed in
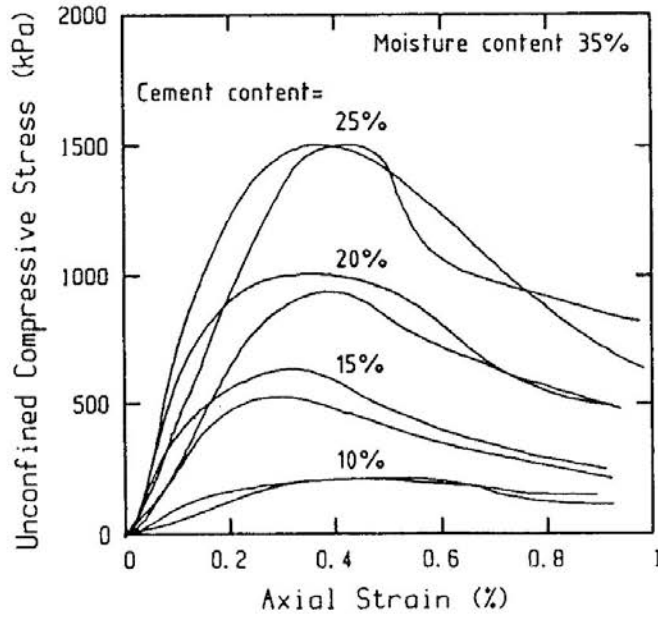
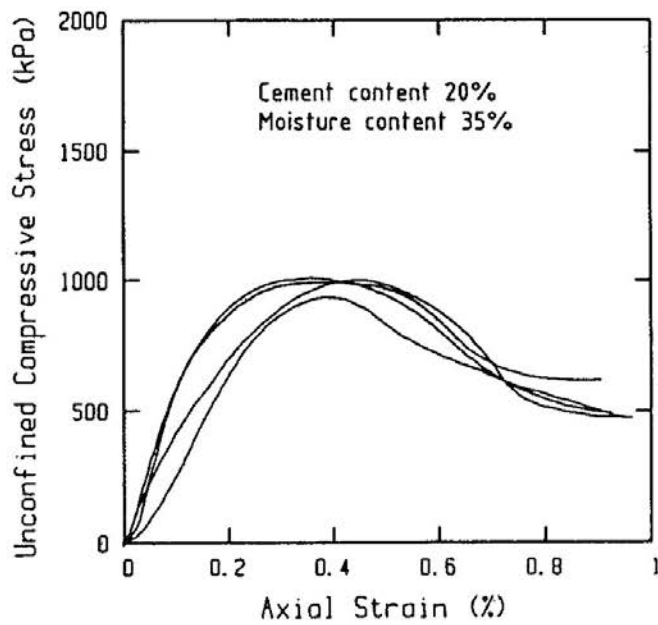**Fig.7   Reproducibility of behaviour of the artificially cemented carbonate soil**

Fig.8   Reproducibility of behaviour of the artificially cemented carbonate soil (cement content 20%, moisture content 35%)
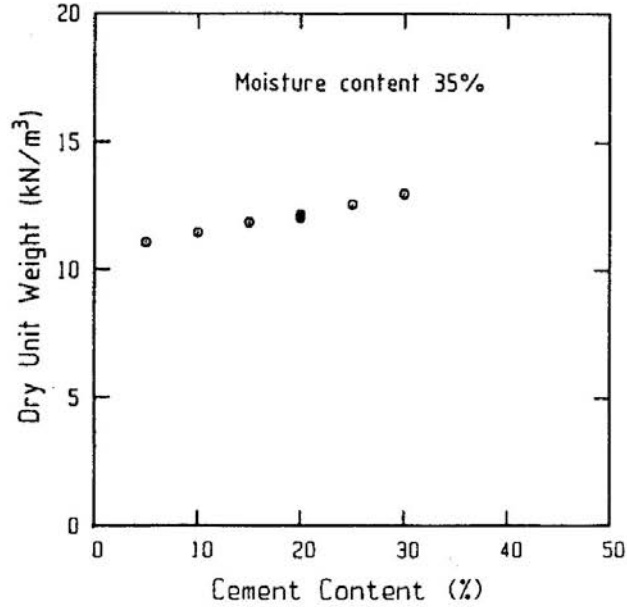
Fig.9   Dry unit weight as a function of the cement content

this section. Various authors (e.g. Jewell and Andrews, 1988; Jewell and Khorshid, 1988) have commented previously on the relationship between cementation, unit weight and moisture content on the behaviour of the naturally cemented material. Fig.9 shows the dry unit weight of the material which appears to increase linearly with the cement content over the range investigated. Fig.10 shows that the peak strength of the material increases markedly with the dry unit weight. For comparison purposes it is noted that the natural calcarenite from the site of the North Rankin 'A' gas production platform on the North-West Continental Shelf of Australia has an average dry unit weight of approximately $12.13kN/m^3$ (Mostyn, 1988).

Fig.11 shows how the deformation modulus of the artificially cemented material varies with the dry unit weight. E_{25} and E_{50} are the secant moduli at 25% and 50% of the peak stress level and E_0 is the initial tangent modulus. It is very interesting to note that each modulus increases with increasing dry unit weight, although for a given dry unit weight the values of the three moduli are reasonably close. This is another reflection of the linearity of the axial stress versus axial strain curves (Fig.2) below half of the peak stress. Samples with a cement content of 20% have elastic moduli that range from 360 to 500Mpa. For comparison, it can be noted that the modulus of calcarenite from the North Rankin 'A' site derived from drained triaxial compression tests, ranges from 108 to 540MPa (Allman, 1988). Thus the artificially cemented soil has similar stiffness to this naturally cemented material.
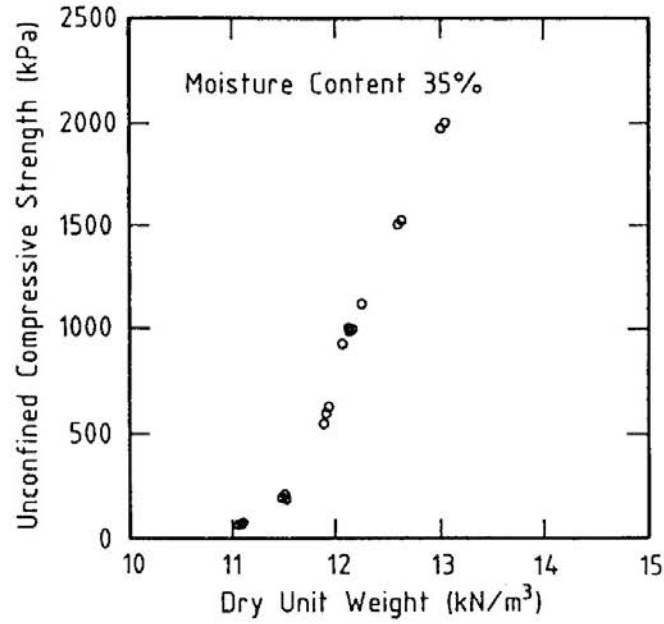
171

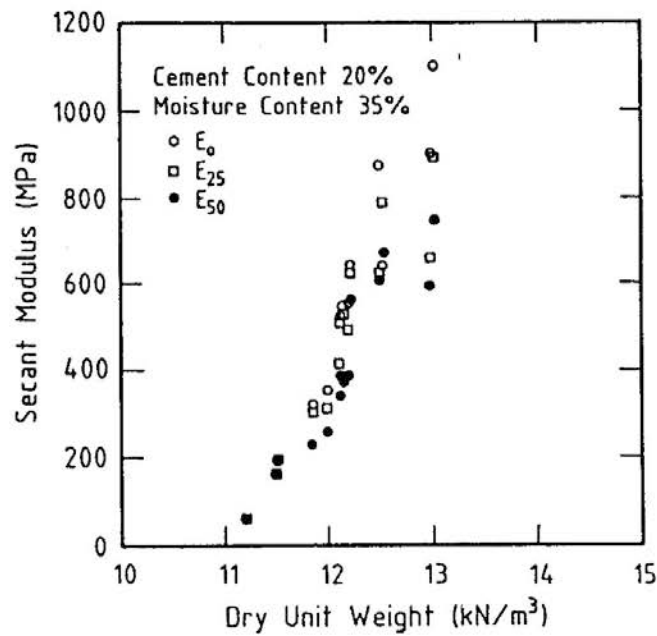**Fig.10 Variation with dry unit weight of the unconfined compressive strength**

Fig.11 Variation with dry unit weight of the secant modulus
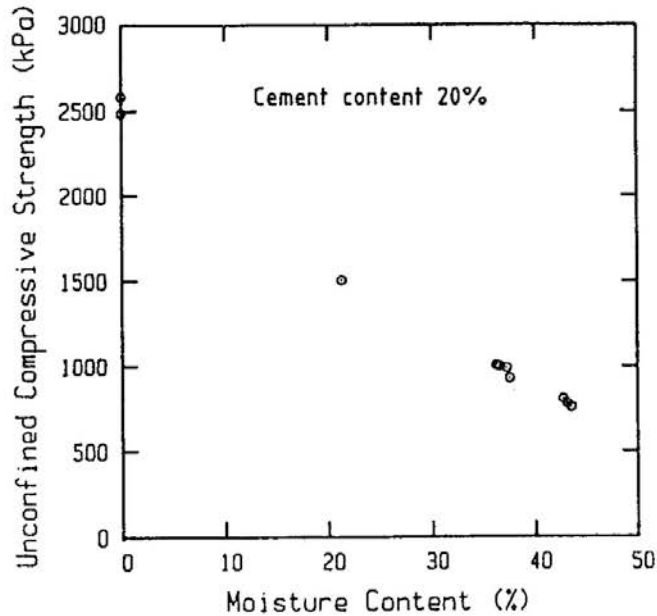
Fig.12 Variation with moisture content of the unconfined compressive strength

Fig.12 shows that the peak strength of the sample depends very much on the moisture content at the time of testing. As the moisture content decreases, the peak strength of the sample increases. This indicates that it is very important that natural samples which are to be tested in the laboratory should be properly and securely wrapped immediately after the core is recovered, in order to minimise moisture loss.

Rate of straining

The rate of axial displacement also affects the peak strength of the artificially cemented material. Fig.13 shows that the peak strength increases slightly with increasing rate of straining, for strain rates between 0.01 to 2mm/minute (7.5×10^{-5} to 1.5×10^{-2} strain/minute). The loading rate of 0.01mm/minute gives the lowest peak strength, which may be caused by the material creeping significantly under load at this slow loading rate. These results imply that for testing which involves cyclic loading, selection of the frequency of cycling may need to be carefully considered.

Fig.13 Effect of rate of loading on the unconfined compressive strength
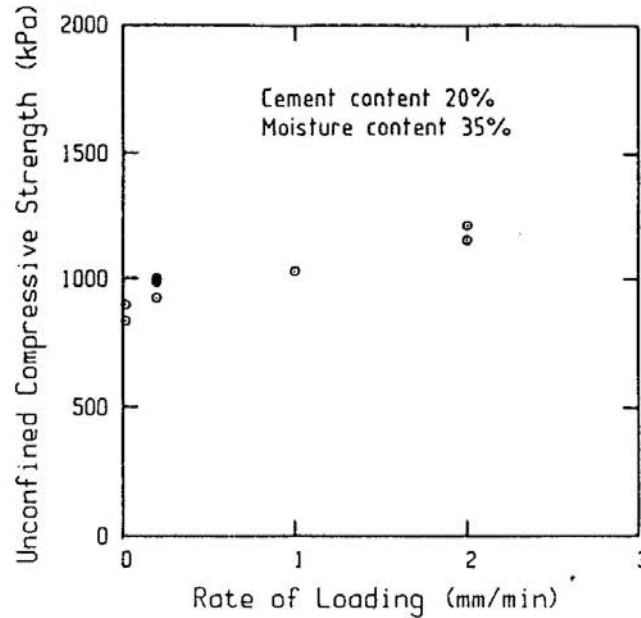
A number of other investigators (e.g. Kobayashi, 1970; Bjerrum, 1973) also found that the rate at which a rock or soil sample was loaded in the laboratory or field can influence the properties measured. The trend usually observed is that for high rates of strain application, both the measured modulus and strength can be increased significantly (Johnston et al., 1980).

COMPARISON WITH A CALCARENITE

Table 1 contains a comparison between some of the characteristics and properties of the artificially cemented carbonate soil with a nominal cement content of 20% and the natural calcarenite from the site of the North Rankin 'A' gas production platform. It is clear that the two materials have similar mechanical properties. Data for the natural calcarenite were abstracted from Allman (1988) and Mostyn (1988).

Currie et al. (1988) reported unconfined compression strength values for the core specimens of natural calcarenite recovered from the site of North Rankin 'A' gas production platform to be in the range 0.30-2.07MPa. The average unconfined compression strength was 1.3MPa with a standard deviation of 0.5MPa. The moisture content for these specimens was not reported but was likely to be in the range 25-35%.

174

	Unit	Calcarenite	Artificially cemented soil	Reference for Calcarenite
$CaCO_3$	%	90-96	>90	Allman (1988)
Dry unit weight	kN/m^3	12.13	~12.3	Mostyn (1988)
		(14.81-17.85)		Allman (1988)
Void ratio		1.22	~1.30	Mostyn (1988)
Moisture content	%	~40	~35	
Effective peak friction angle ϕ' [1,5]	degree	~36	~34	Allman (1988)
Cohesion c' [1,5]	kPa	~100-160	~200	Allman (1988)
Unconfined compressive strength [2]	MPa	~0.39-0.65	~0.74	
Young's modulus E' [3,5]	MPa	~108-540	~120-220	Allman (1988)
Poisson's ratio ν' [4,5]		~0.09-0.30	~0.15-0.25	Allman (1988)

Notes:

(1) Values for ϕ' and c' were determined from triaxial compression tests.

(2) Value for unconfined compressive strength was backfigured using: $q_u = \frac{2c'cos\phi'}{(1-sin\phi')}$.

(3) Values for E' were determined from triaxial compression tests.

(4) Value for Poisson's ratio was calculated from the slope of the volume strain-axial strain curve using the theory of elasticity, i.e. $\nu' = \frac{1}{2}(1-\frac{\varepsilon_v}{\varepsilon_{ax}})$, where ε_v is volumetric strain, and ε_{ax} is axial strain.

(5) In the triaxial compression tests, the confining pressures range from 20 to 500 kPa.

Values of unconfined compression strength for the natural calcarenite were also calculated from the Mohr-Coulomb strength criterion using values of c' and ø' (c' is the cohesion and ø' is the peak friction angle) provided by Allman (1988). These are average values of c' and ø' deduced from a set of triaxial test results carried out on the calcarenite, as reported by Carter et al. (1988). It is the range of values for unconfined compressive strength of the natural calcarenite calculated in this way that is listed in Table 1. The value backfigured for the unconfined compressive strength for the artificially cemented carbonate soil, using c' = 200 and ø' = 34°, was 0.74MPa. (It is worth noting that this calculated strength agrees very well with the measured unconfined compression of 0.75MPa for a sample of the artificially cemented material with a moisture content of 43% – see Fig.12). The triaxial samples used to determine these values of c' and ø' for the artificial material had a moisture content of about 43%. Moisture content has a significant influence on the

175

strength and for comparison purposes, it is reported that a sample of the artificially cemented soil with moisture content of 35% has an unconfined compressive strength of 1.0MPa.

For completeness, values of the drained deformation parameters, viz. Young's modulus E' and Poisson's ratio ν', for both materials are included in Table 1. Both sets of values have been determined from CID triaxial tests. Further discussion of these deformation parameters for the artificially cemented soil will be given in a forthcoming paper describing the triaxial testing of this material. It should be pointed out that the values of E' determined from the triaxial tests are lower than the values of E' determined from the unconfined compression tests.

The natural calcarenite and the artificially cemented soil were also compared visually and chemically using optical and electron microscopy and spectral analysis. Some typical results of this study are shown in Figs. 14, 15 and 16.

The calcarenite occurring at North Rankin has been described as being weakly to moderately cemented (Nyland, 1988), while the artificially cemented soil can also be described as being moderately cemented. In Fig.14 the photographs show that the two materials have similar structures, although the artificially cemented soil is more uniform. The calcarenite seems to have a non-uniform distribution of silty and shelly materials. Fig.15a shows a scanning electron micrograph of the cementation in the artificially cemented soil. The cementation appears to be composed of needle-like crystals probably of calcium sulphate (since gypsum plaster is predominantly composed of calcium sulphate) which are precipitated inorganically. It can be seen that the soil particles are encrusted by the calcium sulphate crystals. This form of cementation may be compared with the types of natural cementation occurring in the calcarenite. These are shown in Figs.15b and 15c. Fig.15b shows the soil particles being encrusted by the needle-like crystals of aragonite. However, Fig.15c shows another form of cementation present in the natural material which is composed of calcite crystal euhedra. These crystals have been precipitated inorgaincally in the calcarenite (Allman, 1988). Although the forms of cementation in the calcarenite and the artificially cemented soil are different, the soil particles of both soils are cemented into a structure which is open and contains a large amount of interparticle voids. Clearly, the large interparticle void space contributes to the collapsing nature of both soils.

Figs.16a and 16b show the results of spectral analyses of the two materials. The elements present in the artificially cemented soil are calcium *(Ca)* and sulphur *(S)*. They are expected to be present since the cement is mostly calcium sulphate and the

176
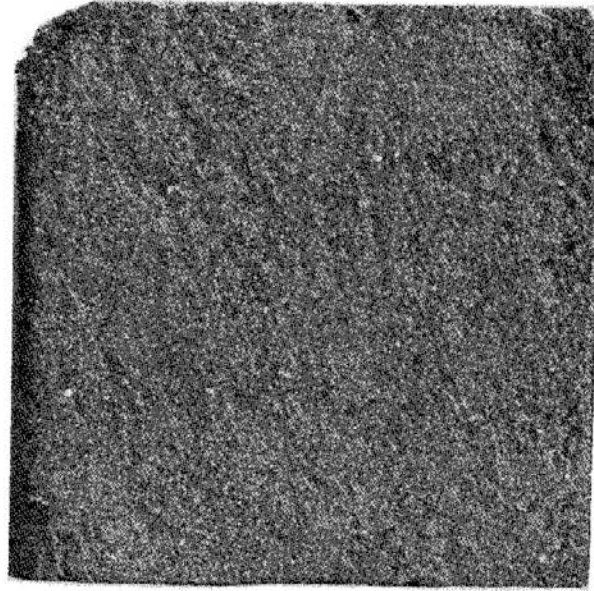
(a) Artificially cemented soil
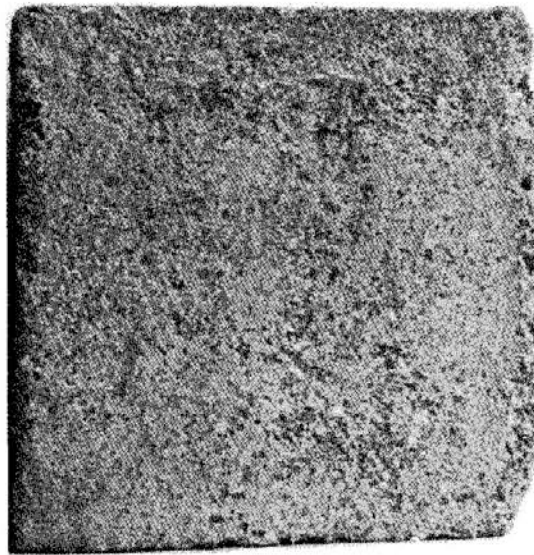
(b) North Rankin calcarenite

Fig.14   Photographs of sections of the artificially cemented soil and natural calcarenite

(a) Calcium sulphate crystal in artificially cemented soil

(b) Aragonite needles in calcarenite (after Allman, 1988)
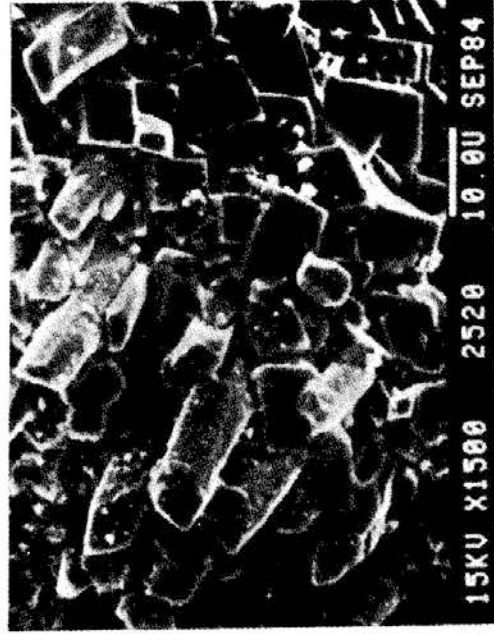
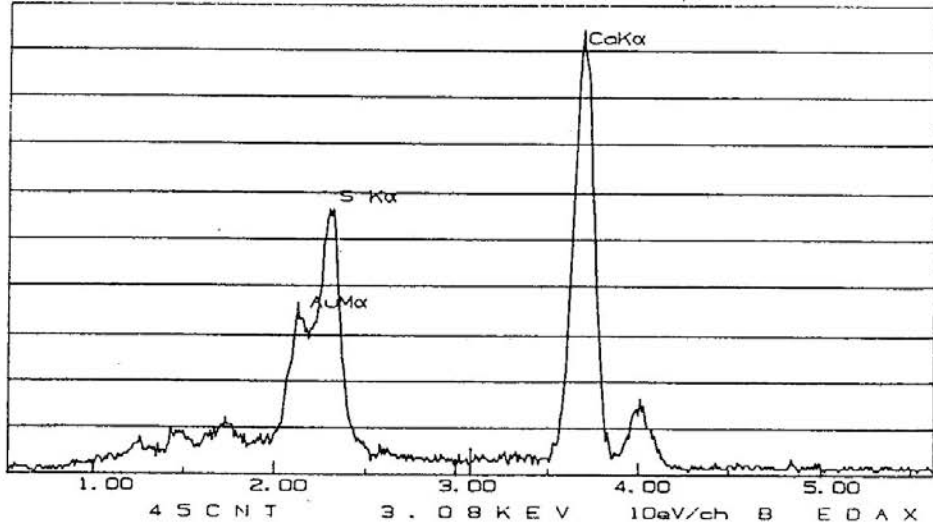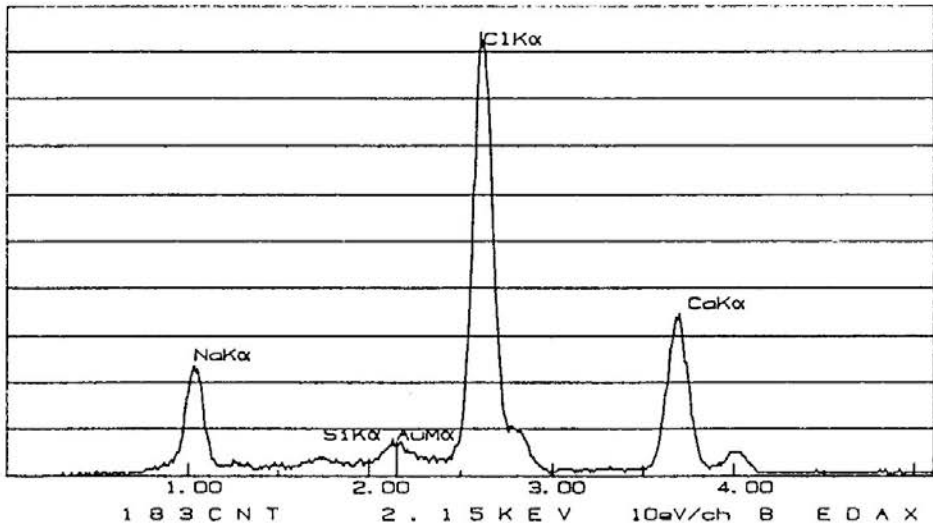(c) Calcite crystal euhedra in calcarenite (after Allman, 1988)

Fig.15 Various types of cementation in the artificially cemented soil and natural calcarenite

(a) Spectral analysis of the artifcially cemented soil

(b) Spectral analysis of the calcarenite

Fig.16   Spectral analyses of the artificially cemented soil and natural calcarenite

soil particles are composed predominantly of calcium carbonate. However, in the natural calcarenite the elements present are sodium *(Na)*, chlorine *(Cl)*, calcium *(Ca)* and silicon *(Si)*. The presence of sodium and chlorine is an indication of sodium chloride (probably from sea water), and the presence of calcium and silicon is an indication of carbonate and silica materials occurring in the calcarenite. Some traces of gold are also shown in the spectra and its presence is due to a layer of gold which was required for coating the soils before they could be analysed.

CONCLUSIONS

By compacting the calcareous soil from an unconsolidated state to a consolidated condition and using plaster as a suitable cementing agent to provide particle bonding, it was possible to manufacture an artificially cemented soil which exhibits behaviour similar to at least one naturally cemented calcareous soil, viz. calcarenite from the site of the North Rankin 'A' gas production platform. Results of unconfined compression tests on samples of the artificially cemented soil have been presented. The results indicate that the manufacturing process described is reliable (and simple) and capable of producing samples with reproducible behaviour. Most importantly, the inherent variability of the natural material has been avoided and results of the tests on this artificially cemented carbonate soil should be of assistance in understanding the fundamental behaviour of naturally cemented calcareous sediments. Other types of test such as the triaxial compression and direct shear test have also demonstrated the suitability of the artificially prepared material for a study of the fundamental mechanical behaviour of calcarenites. The results of these other tests have been described elsewhere (Boey & Carter, 1988).

ACKNOWLEDGEMENTS

REFERENCES

Allman, M.A. (1988). *"The Behaviour of Piles in Cemented Calcareous Soil"*, Ph.D. Thesis, University of Sydney, Australia.

Angemeer, J., Carlson, E., Stroud, S. & Kurzeme, M. (1975). "Pile Load Tests in Calcareous Soils Conducted in 400 Feet of Water from a Semi-Submersible Exploration Rig", *Proc. 7th Annual Offshore Tech. Conf.,* Houston, Paper No. OTC 2311, pp. 659-670.

Bjerrum, L. (1973). "Problems of Soil Mechanics and Construction on Soft Clays and Structurally Unstable Soils", *Proc. 8th Int. Conf. S.M.F.E.,* Mexico, 3, pp.111-159.

Boey, C.F. & Carter, J.P. (1988). "Mechanical Testing of Artificially Cemented Carbonate Soil", *Proc. 5th Australia-New Zealand Conf. on Geomechanics,* Sydney, pp.145-149.

Carter, J.P., Johnston, I.W., Fahey, M., Chapman, G.A., Novello, E.A. & Kaggwa, W.S. (1988). "Triaxial Testing of North Rankin Calcarenite", *Proc. Int. Conf. on Calcareous Sediments,* Perth, Vol.2, A.A. Balkema, Rotterdam, pp.515-530.

Chan, K.F. (1986). *"Behaviour of Model Piles in Calcareous Sand",* M.Eng.Sc. Thesis, University of Sydney, Australia.

Chua, E.W. (1983). *"Bearing Capacity of Shallow Foundations in Calcareous Sand",* M.Eng.Sc. Thesis, University of Sydney, Australia.

Clough, G.W. & Bachus, R.C. (1981). "An Investigation of Sampling Disturbance in Weakly Cemented Soils", *Proc. Engineering Foundation Conf. in Updating Subsurface Sampling and In-situ Testing,* Santa Barbara, California.

Currie, P.K., Cuckson, J. & Jewell, R. (1988). "Testing of Chemically Stabilised Calcareous Sediments", *Proc. Int. Conf. on Calcareous Sediments,* Perth, Vol.2, A.A. Balkema, Rotterdam, pp.587-595.

Datta, M., Gulhati, S.K. & Rao, G.V. (1979). "Crushing of Calcareous Sands During Shear", *Proc. 11th Annual Offshore Tech. Conf.,* Houston, Texas, Paper No. OTC 3525, pp.1459-1467.

Dutt, R.N., Moore, J.E., Mudd, R.W. & Rees, T.E. (1985). "Behaviour of Piles in Granular Carbonate Sediments from Offshore Philippines", *Proc. 17th Annual Offshore Tech. Conf.,* Houston, Texas, Paper No. OTC 4849, pp.73-82.

Fahey, M. & Jewell, R. (1988). "Model Pile Tests in Calcarenite", *Proc. Int. Conf. on Calcareous Sediments,* Perth, Vol.2, A.A. Balkema, Rotterdam, pp.555-564.

Frydman, S., Hendron, D., Horn, H., Steinback, J., Baker, R. & Shaal, B. (1980). "Liquefaction Study of Cemented Sands", *Journal of the Geotechnical Eng'g. Div.,* ASCE, Vol.106, No.GT3, pp.275-297.

Hull, T.S., Poulos, H.G. & Alehossein, H. (1988). "The Static Behaviour of Various Calcareous Sediments", *Proc. Int. Conf. on Calcareous Sediments,* Perth, Vol.1, A.A. Balkema, Rotterdam, pp.87-96.

Iwabuchi, J. (1986). *"The Influence of Cementation on Liquefaction Resistance of Sands",* Ph.D. Thesis, Virginia Polytechnic Institute and State University.

Jewell, R.J. & Andrews, D.C. (1988)(Eds). *"Engineering for Calcareous Sediments – Vol.1, General Proceedings",* A.A. Balkema, Rotterdam.

Jewell, R.J. & Khorshid M.S. (1988)(Eds). *"Engineering for Calcareous Sediments – Vol.2, North Rankin A Foundations Project and State of the Art Reports"*, A.A. Balkema, Rotterdam.

Johnston, I.W., Williams, A.F. & Chiu, H.K. (1980). "Properties of Soft Rock Relevant to Socketed Pile Design", *Proc. Int. Conf. on Struct. Founds. on Rock,* Sydney, Vol.1, pp.55-64.

Johnston, I.W., Carter, J.P., Novello, W.A. & Ooi, L.H. (1988). "Constant Normal Stiffness Direct Shear Testing of Calcarenite", *Proc. Int. Conf. on Calcareous Sediments,* Perth, Vol.2, A.A. Balkema, Rotterdam, pp.541-553.

Kobayashi, R. (1970). "On Mechanical Behaviour of Rocks Under Various Loading-Rates", *Rock Mech. in Japan,* 1, pp.56-58.

Lee, C.Y. (1988). *"The Behaviour of Grouted Piles in Offshore Foundations"*, Ph.D. Thesis, University of Sydney, Australia.

File no.: TI-19 times 78 (CY 4/1)

Lu, B.T.D. (1986). "Axial Behaviour and Capacity of Driven Piles in Calcareous Sands", *Proc. 18th Annual Offshore Tech. Conf.,* Houston, Texas, Paper No. OTC5148, pp.579-588.

Mostyn, G. (1988). "Statistical Evaluation of Design Parameters for Gravity Based Anchor System", *Proc. Int. Conf. on Calcareous Sediments,* Perth, Vol.2, A.A. Balkema, Rotterdam, pp.711-717.

Nauroy, J.F. & Le Tirant, P. (1983). "Model Tests of Piles in Calcareous Sands", *Proc. ASCE Conf. on Geotechnical Practice in Offshore Eng'g.,* Austin, pp. 356-369.

Nauroy, J.F., Brucy, F. & Le Tirant, P. (1985). "Static and Cyclic Load Tests on a.Drilled and Grouted Pile in Calcareous Sand", *Proc. 4th Int. Conf. on Behaviour of Offshore Structures,* Delft, The Netherlands, pp.577-587.

Nyland, G. (1988). "Detailed Engineering Geological Investigation of North Rankin 'A' Platform Site", *Proc. Int. Conf. on Calcareous Sediments,* Perth, Vol.2, A.A. Balkema, Rotterdam, pp.503-512.

Ping, W.C.V., Locke, G.E., de Mello, J.R. & de Matos, S.F.D. (1984). "Performance Assessment of Deep Penetration Offshore Piles Driven into Calcareous Soils", *Proc. 16th Annual Offshore Tech. Conf.,* Houston, Paper No. OTC4836, pp.513-518.

Poulos, H.G. (1984). "Cyclic Degradation of Pile Performance in Calcareous Soils", *Analysis and Design of Pile Foundations,* ASCE, San Francisco, pp.99-118.

Poulos, H.G., Uesugi, M. and Young, G.S. (1982), "Strength and Deformation Properties of Bass Strait Carbonate Sands", *Geotech, Eng'g.,* Vol.13, pp.189-211.

Puyuelo, J.G., Sastre, J. & Soriano, A. (1983). "Driven Piles in a Granular Calcareous Deposits", *Proc. Conf. on Geotech. Practice in Off. Eng'g.,* Austin, Texas, pp.440-456.

Ripley, I., Keulers, A.J.C. & Creed, S.G. (1988). "Conductor Load Tests", *Proc. Int. Conf. on Calcareous Sediments,* Perth, Vol.2, A.A. Balkema, Rotterdam, pp.429-438.

Sangrey, D.A. (1977). "Marine Geotechnology – State of the Art", Marine Geotechnology, Vol.2, *Marine Slope Stability,* pp.45-80.

Saxena, S.K. & Lastrico, R.M. (1978). "Static Properties of Lightly Cemented Sand", *Journal of the Geotechnical Eng'g. Div., ASCE,* Vol.104, No. GT12, pp.1449-1464.

Semple, R.M. (1988). "The Mechanical Properties of Carbonate Soils", *Proc. Int. Conf. on Calcareous Sediments,* Perth, Vol.2, A.A. Balkema, Rotterdam, pp.807-836.

Williams A.F. & van der Zwagg, G.L. (1988). "Analysis and Evaluation of Grouted Section Tests", *Proc. Int. Conf. on Calcareous Sediments,* Perth, Vol.2 A.A. Balkema, Rotterdam, pp.493-502.

DISCUSSION

Paper "Risks in Geotechnical Engineering: Conceptual and Practical Suggestions" by Victor F.B de Mello, *Geotechnical Engineering*, Vol.19, No. 2., Dec 1988.

A broad and scholarly paper by Prof. V. F. B. de Mello, "Risks in Geotechnical Engineering: Conceptual and Practical Suggestions," appeared recently in "Geotechnical Engineering" Vol. 19, No. 2, December 1988. In his paper de Mello lists a large number of references, covering a wide range in this broad and difficult subject. It is noted that the list does not include Prof. Arthur Casagrande's masterful paper, "The Role of the 'Calculated Risk' in Earthwork and Foundation Engineering," given in 1964 as the Second Terzaghi Lecture of ASCE. It was published in the ASCE Journal of the Soil Mechanics and Foundation Division, Vol. 91, No. SM4, July 1965.

Casagrande describes in considerable detail six large and conspicuous projects on which he was closely associated, to illustrate the uncertainties due to imperfect knowledge of subsurface conditions and properties which geotechnical engineers must often accept in their work. In addition, Casagrande discusses various types of risks, including those due to human imperfections, and also the consequences of failures. His paper is recommended for reading and study by those who often struggle with obtaining realistic factors of safely, even when using the latest techniques.

Philip Keene
Consulting Geotechnical Engineer,
Middletown, Connecticut, USA.

BOOK REVIEW

Subsidence – Occurrence, Prediction and Control, by B.N. Whittaker and D.J. Reddish, Elsevier, Amsterdam, 1989, 528 pages. Available from Elsevier Science Publishing Co., Inc. P.O. Box 882, Madison Square Station, New York NY 10159, USA.

This recently published book is the latest offering in the Elsevier Series on "Developments in Geotechnical Engineering" which currently numbers 56 in total. Both authors of this rather impressive book are from the UK, indeed, they are both from the Department of Mining Engineering of the University of Nottingham.

The book essentially deals with the adverse surface subsidence effects of the mining/extractive industries and is clearly mining subsidence oriented; not to be confused with settlements related to soil mechanics causes.

The aims of the book, as set out by the authors, are to bring together existing world knowledge, experience and research on the subject; to collate field data on subsidence from many countries and so to make international comparisons; to review the important topic of subsidence prediction; to examine methods of controlling subsidence and finally to achieve a better understanding of the mechanics of mining subsidence. On the whole the authors have reached their amins although they might not have fully achieved the extensive international coverage they sought.

The book will be of particular interest to the practising mining or geotechnical engineer concerned with the causes, prediction and control of the surface effects of mining subsidence and while in no sense a manual, nor is it meant to be, the book will definitely provide considerable and sound practical guidance and reference for the practitioner; the book is certainly not a theoretical treatise.

The thin, well bound, hardcover, size and form of the book belies the massive amount of wordage and illustration it contains. There are over 500 pages of neat, small print text, divided into 18 chapters and 1 appendix. Only three of the chapters deal with aspects other than underground coal mining subsidence and these cover; natural (geological) subsidence, rock salt and potash subsidence; and subsidence arising from ground water, or oil and gas field extraction. For the record the contents of the coal mining subsidence chapters relate to; the historical development of mining subsidence theory and concepts; mining and ground movements; methods of predicting mining subsidence; observed behaviour of mining subsidence; subsidence prediction by the UK empirical model; computer based prediction; near sur-

face tunnels subsidence; room and pillar mining subsidence; steeply inclined seams; sloping ground surfaces; the time factor; geological factors; abandoned mine workings; effects on structures; and ground movement behaviour – subsidence models.

This subdivision and treatment of separate topics in individual chapters aids both the easy first time reading and subsequent ready reference is further assisted by the inclusion of a triple index system, covering places, subjects and authors, as well as by the extensive single alphabetical reference list at the end of the text. About the only publication fault noted was that pages 471 to 478 were duplicated; in the reviewers copy at least!

The layout of the text in each chapter is clear, albeit produced in rather small print size, and well subdivided under headings.

The book is extensively and well illustrated by numerous clear and well labelled and captioned figures, black and white photographs and tables. The mathematical formulae, which are not extensive, are well printed and clear.

Regarding the technical content of the publication the authors have aimed at, and in the reviewers opinion, achieved, a well judged and methodical build up from theory to observed and from established practice in simple cases to the coverage of more complex situations by development of the previously discussed simpler predictive models. Emphasis is placed on the empirical/semiquantitative approach using relatively straight forward formulas, graphs and tables to achieve the objectives. Complex mathematical, numerical or computer methods are avoided – thus making the text both reader friendly yet directly and practically oriented and easy to apply. A small number of worked examples are woven into the text of those chapters dealing with subsidence prediction and these are particularly useful and illustrative.

In conclusion the book provides an extensive, readily useable and directly applicable coverage of most mining subsidence situations and readers, particularly in the European sphere of mining, should find the text a very acceptable and indispensable reference source and initial solution provider.

A.D. Burnett

BOOK REVIEW

Rock Mechanics in Hydroengineering.

This book covers a broad spectrum of Rock Mechanics including rock mass properties, fundamental stress and deformation response, failure mechanisms, analytical and numerical techniques, hydraulics of fractured rock masses and field applications, particularly useful to the geotechnical engineer. The addition of chapters on mineralogy, structural geology and geophysical methods makes the book also attractive to the geologists.

Stability of slopes and underground excavations and flow modelling have been discussed in detail with some relevant discussion also on the stabilization methods such as grouting and anchoring. These sections are useful to practising geotechnical engineers and geologists. The author has also attempted to elucidate on numerical modelling techniques including the Finite Element and Boundary Element methods, but only a basic treatment of this subject matter is provided, perhaps for the benefit of the novice.

This book can be recommended as a standard textbook for both undergraduate and post graduate levels in Civil (Geotechnical) Engineering and Engineering Geology. It will also serve as a basic guide as well as a source of relevant information for researchers in the field of Rock Engineering. The book is also available from the Elsevier Science Publishing Co. Inc., P.O. Box 882, Madison Square Station, New York, NY 10159, U.S.A.

Dr B. Indraratna

CONFERENCE NEWS

Third Int. Symp. on Pressuremeter. Oxford UK, 2-6 April 1990. All enquiries to: Dr. Houlsby, Dept. Eng. Science, Parks Rd, Oxford OX1 3P5, UK.

Tenth S.E. Asian Conf. on Geotechnical Engineering. Taipei, 16-20 April 1990. All enquiries to: Dr. Ou, Ret-Ser Eng. Agency, 11/F, 207 Sung-Chiang Rd, Taipei, Taiwan.

Fourth Int. Conf. on Geotextiles and Geomembranes. The Hague Netherlands, 28 May-1 June, 1990. All enquiries to: Holland Organizing Centre, 16 Lange Voorhout, 2514 EE The Hague, Netherlands.

ASCE Spec. Conf. on Design and Performance of Earth Retaining Structures. Ithaca, NY, USA, 18-21 June 1990. All enquiries to: Dr. P. Lambe, Dept. Civ. Eng., N. Carolina State Univ., Campus Box 7908, Rayleigh, NC 27695, USA.

VIth Int. Congress of the IAEG. Amsterdam, August 6-10, 1990. All enquiries to: Dr. L. Primel, Secretary IAEG, Laboratoire Central des Ponts et Chausees, 58 Boulevard Lefebvre, 75732 Paris Cedex 15, France. Tlx: LCPARI 200361 F.

ISRM 7th International Congress on Rock Mechanics. Aachen GERMANY FR. 1991 September 16-20. All enquiries to' Deutsch Gesellschaft fur Erdund Grundbau e.V., Kronprinzenstr. 35a, D-4300 Essen I, GERMANY FR. TLP: 49/201/227677; TLX: 887414 ESN.

9th Asian Regional Conference. Bangkok, Thailand, 1991. All enquiries to: SEAGS, PO Box 2754, Bangkok 10501, Thailand.

6th Int. Conf. on Landslides. Christchurch, New Zealand, 10-14 Feb. 1992. All enquiries to: Dr. D. Bell, Univ. of Canterbury, Christchurch, New Zealand.

XIII International Conference on Soil Mechanics and Foundation Engineering. New Delhi, India, January, 1994. All enquiries to: Prof. Gulhati, Secy-General 13th ICSMFE, India Institute of Technology, New Delhi, 110016, India.

ANNOUNCEMENTS

Golden Jubliee Commemorative Volume of the Southeast Asian Geotechnical Society

Geotechnical Engineering in Southeast Asia, a commemorative volume of the Southeast Asian Geotechnical Society, is now available from Balkema Publishers. This volume contains 11 contributions from Southeast Asia ranging from the behaviour of piles in soft organic clays to landslides and their control. It also includes bibilographies of books, journals, conference publications, theses, etc (c. 2,200 titles) and a directory of consultants and contractors in Southeast Asia. This 352 page document (US$40) can be obtained from:

A. A. Balkema Book Distributors
P.O. Box 1675, NL-3000 BR Rotterdam
Netherlands

SEAGS Newsletter

All correspondence related to the SEAGS Newsletter should be addressed to:

Southeast Asian Geotechnical Society
c/o Division of Geotechnical and Transportation Engineering,
Asian Institute of Technology,
P.O. Box 2754
Bangkok, Thailand 10501.

10th SOUTHEAST ASIAN GEOTECHNICAL CONFERENCE, TAIPEI 1990

In the next few years a number of major projects will be undertaken in Taiwan. The construction of an extensive Mass Rapid Transit System for Taipei Metropolis has already started and will reach its peak by 1992. The construction of the second freeway is just about to start and it will take four years to complete. A tunnel linking Taipei City and Eastern Taiwan is being planned and an extension of the railroad tunnel in Taipei City will be constructed soon.

The 10th SEAGC will be held in the brand new Taipei International Convention Centre in 1990. The great scenic spots of this beautiful island and the colorful life in

Taipei City, day and night, will make the 10th SEAGC even more attractive to delegates and their spouses.

Conference Date: April 16, 1990-April 20, 1990
Conference Place: Taipei International Convention Center
Offical Language: English
Conference Theme: "THE GEOTECHNOLOGY FOR TOMORROW"

Main Subject Areas of Papers:
1. **Tunnelling and Underground Construction**
2. **Environmental Geotechnology**
3. **Geotechnical Mapping**
4. **Slope Stability and Landslides**
5. **Engineering Geology and Rock Mechanics**
6. **Ground Improvement**
7. **Deep Foundations**
8. **Others**

Exhibitions:
1. **Recent developments in Geotechnical Engineering equipment and techniques.**
2. **In-situ and laboratory instruments.**
3. **Organizations interested in participating are advised to fill out the Preliminary Registration Form and return to the Secretary-General before July 1st, 1989.**

Other Activities:
Guest Lectures, Site Visits, Post-Conference Tours and Spouse Programs

Contact Address:
Dr. C.D. Ou, Secretary-General
The Organizing Committee, 10th SEAGC
c/o RSEA, No.207, Sung Chiang Rd.,
Taipei, Taiwan, 10430, Republic of China
Telephone: (02)5032233 ext 213
Telefax: (02)5031113, Telex: 21531 RSEA

SI UNITS AND SYMBOLS

The following list of quantities, SI (Systeme International) units and SI symbols, are recommended for use in Geotechnical Engineering.

Quantities	Units	Symbols
Length	kilometre	km
	metre	m
	millimetre	mm
	micrometre	μm
Area	square kilometre	km^2
	square metre	m^2
	square millmetre	mm^2
Volume	cubic metre	m^3
	cubic millimetre	mm^3.
Mass	tonne	t
	kilogramme	kg
	gramme	g
Density P (mass density)	tonne per cubic metre	t/m^3
	kilogramme per cubic metre	kg/m^3
Unit weight γ (weight density)	kilonewton per cubic metre	kN/m^3
Force	meganewton	MN
	kilonewton	kN
	newton	N
Pressure	megapascal	MPa
	kilopascal	kPa
Energy	megajoule	MJ
	kilojoule	kJ
	joule	J
Coefficient of volume compressibility or swelling m_v	1/megapascal	MPa^{-1}
	1/kilopascal	kPa^{-1}
Coefficient of consolidation or swelling c_v	square metre per second	m^2/s
	square metre per year	$m^2/year$
Hydraulic conductivity k (formerly coefficient of permeability)	metre per second	m/s

NOTES: The term specific gravity is obsolete and is replaced by relative density.
The former term relative density $(e_{max}-e)/(e_{max}-e_{min})$ is replaced by the term density index, I_D.